

UNIVERSITY OF CALGARY

Neural Network Based SVC Controller

by

Hong Wang

A THESIS

SUBMITTED TO THE FACULTY OF GRADUATE STUDIES
IN PARTIAL FULFILMENT OF THE REQUIREMENTS FOR THE
DEGREE OF MASTER OF SCIENCE

DEPARTMENT OF ELECTRICAL AND COMPUTER
ENGINEERING

CALGARY, ALBERTA

November, 2004


© Hong Wang 2004

UNIVERSITY OF CALGARY
FACULTY OF GRADUATE STUDIES

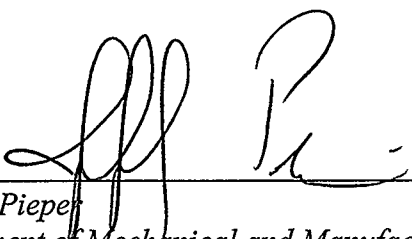
The undersigned certify that they have read, and recommend to the Faculty of Graduate Studies for acceptance, a thesis entitled "Neural Network Based SVC Controller" submitted by Hong Wang in partial fulfillment of the requirements for the degree of Master of Science.



Supervisor, Dr. O.P. Malik
Department of Electrical and Computer Engineering



Dr. Ed. Nowicki
Department of Electrical and Computer Engineering



Dr. Jeff Pieper
Department of Mechanical and Manufacturing Engineering

Date: 2011.10.15

ABSTRACT

A Static Var Compensator (SVC) controller used to control the output of the SVC to damp power system oscillations is developed in this dissertation. The proposed SVC controller is based on the discrete time filtered direct control theory by which a multi-layer neural network with the hyperbolic tangent activation function is derived. The Lyapunov stability technique and advanced weight tuning algorithm based on the modified delta rule and projection algorithm are used to design the neural network based controller to realize the objective of damping and to keep the stability of the entire closed loop system. Simulation studies with the proposed controller on a single machine infinite bus system show the damping effectiveness of the proposed controller. Results of the simulation studies show that the entire power system stability is greatly improved through the employment of the proposed SVC controller.

ACKNOWLEDGEMENTS

It is a pleasure to express my deep thanks and gratefulness to my supervisor Dr. O.P. Malik for his valuable help and guidance during this period. This dissertation would be impossible without his advice, guidance and encouragement from time to time. From him I have learned so much not only in the area of my speciality but also in the serious and careful attitude toward scientific research.

Also, I appreciate very much all the professors and friends who give me advice and discussions regarding this project.

Finally, my hearty gratitude is expressed to my beloved family: my parents and my wife. Their endless support and encouragement are invaluable for me.

To my Parents and my Wife Xiaoming Zhang

TABLE OF CONTENTS

APPROVAL PAGE.....	ii
ABSTRACT.....	iii
ACKNOWLEDGEMENT.....	iv
DEDICATION	v
TABLE OF CONTENTS	vi
LIST OF FIGURES	ix
LIST OF SYMBOLS AND NOMENCLATURE.....	xii
CHAPTERS	
1. INTRODUCTION.....	1
1.1 Power System Stability and Oscillations.....	1
1.1.1 Bulk Electric Power System and SVC.....	1
1.1.2 Power System Stability.....	5
1.1.3 Oscillations in Power Systems.....	6
1.2 Damping Control Strategies and Types of Power System Stabilizers.....	6
1.2.1 Damping at Generator Locations.....	7
1.2.2 Damping in Transmission Paths.....	7
1.2.3 Types of Power System Stabilizers.....	8
1.3 SVC for Oscillation Damping.....	10
1.4 Artificial Neural Network Based PSS.....	12
1.4.1 Neural Networks for Control.	12
1.4.2 Neural Network Based PSS.....	13
1.5 Dissertation Objectives.....	14
1.6 Contributions of Dissertation.....	16
1.7 Thesis Organization	17
2. ARTIFICIAL NEURAL NETWORKS.....	18
2.1 Introduction.....	18
2.2 Neuron Model.....	19
2.3 Architecture of Neural Networks.....	23
2.3.1 Single Layer Structure.....	24
2.3.2 Multilayer Perceptron.....	24

2.3.3 Other Neural Network structures.....	25
2.3.3.1 Radial Basis Function Neural Network.....	25
2.3.3.2 Cerebella Model Articulation Controller.....	26
2.3.3.3 Recurrent Architecture.....	27
2.4 Learning Algorithms.....	28
2.4.1 Hebbian Learning Rule.....	29
2.4.2 Delta Rule.....	30
2.5 Back Propagation Algorithm.....	32
2.6 Selection of Neural Network for SVC Controller.....	32
2.7 Summary	34
3. NEURAL NETWORK BASED CONTROL DESIGN.....	36
3.1 Introduction.....	36
3.2 Plant Model.....	37
3.2.1 Continuous System Model.....	37
3.2.2 Discrete Time System Model.....	38
3.3 Control Applications.....	39
3.3.1 Model Reference Adaptive Inverse Control.....	39
3.3.2 Model Reference Adaptive Control.....	40
3.3.3 Model Predictive Control.....	41
3.3.4 Neural Network Based Indirect Control Design.....	42
3.4 Proposed Multilayer Neural Network Based Direct Control Design.....	43
3.4.1 Tracking Problem.....	44
3.4.2 System Dynamics.....	45
3.4.3 Selection of Input of the Proposed NN.....	47
3.4.4 Weight Update Functions.....	48
3.4.5 Projection Algorithm.....	51
3.4.6 Modification of the Weight Tuning Functions.....	51
3.4.7 Stability Proof.....	53
3.5 Summary.....	58
4. SIMULATION STUDIES OF NN SVC CONTROLLER IN A SINGLE MACHINE INFINITE BUS SYSTEM.....	59
4.1 Introduction.....	59

4.2 Modeling of the Single Machine Infinite Bus System with an SVC at the Middle Bus.....	59
4.3 Conventional SVC Supplementary Controller.....	62
4.4 Design of the Proposed SVC NNPS.....	64
4.5 Control Simulation Studies.....	64
4.5.1 Network Training.....	65
4.5.2 Normal Operating Condition.....	66
4.5.3 Leading Power Factor Condition.....	69
4.5.4 Light Load Test.....	70
4.5.5 Voltage Reference Change of the Generator Bus.....	72
4.5.6 Voltage Reference Change of the Middle Bus.....	74
4.5.7 Different Sampling Intervals.....	76
4.5.8 Three Phase Short Circuit Tests.....	78
4.5.9 Comparisons of the Damping Effectiveness Between Generator PSS and the Proposed SVC Controller.....	82
4.5.10 Test Of the Coordination with the Generator CPSS.....	83
4.5.11 Test of the Stability Margin	84
4.6 Summary.....	85
5. CONCLUSIONS AND FUTURE STUDIES.....	87
5.1 Conclusions	88
5.2 Future Studies.....	90
REFERENCES.....	91
APPENDIX.....	97

LIST OF FIGURES

1.1 Typical True 48-Pulse SVC	3
1.2 Typical Seven Level Cascading Structure of SVC.....	4
2.1 Structure of A Neuron with Multiple Inputs.....	19
2.2 Hyperbolic Tangent Function.....	22
2.3 Layer with s Neurons.....	23
2.4 Typical Three Layer Neural Network	25
2.5 Recurrent Architecture.....	28
2.6 Supervised Learning.....	29
2.7 Architecture of the Proposed Neural Network.....	34
3.1 Structure of the Adaptive Inverse Control System.....	39
3.2 Architecture of the Model Reference Controller.....	40
3.3 Model Predictive Control.....	41
3.4 NN Indirect Control.....	43
3.5 Proposed NN Controller.....	49
4.1 Single Machine Infinite Bus System with an SVC.....	60
4.2 SVC Controller Configuration	61
4.3 Closed Loop System with the Proposed SVC NNPSS	63
4.4 Training of the Network. Initial Condition $P=0.7$ p.u., p.f. = 0.85 lag	65
4.5 Generator Angular Speed in Response to a 0.2 p.u. Step Increase in Torque. Initial Condition $P=0.7$ p.u., p.f. = 0.85 lag.....	67
4.6 Voltage at the Middle Bus in Response to a 0.2p.u. Step Increase in Torque. Initial Condition $P=0.7$ p.u., p.f. = 0.85 lag.....	67

4.7	Output of PSS in Response to a 0.2 p.u. Step Increase in Torque. Initial Condition P=0.7p.u., p.f. = 0.85 lag.....	68
4.8	Output of AVR in Response to a 0.2p.u. Step Increase in Torque. Initial Condition P=0.7p.u., p.f. = 0.85 lag.....	68
4.9	Generator Angular Speed in Response to a 0.2p.u. Step Increase in Torque. Initial Condition P=0.7p.u., p.f. = 0.9 lead.....	69
4.10	Voltage at the Middle Bus in Response to a 0.2p.u. Step Increase in Torque. Initial Condition P=0.7p.u., p.f. = 0.9 lead.....	70
4.11	Generator Angular Speed in Response to a 0.1 p.u. Step Increase in Torque. Initial Condition P=0.2 p.f.=0.85 lag.....	71
4.12	Voltage at the Middle Bus in Response to a 0.2p.u. Step Increase in Torque. Initial Condition P=0.2p.u., p.f. = 0.85 lag.....	71
4.13	Generator Angular Speed Response to a 0.03 p.u. Step Increase in the Voltage Reference of the Generator Bus. Initial Condition P=0.7p.u., p.f. = 0.85 lag	72
4.14	Middle Bus Voltage in Response to a 0.03 p.u. Step Increase in the Voltage Reference of the Generator Bus. Initial Condition P=0.7p.u., p.f. = 0.85 lag	73
4.15	Generator Bus Voltage in Response to a 0.03 p.u. Step Increase in the Voltage Reference of the Generator Bus. Initial Condition P=0.7p.u. p.f. = 0.85 lag.....	73
4.16	Generator Angular Speed in Response to a 0.04 p.u. Step Increase in the Voltage Reference of the Middle Bus. Initial Condition P=0.7p.u., p.f. = 0.85 lag.....	74
4.17	Middle Bus Voltage in Response to a 0.4 p.u. Step Increase in the Voltage Reference of the Middle Bus. Initial Condition P=0.7p.u., p.f. = 0.85 lag.....	75
4.18	Generator Bus Voltage Response to a 0.04 p.u. Step Increase in the Voltage Reference of the Middle Bus. Initial Condition P=0.7p.u., p.f. = 0.85 lag.....	75

4.19	Generator Angular Speed in Response to a 0.2 p.u. Torque Increase at Different Sampling Intervals. Initial Condition P=0.7p.u., p.f. = 0.85 lag.....	77
4.20	Output of PSS in Response to a 0.2 p.u. Torque Increase at Different Sampling Intervals. Initial Condition P=0.7p.u., p.f. = 0.85 lag.....	77
4.21	Generator Angular Speed in Response to a Three-Phase Short Circuit at a Tie Line Close to the Generator Bus. Initial Condition P=0.7p.u., p.f. = 0.85 lag.....	78
4.22	Voltage at the Middle Bus in Response to a Three-Phase Short Circuit at a Tie Line Close to the Generator Bus. Initial Condition P=0.7p.u., p.f. = 0.85 lag.....	79
4.23	Output of PSS in Response to a Three Phase Short Circuit at a Tie Line Close to the Generator Bus. Initial Condition P=0.7p.u., p.f. = 0.85 lag.....	79
4.24	Output of AVR in Response to a Three Phase Short Circuit at a Tie Line Close to the Generator Bus. Initial Condition P=0.7p.u., p.f. = 0.85 lag.....	80
4.25	Generator Angular Speed in Response to a Three Phase Short Circuit with Successful Reclosure at a Tie Line Close to the Generator Bus. Initial Condition P=0.7p.u., p.f. = 0.85 lag.....	81
4.26	Generator Angular Speed in Response to a Three-Phase Short Circuit with Unsuccessful Reclosure at a Tie Line Close to the Generator Bus. Initial Condition P=0.7p.u., p.f. = 0.85 lag.....	81
4.27	Different PSS Configurations in Response to a 0.2 p.u. Torque Increase. Initial Condition P=0.7p.u., p.f. = 0.85 lag.....	82
4.28	Different PSS Combinations in Response to a 3 Phase Short Circuit Lasting for 0.1s. Initial Condition P=0.7p.u., p.f. = 0.85 lag.....	83
4.29	Enlarged Fig. 4.27. Initial Condition P=0.7p.u., p.f. = 0.85 lag.....	84
4.30	Generator Speed in Response to a Continuous Mechanical Torque Increase at the Rate of 0.001 p.u per Second. Initial Condition P=1.22p.u., p.f. = 0.90 lag.....	85
A.1	AVR and Exciter Model.....	98

LIST OF SYMBOLS AND NOMENCLATURE

$a, b, c,$	design parameters of triangular function
a_g, b_g	parameters of governor
AVR	automatic voltage regulator
ct	center of function
CMAC	cerebella model articulation controller
CPSS	conventional power system stabilizer
$d(k)$	desired value at instant k
dis	disturbance
$e(k)$	tracking error
E	energy function
$f(x)$	nonlinear function
FACTS	Flexible AC Transmission Systems
FPSS	fuzzy logic power system stabilizer
gov	governor output
$g(x)$	nonlinear function
GAVR	generator AVR
GTO	gate turn-off thyristor
GPSS	generator conventional PSS
HVDC	High Voltage Direct Current
i_d	generator d-axis current
i_{kd}	generator d-axis damper winding current
i_q	generator q-axis current
i_{kq}	generator q-axis damper winding current
i_f	generator field current
i_{sd}	SVC d-axis current
i_{sq}	SVC q-axis current
$J(k)$	performance function
k	time index
K_a	gain of SVC AVR
K_A	gain of generator AVR
K_d	generator damping ratio coefficient
K_{pss}	gain of PSS

k_v	design parameter
LMS	least mean square
NERC	North American Electric System Reliability Council
NN	neural network
NNPSS	proposed neural network based PSS
NO PSS	system without PSS
P	real power output of generator
P_e	electrical power of generator
P_m	mechanical power of generator
PE	persistent excitation
PSS	power system stabilizer
p.f.	power factor
p.u.	per unit
r_s	generator armature resistance
$r(k)$	filtered tracking error at time k
r_f	generator field resistance
r_{kd}	generator d-axis damper winding resistance
r_{kq}	generator q-axis damper winding resistance
r_e	transmission line resistance
r_T	resistance of the step up transformer of SVC
RBF	radial basis function
RNN	recurrent neural network
SAVR	SVC AVR
SCPSS	SVC conventional PSS
SVC	static var compensator
STATCOM	static compensation
TCSC	Thyristor Controlled Series Compensator
T_a	time constant of SVC AVR
T_A, T_b, T_c	time constants of generator AVR
T_g	time constant of governor
T_W	washout time constant of PSS
$T_1 \dots T_4$	time constants of CPSS
T_ω	impulse moment of rotor

$u(k)$	control output
UPFC	Unified Power Flow Controller
V	Lyapunov function
V_{AMIN}	AVR command signal lower limit
V_{AMAX}	AVR command signal upper limit
V_{IMIN}	AVR input signal lower limit
V_{IMAX}	AVR input signal upper limit
V_{RMIN}	AVR regulator lower limit
V_{RMAX}	AVR regulator upper limit
V_{OEL}	AVR over excitation limit
V_{UEL}	AVR under excitation limit
V_{STMAX}	PSS output upper limit
V_{STMIN}	PSS output lower limit
\bar{W}_i	weight of neural network
\hat{W}_i	actual weight of neural network
\tilde{W}_i	estimation error of weight of neural network
x	input of neural network
$x_{des}(k)$	desired trajectory
x_d	generator d-axis synchronous reactance
x_{md}	generator d-axis mutual reactance
x_{kd}	generator d-axis damper winding reactance
x_q	generator q-axis synchronous reactance
x_{mq}	generator q-axis mutual reactance
x_{kq}	generator q-axis damper winding reactance
x_f	generator field reactance
x_e	transmission line reactance
x_T	reactance of the step up transformer of SVC
y	output of neural network
α	learning rate
δ	power angle of generator
ω	angular speed of generator
$\Delta\omega$	deviation of generator angular speed
ΔV	first difference of Lyapunov function

$\Phi(x)$	activation function
$\hat{\Phi}(x)$	actual value of $\Phi(x)$
$\tilde{\Phi}(x)$	estimation error of $\Phi(x)$
σ	variance
$\nabla_w J(k)$	instantaneous gradient of performance function
$\lambda_{n-1}, \dots, \lambda_1$	design parameters
λ_d	generator d-axis flux linkage
λ_{kd}	generator d-axis damper winding flux linkage
λ_q	generator q-axis flux linkage
λ_{kq}	generator q-axis damper winding flux linkage
λ_f	generator field flux linkage
$\varepsilon(k)$	error of neural network
β_i	design parameter
ς_i	design parameter
ξ_i	design parameter
Γ_i	design parameter
φ	activation function

CHAPTER 1

INTRODUCTION

1.1 Power System Stability and Oscillations

The electric power system is one of the most complex industrial systems in the world. It is usually comprised of hundreds of different generators, thousands of transmission lines at different voltage levels and millions of customers. As electricity is generated, transmitted and consumed simultaneously, the unique characteristic decides that the system dynamic stability is a very important factor for the security and reliability of a large scale power system.

1.1.1 Bulk Electric Power System and SVC

Modern electric power systems usually interconnect a large amount of power system components and cover vast geographical area. According to the definition of the bulk electric power system prescribed by the North American Electric System Reliability Council (NERC) in 1995, “ The bulk electric system is a term commonly applied to that portion of an electric utility system, which encompasses the electrical generation resources, transmission lines, interconnections with neighboring systems and associated equipment, generally operated at voltages of 100 kV or higher. ”[1].

The advantages of an interconnected power system are:

- Improved stability of the entire system, because a larger system can reduce the

impact of losing a system component (components) and system faults.

- Shared spinning and unspinning generation capability reserve to reduce the total installation of generation capacity.

With the rapid development of the power electronic technology in recent years, new equipment has been introduced in the power systems such as Flexible AC Transmission Systems (FACTS). FACTS including Static Var Compensator (SVC) or Static Compensation (STATCOM), Thyristor Controlled Series Compensator (TCSC), High Voltage Direct Current (HVDC) and Unified Power Flow Controller (UPFC) can provide more flexible and controllable transmission service than traditional AC transmission systems.

Comparing the various FACTS technologies, SVCs have been widely employed in power systems to regulate the system voltage and improve the system stability. SVC has many advantages over traditional reactive power compensators. It is controlled by high voltage Gate Turn-off Thyristors (GTO) and Diodes based on the electronic power converter principles and can continuously adjust the output of the SVC to generate inductive or capacitive reactive power to the power system. Since the output of an SVC is dynamically adjustable, it has the potential to be used to damp power system oscillations similar to the function of a Power System Stabilizer (PSS) employed on generators.

The common configurations of SVCs introduced in [2,3,4,5] include true pulse structures and multilevel cascading converter structures. The true pulse structure relies on zigzag transformers to shift the phase of the output of each group to create the sinusoidal

waveform in the output of the unit and eliminate the third harmonic pollution produced during the energy conversion. Fig 1.1[2] shows the typical true 48-pulse converter structure.

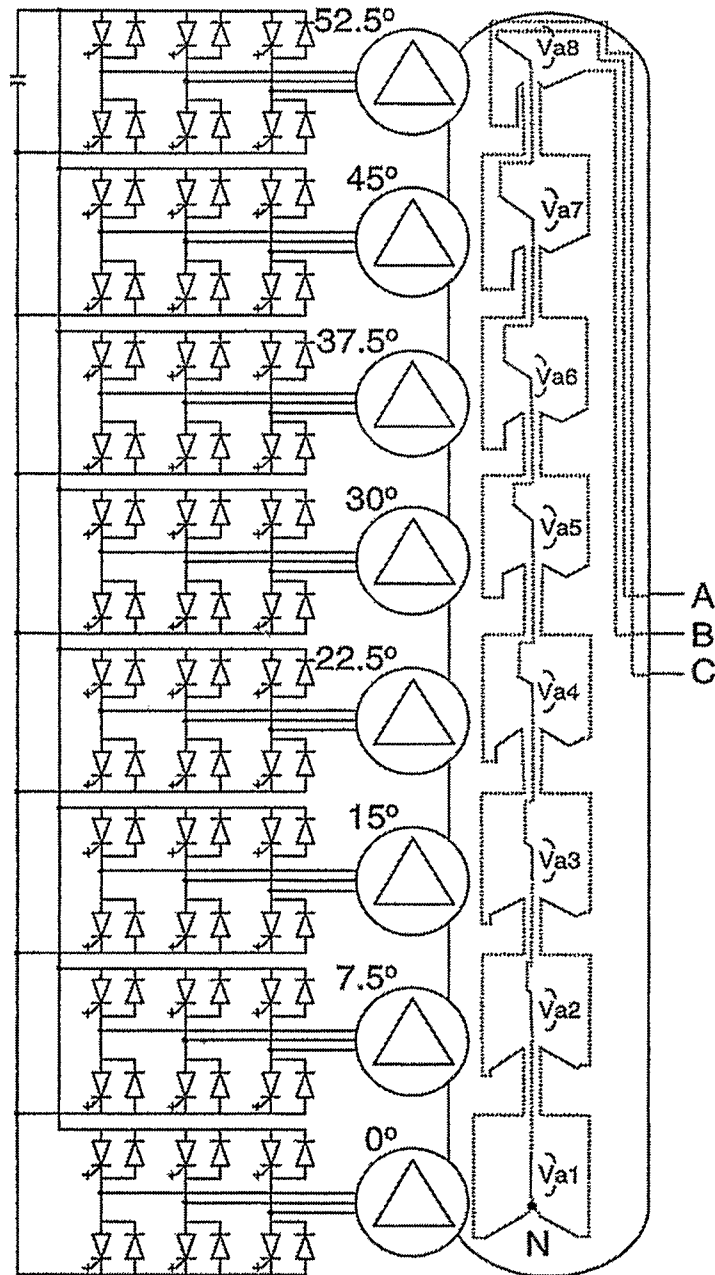


Figure 1.1 Typical True 48-Pulse SVC [2]

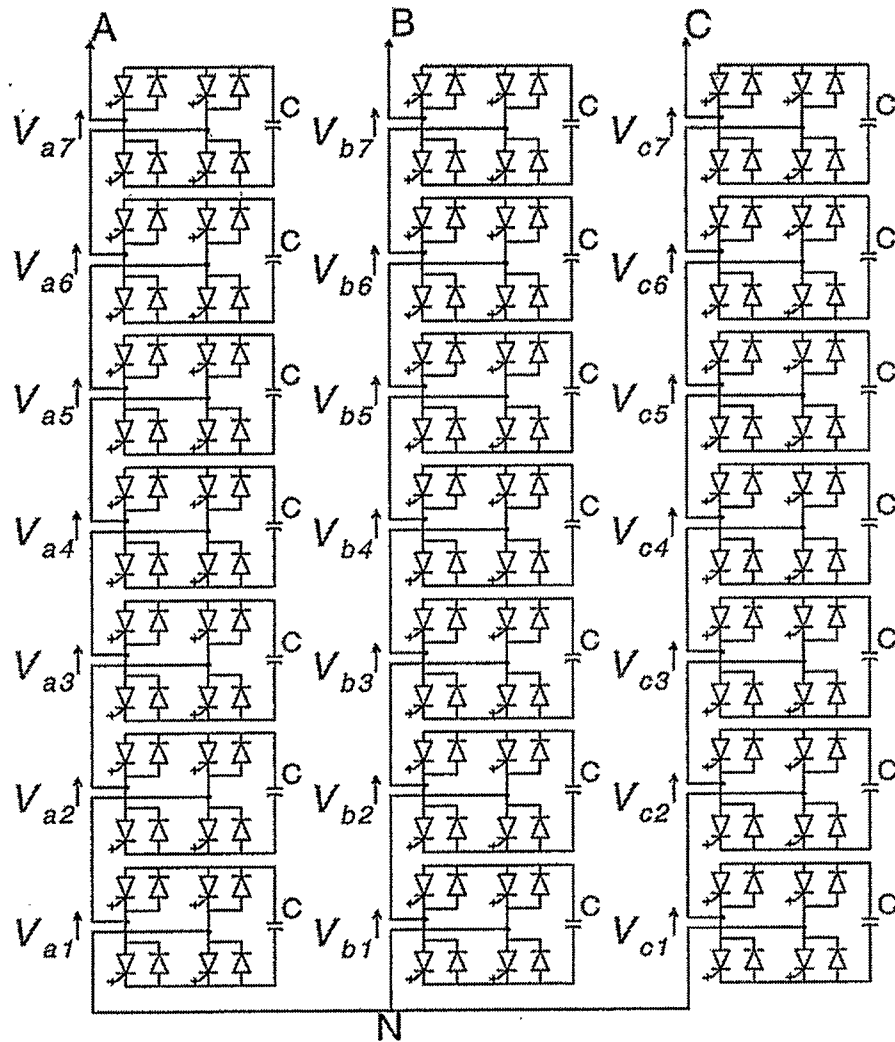


Figure 1.2 Typical 7- Level Cascading Structure of SVC [2]

The multilevel cascading converter structure is more popular these days, as it not only does not need the phase shift transformers but also saves space and investment. The typical seven-level structure is shown in Fig. 1.2 [2]. In practice, the firing angles of GTOs are adjusted dynamically to control the output of the SVC with leading current (capacitive mode) or lagging current (inductive mode) to realize reactive power compensation and voltage control.

In order to directly apply an SVC to a high voltage system bus such as a 500kV or 240kV system bus, the common way is to connect the SVC through a step-up transformer.

1.1.2 Power System Stability

Power system stability [6,7,8] has always been an attractive research topic since the birth of modern electrical power systems. The stability of power systems is generally defined as the ability of all synchronous generators of a system to move from one steady state to another steady state without loss of synchronism when the system is subjected to a disturbance (disturbances) or a contingency (contingencies).

According to characteristics and the nature of disturbances in power systems, power system stability can be classified into two categories, steady state stability and dynamic stability [6,7,8].

- **Steady State Stability** – refers to a system operated around a relatively fixed operating point on which the system is only subjected to small and gradual changes. If the system is able to maintain synchronism after these changes in operating conditions, it is said that it has steady-state stability.
- **Dynamic Stability**- refers to the system transient performance after a system is subjected to a disturbance (disturbances) or a fault (faults). Electric power system disturbance can cause electromechanical oscillations in generators. To analyze the transient stability, the swing equation of synchronous generators is commonly used. This equation is derived from the torque equation of generators in Eq (1.1).

$$T\omega_i \frac{d^2 \delta_i}{dt^2} = P_{mi} - D_i \frac{d}{dt} \delta_i - P_{ei} \quad (1.1)$$

where $T\omega_i$ is the “the impulse moment” of the rotor of the generator i , D_i is the damping coefficient of the generator i , P_{mi} and P_{ei} are the mechanical power and electrical power of the generator i , respectively, and δ_i is the power angle of the generator i [9].

1.1.3 Oscillations in Power Systems

Oscillations in power systems can be divided into two types, local oscillations and interarea oscillations. A local oscillation refers to a single generator oscillating against a large system. Its oscillation frequency is usually around 1-2 Hz. In contrast, the interarea oscillations refer to two areas oscillating against each other. The interarea oscillations are in the range of about 0.1 to 0.7 Hz. The larger system usually has a lower oscillation frequency compared with a smaller system.

In order to make the system stable, the natural damping torque or the damping torque generated by damping controllers like PSSs must decay the magnitude of oscillations. If the magnitude cannot be reduced quickly enough, the generators would be disconnected or the system would collapse partially or even totally.

1.2 Damping Control Strategies and Types of Power System Stabilizers

After many years of research and development in the area of oscillation damping in power systems, many damping methodologies and control algorithms have been developed. Depending on the locations at which the controllers are installed, these methods may be

classified into two categories: damping in transmission paths and damping at generator locations.

1.2.1 Damping at Generator Locations

Utilizing the excitation of generators to directly damp the generator oscillations is the most common way to improve the power system transient stability. Currently, most of the new generating units in North America are equipped with PSSs to improve transient stability and provide effective damping.

The PSS collaborates with the Automatic Voltage Regulator (AVR) to modulate the field excitation of the generator and provide a damping electrical torque on the generator rotor. The input to the generator PSS may use one of the below signals or a combination of them:

- Deviation of angular speed
- Deviation of system frequency
- Deviation of electrical power
- Rotor acceleration

1.2.2 Damping in Transmission Paths

Since FACTS elements in power systems are controlled by power electronic components, which are dynamically adjustable, FACTS equipment is also used for the system oscillation damping.

HVDC and UPFC can directly control the power flow of the transmission paths, so

system oscillations cannot affect the output of these transmission paths. It means that system oscillations can be isolated in one system and will not transfer the system instability to another system connected through the HVDC or UPFC components.

TCSC and SVC also have the ability to damp system oscillations described in [10,11,12,13,14,15]. TCSC usually connects into a transmission line to make the system connections tighter. The controller of a TCSC can adjust the power flow by changing the effective impedance of the transmission line and achieve the objective of damping. An SVC is more like the exciter of a generator. It can affect the system voltage through changing its reactive power output and then produce damping torque in generators.

Although FACTS equipment can perform the damping function, its cost is the main obstacle for its wide application. However, as SVCs are already being used in power systems to compensate for the reactive power and provide voltage support, they have the potential to be used for oscillation damping, and work with generator PSSs to improve the overall power system stability.

1.2.3 Types of Power System Stabilizers

From the above analysis, it can be seen that the principle of SVC PSSs is almost the same as the control design for generator PSSs. So, the design methodologies and algorithms of generator PSSs can be directly used for the SVC controller design. According to the history of PSSs, the development of PSSs experienced three stages, conventional PSS, adaptive PSS and intelligent PSS.

- **Conventional Power System Stabilizer (CPSS)**

CPSS described in [5] is the earliest PSS. It is based on the classical control theory to use a lead-lag compensation network to shift the phase of the output to damp the system oscillations. The transfer function of the commonly used CPSS is:

$$G_{PSS}(s) = K_{PSS} \cdot \frac{sT_w}{(1+sT_w)} \cdot \frac{(1+sT_1)}{(1+sT_2)} \cdot \frac{(1+sT_3)}{(1+sT_4)} \quad (1.2)$$

where K_{PSS} is the gain of the PSS, T_w is the washout time constant. T_1 through T_4 are the time constants used to adjust the phase shift of the output. By appropriately tuning these design parameters, it can produce a desired damping function for the system in a certain operating condition.

However, the power system is highly nonlinear and uncertain, especially the power system parameters change as the system operating conditions change. The fixed parameter CPSS cannot track the variation of the system parameters, so it cannot provide fully effective damping function over a wide range of operating conditions. Hence, CPSSs are easy to design but the damping function is not flexible and effective enough.

In order to solve these problems, extensive research has been carried out to develop new control theories and algorithms to design PSSs such as the adaptive control and intelligent control.

- **Adaptive Power System Stabilizer and Intelligent Power System Stabilizer**

Since 1970s, adaptive control has emerged as an effective control technique and

has greatly boosted the development of PSSs. The adaptive algorithm can update in real time the system parameters used in control computation. This can make the controller track system parameters on-line and tune the control output to provide more effective damping.

Besides adaptive controllers, artificial intelligence based controllers, including fuzzy logic and neural network controllers [16,17,18,19], have been developed in recent years for the design of generator PSSs. These artificial intelligence based control theories can be more adaptive and robust for nonlinear uncertain systems than the adaptive control theory. Controllers based on these theories can universally approach most uncertain nonlinear system through self-learning of parameters. As an alternative to adaptive control, they also have better performance than the CPSS.

The design of a fuzzy controller needs a knowledge base to do fuzzification of the system. The first step is to convert the crisp input signals to the corresponding fuzzy variables. The next step is to create rules for generating the desired fuzzy output according to the input signals and then do the defuzzification to get the desired non-fuzzy output.

The difficulty of a fuzzy control design is to obtain a sufficient base knowledge of the controlled system to make the rules. In contrast, a neural network based control design learns the structure of the system through training procedure. Therefore, in this dissertation a neural network method is developed to design the proposed controller.

1.3 SVC for Oscillation Damping

Considerable effort has been devoted to the control design of SVCs to damp power system oscillations in recent years. Various control techniques and control logics

[10,11,12,13,14,15,18,20] were used to develop SVC controllers. Bulk electrical systems are highly nonlinear, system parameters are more uncertain than that of generators and most system variables cannot be measured locally [10,13,18,20,21]. These factors mean that the control design of SVCs is more challenging.

So far, most SVCs that have already been put in service are only used for voltage control and reactive power compensation. From [10,18,20], SVCs with only voltage control mode do not improve the damping function and even in some certain conditions may have negative impact on system oscillations. Therefore, a supplementary control should be added on the voltage controller to allow the bus voltage to vary. The variation of the voltage should produce an accelerating or decelerating torque on the generator rotors.

This additional control signal can be provided through a voltage loop control or can be added at the output of the voltage control loop. These signals control the firing angles of the GTOs of an SVC in a continuous or discontinuous manner. The discontinuous manner can use “bang-bang” control theory discussed in [10]. The damping results in [10] are not as good as the performance of continuous controllers. Especially, if the system oscillations at different frequencies are combined together, discontinuous control cannot provide robust and effective damping.

Fuzzy and genetic algorithms were also studied in [18,20]. Variable gain fuzzy designs for SVC control have demonstrated improvement in the system damping. In fuzzy design, just like other fuzzy controllers, it is necessary to have a very good understanding of the controlled system. Based on the knowledge of the system, it is possible to fuzzify the input signals, make the rule table and defuzzify the output signals. However, the highly

nonlinear and uncertain parameters in power systems, especially at the middle bus on which the SVC is installed, make full understanding of the controlled system more difficult.

It is seen from a review of the published literature that the simulation model used in verifying the performance of the controllers is a linearized generator model but not the more accurate and complex Park's seventh order model [7] shown in Appendix. Because power systems are highly nonlinear systems, they can only be linearized in a small domain around the current operating point. If the system shifts away from that domain, the linearized model cannot be valid.

1.4 Artificial Neural Network Based PSS

Neural network (NN) controllers have emerged as alternative to the adaptive control for decades. A neural network with sufficient number of hidden layer neurons has theoretical capability to represent most arbitrary mapping. Therefore, NNs can be used in many problems that are not easily handled by traditional analytic approaches.

1.4.1 Neural Networks for Control

Two classes of neural networks, which have received considerable attention in recent years, are

- Multilayer feed-forward neural networks
- Recurrent networks

Multilayer feed-forward networks have proved extremely successful in pattern recognition problems while recurrent networks use the associated memory as well as the

solution of optimization problems [23]. From a system theoretic point of view, both networks can represent non-linear systems.

There are many types of feed-forward neural networks (NN) introduced in the published literature like multilayer perceptron, radial basis function (RBF), cerebella model articulation controller (CMAC), etc.

Control designs with multilayer neural network for both continuous and discrete time systems are treated in [21,22,24,25,26,27,28]. These designs use different networks and activation functions, and all of those algorithms got effective control effect.

1.4.2 Neural Network Based PSS

So far it is very rare that the neural network control theory is used in practice for the SVC controller design, but neural network based generator PSSs have been researched by many scholars [19,23,29,30] since 1990s.

In [19], an adaptive indirect neural network control based PSS was designed. It used two neural networks in the controller. One network is used to work as an identifier to identify the system parameters. Another one is used to realize the system control. The identifier approaches the system parameters at each loop and sends them to the control network to correct the output and reduce the error between the desired output and the actual output. The simulation results show that the controller has better performance than CPSS. However this controller needs two neural networks that means more computational resource are needed to do the computation.

In [30], a Radial Basis Function (RBF) neural network was used to identify system control parameters K_{PSS} , T_1 and T_2 . The transfer function, Eq(1.3), of the controller is the same as that of the CPSS. The inputs of the network are deviations of P real power, Q reactive power and V voltage. The input of the CPSS is the deviation of the generator angular speed $\Delta\omega$. This method is a simple approach for the real-time tuning of the conventional PSS. However, the control is still not a direct neural network control. In addition, in the literature, there is no mention of the performance of the RBF PSS in a major disturbance and no comparison between the CPSS and the RBF PSS is given.

$$V_{PSS}(s) = K_{PSS} \cdot \frac{sT_w}{(1+sT_w)} \cdot \frac{(1+sT_1)^2}{(1+sT_2)^2} \quad (1.3)$$

A neural network to tune the fuzzy logic Power System Stabilizer (FPSS) is used in [23]. The neural network based on the variation of operating conditions of the power system tunes two scaling factors used on the outputs of the network and then introduces them into the FPSS. The neural network was trained off-line and the scaled network outputs are the FPSS inputs. The performance is also much better than the fixed CPSS.

Comparing the results of the above literature, neural networks seem to have considerable advantages on the power system stability study. In this thesis, a hyperbolic tangent activation function is used to construct a multilayer neural network and the direct control theory is used to design a digital controller for an SVC to damp system oscillations.

1.5 Dissertation Objectives

The objective of this thesis is to present a systematic methodology for designing a

neural network based direct control algorithm. It is hoped that this research can make a contribution to the development of an SVC controller based on the neural network direct control theory.

In order to develop the proposed SVC NN controller, the following topics are studied and discussed in the dissertation.

- Investigate the theory and principle of neural networks, different network architectures and the learning algorithms. The determination of the appropriate type and structure for the network used for the proposed SVC controller should be made.
- Develop a framework for the design of an SVC controller based on a multilayer neural network.
- Derive a discrete time direct control algorithm for the proposed SVC controller. The proposed neural network controller has self-learning ability and does not need a separate parameter identifier. On the other hand, it should have a stable performance for different operating conditions. All the parameters can be adaptively updated in real time.
- The performance of the proposed NN controller is tested on a single machine infinite bus system. The results are also compared with that of the conventional design method.

1.6 Contributions of dissertation

The main contributions of this dissertation are summarized below:

- The proposed neural network structure uses a multilayer perceptron structure and the hyperbolic tangent function as the activation function of the network. The inputs of the proposed network employ the deviation of the generator angular speed and its delays. The modified Delta rule and projection algorithm are selected for the updating of the NN weights.
- The filtered direct control theory is applied for the design of the SVC control. Comparing indirect control theories that usually need two neural networks to do identification and control, this theory only uses one network to realize both functions. Therefore, the computational complexity of the controller is greatly reduced.
- The behavior of the proposed NN controller is simulated on a single machine infinite bus system with an SVC at the middle bus. The theoretical simulation results verify that the proposed NN controller has more effective damping function than the conventional PSS design.

1.7 Thesis Organization

In addition to the introductory chapter, this dissertation has four chapters as outlined below.

- An overview of the artificial neural networks is given in Chapter 2. Some fundamentals of different artificial neural networks are presented and compared. According to the comparison of the characteristics of different neural networks for the power system control design, the proposed discrete time NN is selected.
- The nonlinear discrete time direct NN control theory is introduced in Chapter 3. The structure of the multilayer NN SVC controller is proposed and the stability proof of the proposed control algorithm is conducted based on the Lyapunov stability theories.
- Computer simulation results in Chapter 4 verify the effectiveness of the proposed controller on a single machine infinite bus system with an SVC at the middle bus.
- Finally, conclusions and suggestions for future work are presented in Chapter 5.

CHAPTER 2

ARTIFICIAL NEURAL NETWORKS

2.1 Introduction

Artificial Neural Networks (NNs) have seen an explosion of interest over the last two decades. They are being successfully applied across an extraordinary range of problem domains especially in the area of intelligent control. This sweeping success of neural networks for control can be attributed to a few key factors.

- **Powerful Modelling Ability:** Neural networks are very sophisticated modeling techniques capable of modeling extremely complex functions. In particular, neural networks can approach most uncertain non-linear dynamic systems. For many years linear modeling has been the commonly used technique in most modeling domains since linear models have well-known optimization strategies. However, in some applications the linear approximation is not always valid. For instance power systems can be linearized effectively only in a very small domain around the current operating point. So using the linear theory to design controllers for power systems meets many problems such as having different performance in a wide range of operating conditions. Therefore, using neural networks is a very good choice to model non-linear power systems with large numbers of variables.
- **Ease of Implementation:** Neural networks approach the nonlinear system by using a certain learning algorithm in an on-line or off-line environment. Although the user does need to have some knowledge of how to select an appropriate neural network

and how to select an effective and efficient learning algorithm, it is not necessary for users to actually reconstruct the plant structure in the NN. The network can learn its structure through the learning process.

In this chapter, the structures of neurons and networks are reviewed. Several types of neural networks, learning algorithms and their applications are discussed. Based on the comparison of the structures and algorithms, the proposed neural network is chosen.

2.2 Neuron Model

Any complex neural network is built up of simple components - neurons. Typically, a neuron in a network has more than one input. A neuron with n inputs can be represented as a structure shown in Fig 2.1.

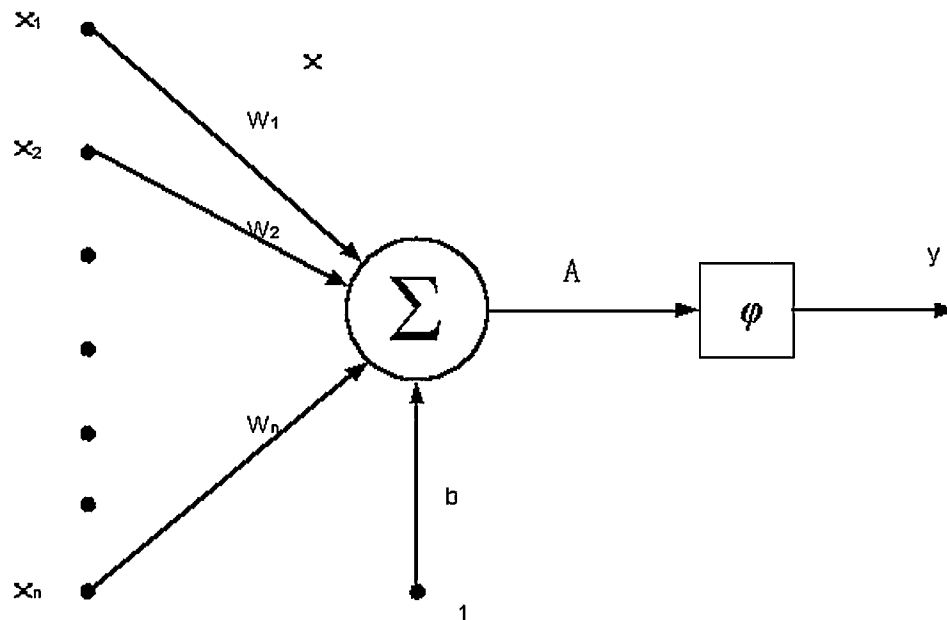


Figure 2.1 Structure of Neuron with Multiple Inputs

In Fig 2.1, $\mathbf{W} = [W_1 \ W_2 \ \dots \ W_n]^T$ is the scalar weight vector of the input vector $\mathbf{x} = [x_1 \ x_2 \ \dots \ x_n]^T$. A standard neuron has a bias b , which is usually neglected in practice. The node with Σ is the adder, which sums all the products of each input and corresponding weight in Eq (2.1).

$$A = W_1x_1 + W_2x_2 + \dots + W_nx_n = \mathbf{W}^T \mathbf{x} \quad (2.1)$$

ϕ is the activation function of the neuron. The activation is a function used to transform the activation level of a neuron into an output signal. Typically, activation functions have a "saturating" effect. Usually the output of the activation function is normalized in a closed interval $[0,1]$ or alternatively $[-1,1]$.

Many types of activation functions are used in the literature. Only a few of these are used by default; the others are available for customization. The commonly used activation functions are given below:

- **Threshold Function 1:** It refers to a step like simple function and but is non differentiable. Its rule is shown in Eq (2.2).

$$y = \begin{cases} 1 & \text{if } x > 0 \\ 0 & \text{otherwise} \end{cases} \quad (2.2)$$

- **Threshold Function 2:** It also refers to a simple and non differentiable step like function Eq (2.3). The difference between the thresholds 1 and 2 is that the output of threshold 2 can be negative or positive.

$$y = \begin{cases} 1 & \text{if } x > 0 \\ -1 & \text{otherwise} \end{cases} \quad (2.3)$$

- **Saturated Linear Function:** It is also called piecewise linear and differentiable function shown in Eq. (2.4).

$$y = \begin{cases} 1 & \text{if } x > 1 \\ x & \text{if } -1 \leq x \leq 1 \\ -1 & \text{if } x < -1 \end{cases} \quad (2.4)$$

- **Sigmoid Function:** It is positive and differentiable function shown in Eq. (2.5).

$$y = \frac{1}{1 + e^{-x}} \quad (2.5)$$

- **Gaussian Function:** It is a differentiable function shown in Eq. (2.6). σ is the variance of the function.

$$y = e^{-x^2/\sigma^2} \quad (2.6)$$

- **Triangular Function:** It is a differentiable function shown in Eq (2.7). a , b and c are the design parameters.

$$y = \begin{cases} 1 & \text{if } a = -\infty \\ \frac{x-a}{b-a} & \text{if } a \leq x \leq b \\ \frac{c-x}{c-b} & \text{if } b \leq x \leq c \\ 1 & \text{if } c = \infty \\ 0 & \text{otherwise} \end{cases} \quad (2.7)$$

- **Hyperbolic Tangent Function:** It is a differentiable function shown in Eq. (2.8) and its characteristic is given in Fig (2.2).

$$y = \frac{e^x - e^{-x}}{e^x + e^{-x}} \quad (2.8)$$

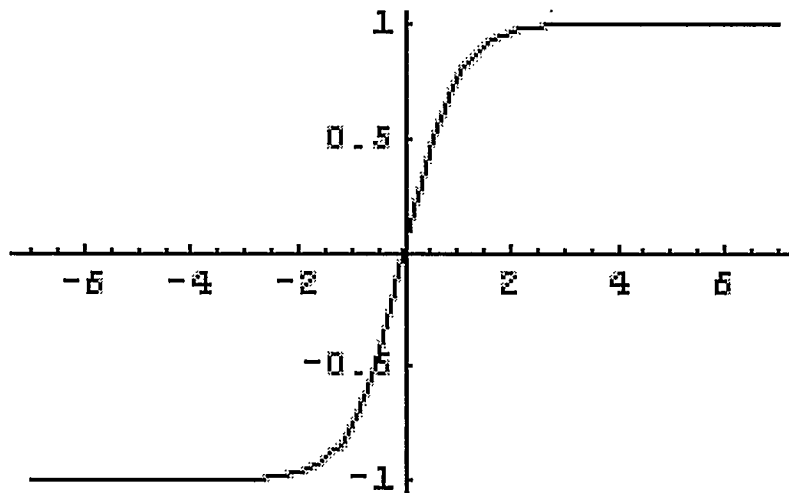


Figure 2.2 Hyperbolic Tangent Function

Among the above activation functions, sigmoid, hyperbolic tangent and gaussian are used more commonly in the multilayer structures. Triangular and rectangular functions were originally used in the fuzzy logic algorithm and have the advantage of computational efficiency. In recent years, these two functions are also used to construct CMAC networks. In order to approach high nonlinear systems, CMAC networks usually have to use tens to a hundred layers.

By comparing the characteristics of the activation functions, the hyperbolic tangent function is more typical and common. Therefore, it is chosen for the proposed network.

After putting all the components of a neuron together, Eq. (2.9) can be used to represent the whole neuron.

$$y = \varphi(\mathbf{W}^T \mathbf{x}) \quad (2.9)$$

2.3 Architecture of Neural Networks

Neurons can be constructed as a layer or a network. Using different network structures and activation functions yields different network behaviour. According to [22, 24,25,27,28,31,32,33], neural networks can be divided into several categories.

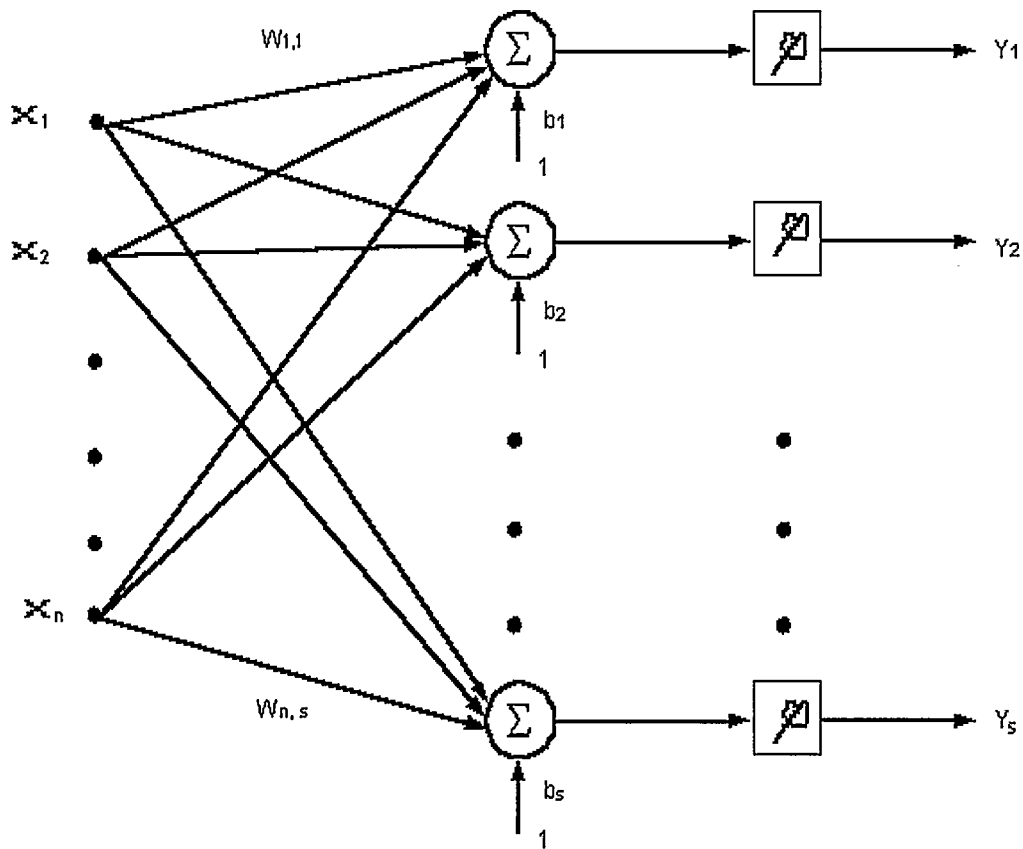


Figure 2.3 Layer with s Neurons

2.3.1 Single Layer Structure

A single layer structure that has s neurons, n inputs and s outputs is shown in Fig. 2.3. Each of the inputs is connected to each of the neurons; hence, the weight matrix is an n by s matrix. The dimensions of the input vector \mathbf{x} and the output vector \mathbf{y} are n by 1 and s by 1, respectively. Therefore, the whole layer can be denoted the same as Eq (2.9), only change the variables \mathbf{y} , \mathbf{x} and \mathbf{W} to vectors and matrix, respectively.

However, a single layer perceptron structure, no matter how many neurons it has or what the kind of activation function is chosen, can only model a linear function. It cannot fully approach a complex nonlinear system. The common way of approaching a nonlinear system is to use a multilayer structure.

2.3.2 Multilayer Perceptron

A multilayer perceptron neural network [21,33] is constructed through putting several single layers together and making the outputs of one layer to be the inputs of another layer. This structure actually is a first-order basis function. The net value is a linear combination of the inputs. Theoretically, this structure belongs to static structure because it only uses the present inputs to decide the current outputs.

However, in the discrete time control design extra delayed signals can be added to cooperate with the current inputs to reinforce the memory of the past of the network. This method is easy to implement and efficient. Fig. 2.4 is a typical three-layer NN structure.

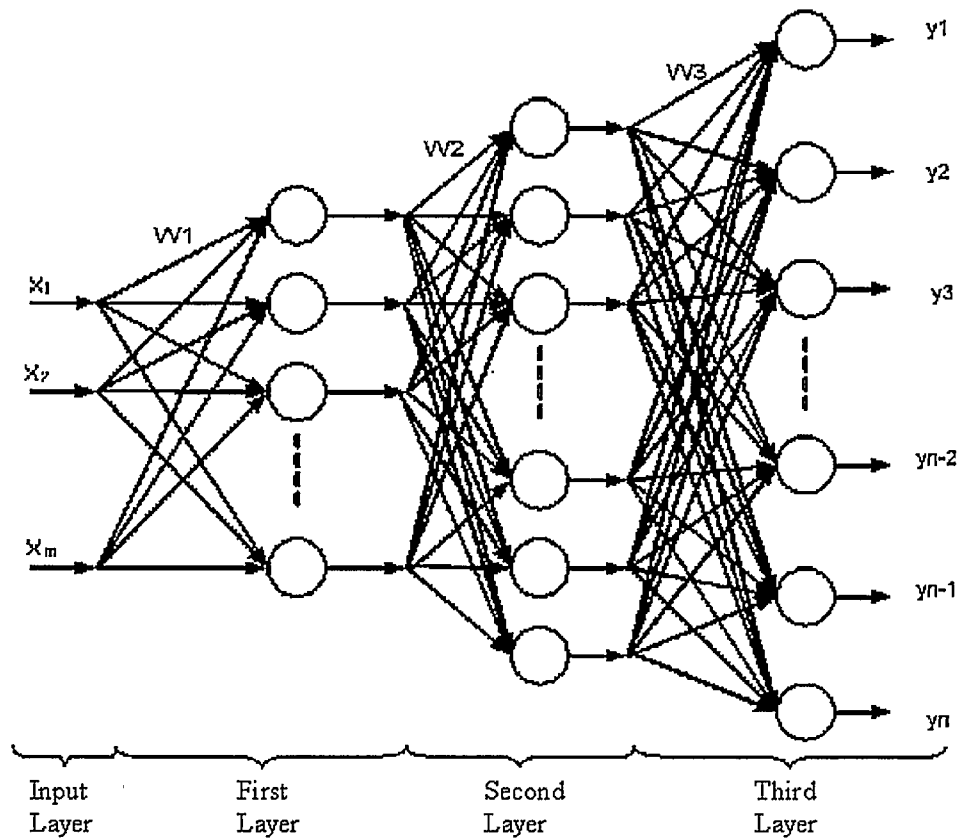


Figure 2.4 Typical Three Layer Neural Network

2.3.3 Other Neural Network Structures

Besides the typical multilayer structure, many other neural network structures are also used in the control design. A brief introduction and comparison of these structures is given in the section.

2.3.3.1 Radial Basis Function

Radial-basis function (RBF) is a hypersphere-type function. This architecture involves a second-order (nonlinear) basis function. The net value represents the distance to

a reference pattern. An RBF NN [30,33] is equivalent to a multilayer feed forward network. It has an input layer, one hidden layer and one output linear layer. In the hidden layer, each node calculates the activation function $\Phi(x)$. In traditional RBF networks, $\Phi(x)$ is usually the Gaussian function given in Eq. (2.10),

$$\Phi(x) = e^{-\|x-ct_j\|^2/\sigma^2} \quad (2.10)$$

where ct_j is the centre of the function. The entire network is described in Eq (2.12).

$$y = W^T \Phi(x) \quad (2.11)$$

The structure of RBF networks is simple and clear. For complex systems, the number of hidden layer nodes can be increased to reflect the increased complexity. But the modified Gaussian function involves more mathematical calculations than other activation functions. Therefore, RBF NN needs more resource to do the computation than the multilayer perceptron structure.

2.3.3.2 Cerebella Model Articulation Controller (CMAC)

CMAC network is a perceptron like associative memory that performs nonlinear function mapping over a region of the function space [17,35,44]. It usually uses triangular or rectangular functions as the activation function. CMAC has the advantage of learning fast and the ability to construct a large network.

A multi-input multi-output CMAC with output $y(x): R^m \rightarrow R^n$ is a nonlinear mapping defined as Eq (2.12).

$$y_i(x) = \sum_{j_m=1}^{N_m} \cdots \sum_{j_1=1}^{N_1} w_{i,(j_1,\dots,j_m)} \Phi_{j_1,\dots,j_m}(x) \quad (2.12)$$

where $i = 1, 2, \dots, n$ and $N_m = 1, 2, \dots, n$.

CMAC has the advantage in the computational efficiency and it usually needs tens to a hundred layers to approach a nonlinear system. The structure means that the network has thousands to hundreds of thousands weights. Therefore, the hardware of the controller requires extensive storage space.

2.3.3.3 Recurrent Architecture

Recurrent neural network (RNN) [8] does not only utilize the input signals but also uses the outputs of the network itself. The configuration of a recurrent network is shown in Fig. 2.5. The advantage of the recurrent configuration is that the network has memory provided by the past inputs. Therefore, it is more dynamic than the feed forward structure.

However, if a recurrent neural network has too many hidden nodes and does too much iteration on a data set, the network might start to memorize the input data. Therefore, the network might have 'learned' the data set, but will have poor results when it is presented with a totally new data set to evaluate.

Another drawback of RNNs is that RNN is more difficult to train than a NN with a multilayer perceptron structure. As the outputs have impacts on the system computation, the training algorithm could become unstable; the error between the target and the output of the RNN may not be monotonically decreasing; the gradient computation is more

complicated; there may be long-range dependencies and the convergence times may be long.

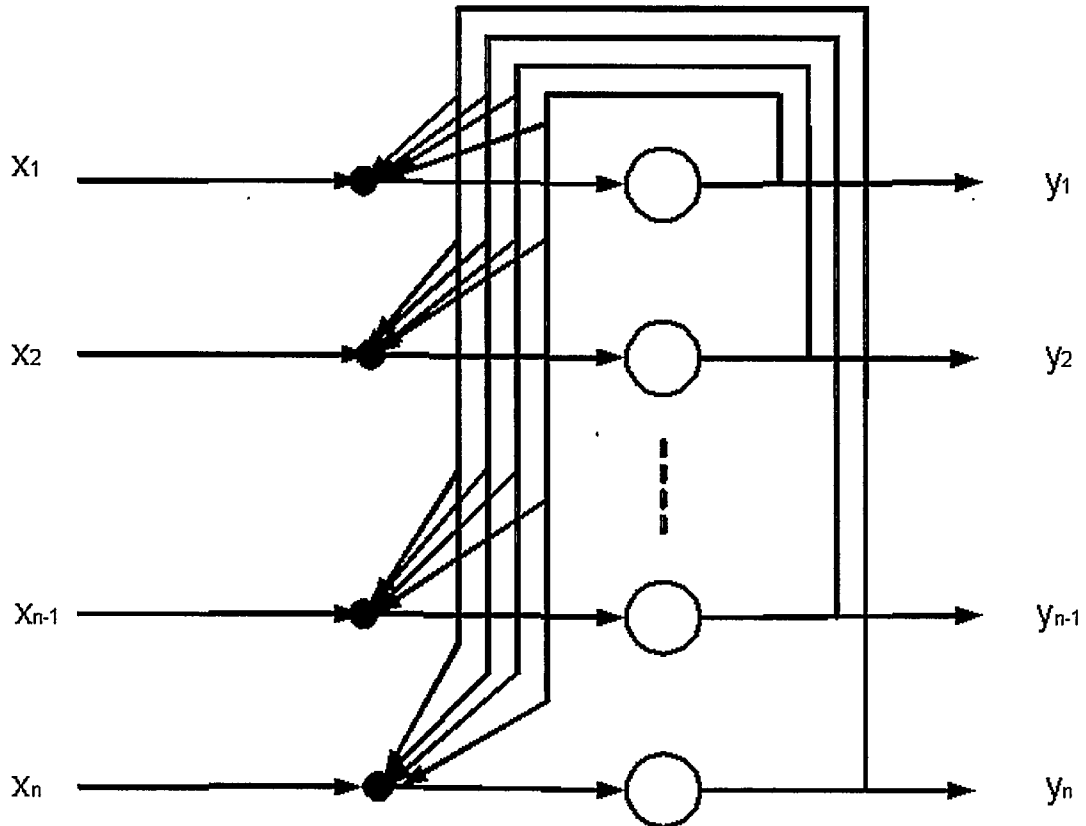


Figure 2.5 Recurrent Architecture

2.4 Learning Algorithms

According to the different structures of networks, an appropriate learning algorithm should be selected to improve the learning rate and keep the convergence of the system [45,46,47]. All learning methods can be classified as

- **Supervised Learning:** It refers to a process that incorporates an external teacher and/or global information. Examples of supervised learning algorithms are error

correction learning (Delta Rule), reinforcement learning, stochastic learning and internal control. Its structure is shown in Fig (2.6).

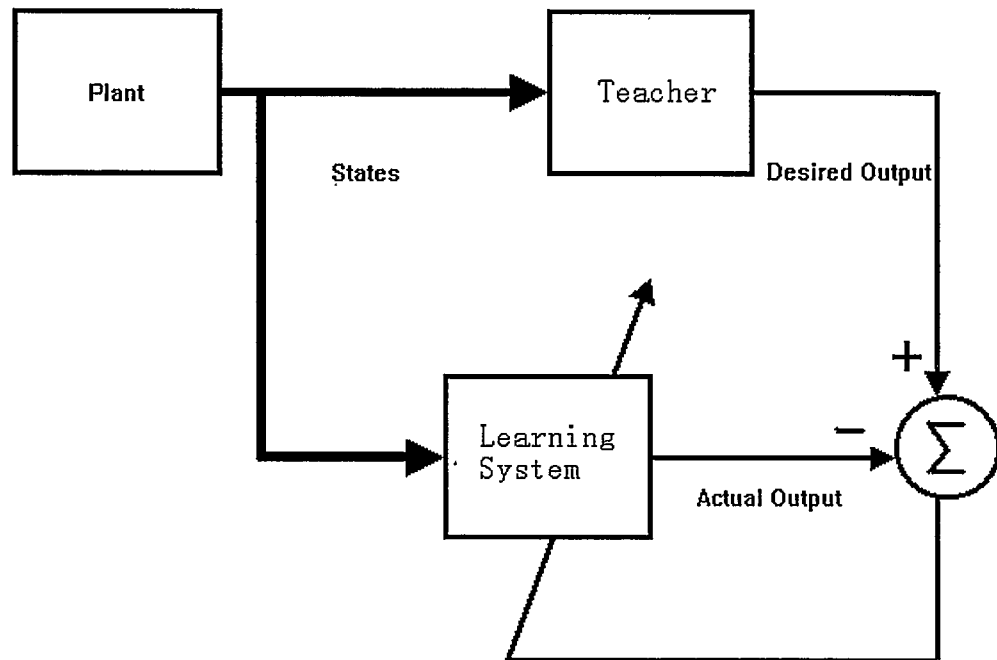


Figure 2.6 Supervised Learning

- **Unsupervised Learning.** It, also referred as self-organization, is a process that incorporates no external teacher and relies upon only local information and internal control.

There are a variety of learning laws and algorithms that are in common use to update the connection weights. Most of these algorithms are originated from the well-known and oldest learning law, Hebbian Rule.

2.4.1 Hebbian Learning Rule

Hebbian learning algorithm [36] is the first and the best known learning rule introduced by Donald Hebb. This basic rule is: If a neuron receives an input from another neuron, and if both are highly active (mathematically have the same sign), the weight between the neurons should be strengthened. Hebbian learning adjusts the network's weights such that its output reflects its familiarity with an input. On average the more probable an input, the larger the output will become. Unfortunately, plain Hebbian learning law continually strengthens its weights without bound unless the input data is properly normalized. There are only a few applications for the plain Hebbian learning. However, almost every unsupervised and competitive learning procedure can be considered Hebbian in nature.

Mathematical description of the Hebbian learning algorithm is given in Eqs (2.13) and (2.14).

$$\Delta W_{ij}(k) = \alpha y_j(k) x_i(k) \quad (2.13)$$

$$W_{i,j}(k+1) = W_{i,j}(k) + \Delta W_{ij}(k) \quad (2.14)$$

where x_i and y_j are the outputs of the neuron i and j , respectively, and α is the learning rate with a positive value between 0 to 1.

2.4.2 Delta Rule

The Delta rule [37,38] is a further variation of the Hebb's Rule, and it is one of the most commonly used algorithms for the weight updating of NNs. This rule is based on the idea of continuously modifying the strengths of the input connections to reduce the

difference (the delta) between the desired output value and the actual output of a neuron [37].

Delta rule changes the connection weights in a way that minimizes the mean squared error of the network. The error is back propagated into previous layers one layer at a time. The process of back-propagating the network errors continues until the first layer is reached. The network type called feed-forward, back-propagation derives its name from this method of computing the error term. This rule is also referred to as the Widrow-Hoff Learning Rule and the Least Mean Square (LMS) Learning rule.

The error between the desired output and the actual output is the Delta in Eq (2.15), where $des(k)$ is the desired signal at time k and $y(k)$ is the actual output at instant time k .

$$e(k) = des(k) - y(k) \quad (2.15)$$

The Lyapunov function (energy function) can be defined as:

$$E(k) = \frac{1}{2} \sum_i e_i^2(k) \quad (2.16)$$

The update function of the weight $W_{i,j}$ can use the geometrical method to get Eq (2.17), where α is the learning rate with a value between 0 and 1 and $x_j(k)$ is the input of the neuron.

$$W_{i,j}(k+1) = W_{i,j}(k) + \alpha e_i(k) x_j(k) \quad (2.17)$$

2.5 Back Propagation Algorithm

The back propagation algorithm [8,36,38,39,40,41] is a powerful and widely known algorithm for training multilayer neural networks to associate patterns. It is used for the learning of multilayer neural networks, which have one input layer, one output layer and at least one hidden layer. This algorithm is effective for the system approximation by reducing the energy function $E(k)$, Eq (2.18), of the output corresponding to the desired plant output.

$$E(k) = \frac{1}{2} (\hat{y} - y)^2 \quad (2.18)$$

where \hat{y} and y are the output of NN and the plant, respectively.

The weight update function consists of three equations shown in Eq (2.19) through (2.21). Then substitute them back to Eq (2.14) to get the new weights.

$$\Delta W_{ji}(k) = \alpha \varphi_j \hat{y}_i \quad (2.19)$$

$$\varphi_i(k) = \hat{y}_i (1 - \hat{y}_i) (y_j - \hat{y}_j) \quad \text{Output layer} \quad (2.20)$$

$$\varphi_i(k) = \hat{y}_i (1 - \hat{y}_i) \sum_m \Phi_m W_{mj} \quad \text{Hidden layer} \quad (2.21)$$

2.6 Selection of Neural Network for SVC Controller

Comparing the above networks and learning algorithms, the multilayer perceptron structure with hyperbolic tangent function as the activation function is selected for the proposed NN and the modified Delta rule is used to update the weights of the NN.

Several different size neural networks were selected to do the comparison of the effectiveness and computational cost in the simulation system. At the beginning, a very large size network with four layers was chosen and put into the proposed controller in the simulation system to make it work. Then the number of layers and the number of neurons in each layer were gradually reduced and tested until the system performance cannot be sustained or deteriorated obviously. According to the comparison of the results, the size of the network with the acceptable performance and the relative small cost can be selected.

The proposed NN shown in Fig. 2.7 has three layers and an input layer. There are 10 neurons in the first and second layers. The hyperbolic tangent function was chosen as the activation functions for both the first layer and the second layer choose. In the third layer, the output layer, the activation function is selected as a linear function. \mathbf{W}_1 , \mathbf{W}_2 and \mathbf{W}_3 are weight matrix and vector corresponding to the hidden layers and the output layer, respectively. \mathbf{W}_1 is a 3 by 10 matrix, \mathbf{W}_2 is a 10 by 10 matrix and \mathbf{W}_3 is a 10 by 1 vector.

For given $input \in R$, the proposed three-layer NN has a net output with mathematical relationship in Eq (2.22),

$$\hat{y} = w_3^T \Phi(w_2^T \Phi(w_1^T Input)) \quad (2.22)$$

where $\Phi(\cdot)$ is the hyperbolic tangent function.

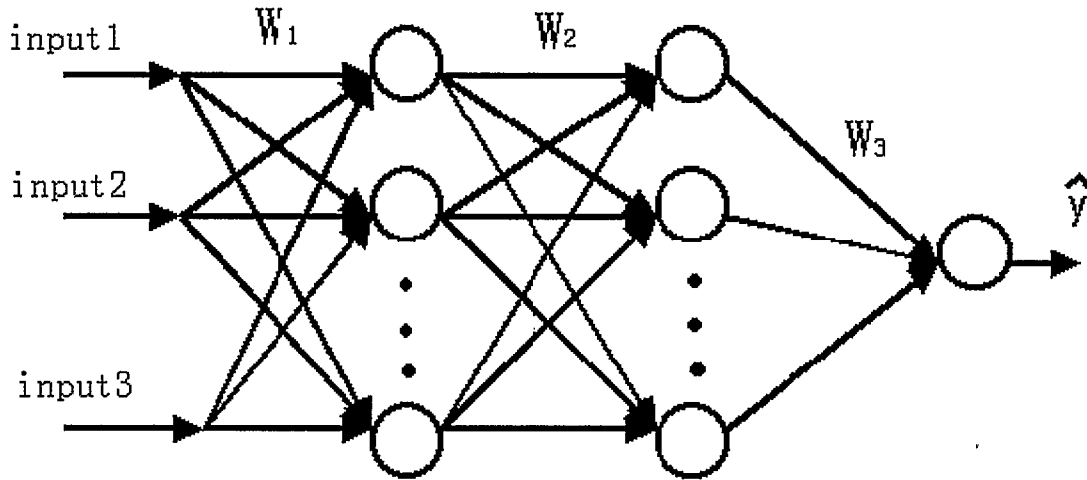


Figure 2.7 Architecture of the Proposed Neural Network

2.7 Summary

In this chapter, some structures and algorithms of neural networks are introduced to do selection and comparison. The fundamental element of a neural network is a neuron, which includes a set of weights, an adder and an activation function. Through the discussion of different functions, the hyperbolic tangent function is a typical and wide used activation function, which is also selected for the proposed NN.

Multilayer structure should be used for the proposed NN as a single layer NN is not sufficient to approach the complexity of nonlinear systems. Different feed-forward architectures and recurrent architecture are also introduced in the chapter. After comparing the characteristics of different network structures, the multilayer perceptron structure that is easy to construct and simple in computation is selected for the proposed NN.

The Delta rule is the most commonly used algorithm for the training of neural networks and back-propagation algorithm is employed for the updating of the weights of a multilayer NN. In this dissertation, these algorithms are also the fundamental algorithms for the proposed NN. Based on a comparison of the network performance the size of the proposed NN is optimized and determined.

CHAPTER 3

NEURAL NETWORK BASED CONTROL DESIGN

3.1 Introduction

Power systems are highly nonlinear, large scale, dynamic, continuous and time variant parameter systems. The nonlinearity and uncertainty of the power system makes it difficult to control. In the earlier phase of the research on PSSs, the power system was treated as a linearized system and linear control theories were used to design power system stabilizers. Because of the uncertainty and nonlinearity of power systems, linear solutions cannot fully satisfy the system requirements.

Many control efforts have been devoted to the development of PSS with nonlinear control theories such as: adaptive control [10], fuzzy logic control [16,18,20] and neural network based control [8,19,30]. From the discussion in Chapter 2, neural networks have the potential to approach most nonlinear and uncertain systems. Therefore, neural network technique has the advantages to be used in PSS design.

Comparing applications of neural networks in PSSs, using neural networks to realize SVC controls is rare in the published literature. In generator PSS design, various neural networks and control algorithms are used. The indirect control method, that includes two networks, one as a system identifier and another as a neuro-controller, is used in [8] and [19]. A neural network to identify system parameters and then self-tune a conventional PSS

is described in [30]. These PSS controls can be designed on both the discrete time model and continuous time model.

In this chapter, several neural network based control methods are introduced. A comparison of these methods is conducted. Finally, the proposed control design method, the multilayer discrete time neural network based controller, is presented and proved. It only has one network and uses the direct control theory.

3.2 Plant Model

Modelling the objective system is a very important step to design an effective and stable control algorithm. According to the different characteristics of the objective system, the plant model can be classified as two categories, continuous time model or discrete time model.

3.2.1 Continuous System Model

An n th order nonlinear dynamic system [32] can be described in the following form, Eq (3.1), or equivalent form, Eq (3.2).

$$\begin{aligned}
 \dot{x}_1 &= x_2 \\
 \dot{x}_2 &= x_3 \\
 &\dots \\
 \dot{x}_n &= f(x) + g(x)u + dis \\
 y &= x_1
 \end{aligned} \tag{3.1}$$

$$\begin{aligned} x^{(n)} &= f(x, \dot{x}, \dots, x^{(n-1)}) + g(x, \dot{x}, \dots, x^{(n-1)})u + dis \\ y &= x \end{aligned} \quad (3.2)$$

where f and g are unknown but bounded functions, $u \in R$ and $y \in R$ are the control input and output of the system, respectively, and dis is an external bounded disturbance.

By converting the system to the state space form, the above system can be written as:

$$\begin{aligned} \dot{x} &= Ax + B(f(x) + g(x)u + dis) \\ y &= C^T x \end{aligned} \quad (3.3)$$

where

$$A = \begin{bmatrix} 0 & 1 & 0 & \dots & 0 \\ 0 & 0 & 1 & \dots & 0 \\ \dots & \dots & \dots & \dots & \dots \\ 0 & 0 & 0 & \dots & 1 \\ 0 & 0 & 0 & \dots & 0 \end{bmatrix}, \quad B = \begin{bmatrix} 0 \\ 0 \\ \vdots \\ 0 \\ 1 \end{bmatrix}, \quad C = \begin{bmatrix} 1 \\ 0 \\ \vdots \\ 0 \\ 0 \end{bmatrix}$$

and $x = [x, \dot{x}, \dots, x^{(n-1)}]^T = [x_1, x_2, \dots, x_n]^T \in R^n$ is a vector of states.

3.2.2 Discrete Time System Model

Corresponding to the continuous system the m th-order discrete time nonlinear system [22,26] can be represented as Eq (3.4).

$$\begin{aligned} x_1(k+1) &= x_2(k) \\ x_2(k+1) &= x_3(k) \\ &\dots \\ x_n(k+1) &= f(x(k)) + g(x(k))u(k) + dis(k) \end{aligned} \quad (3.4)$$

where $x(k) = [x_1(k), x_2(k), \dots, x_n(k)]^T$ with $x_i(k) \in R^m : i = 1, 2, \dots, n$, $u(k) \in R^m$ and $dis(k) \in R^m$ denotes a disturbance vector acting on the system at time k . In addition, $f : R^m \rightarrow R^m$ and $g : R^{m \times m} \rightarrow R^{m \times m}$ are unknown smooth functions. Two assumptions are chosen as $\|dis(k)\| \leq dis_{Max}$ and $g_{min} \leq \|g(x(k))\| \leq g_{max} \quad \forall x$.

3.3 Control Applications

Many control theories have been developed in recent years. From the published literature, the following control theories may be used to design the neural network based PSSs and SVC controllers.

3.3.1 Model Reference Adaptive Inverse Control

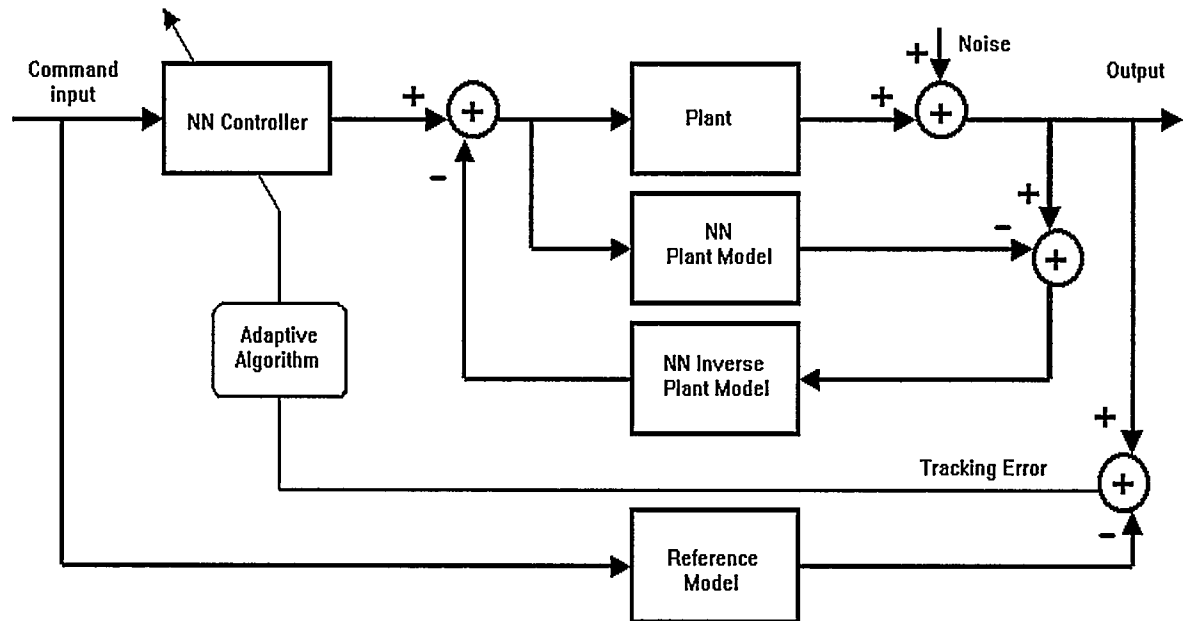


Figure 3.1 Structure of the Adaptive Inverse Control System

The adaptive inverse control Fig 3.1 is proposed in [21,42]. The adaptive algorithm receives the error between the plant output and the reference model output. The controller parameters are updated to minimize the tracking error. The basic model reference adaptive control approach may be affected by the noise generated by the sensor. In order to cancel the noise, another NN plant model can be added as an alternative.

3.3.2 Model Reference Adaptive Control

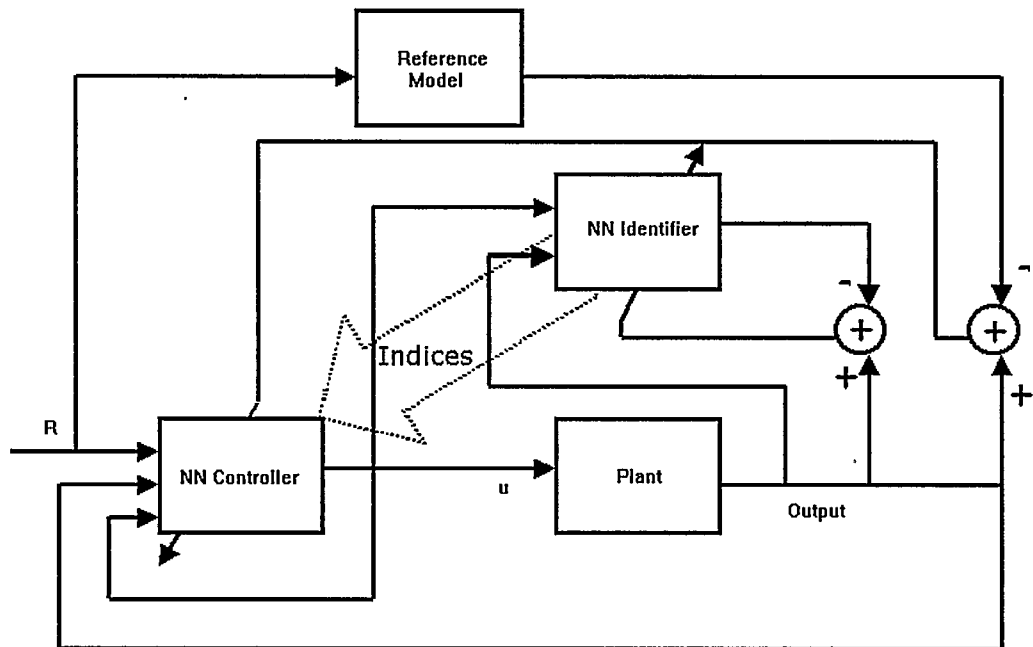


Figure 3.2 Architecture of the Model Reference Controller

The model reference control architecture [8,21,43] shown in Fig. 3.2 has been widely used in the system control design. As the inverse control technique, this algorithm uses two sets of networks: a controller network and a model network. Many on-line or off-

line algorithms can be employed to train the model network. In each iteration, the identifier will transmit the identified system parameter indices to the NN controller. The controller will adaptively force the plant output to track the output of the reference model.

3.3.3 Model Predictive Control

The structure of the Model Predictive Control [8,44] is shown in Fig. 3.3. The algorithm optimizes the plant response over a specified time horizon. This architecture requires a neural network plant model, a neural network controller with a performance function to evaluate system response and an optimization procedure to select the best control input.

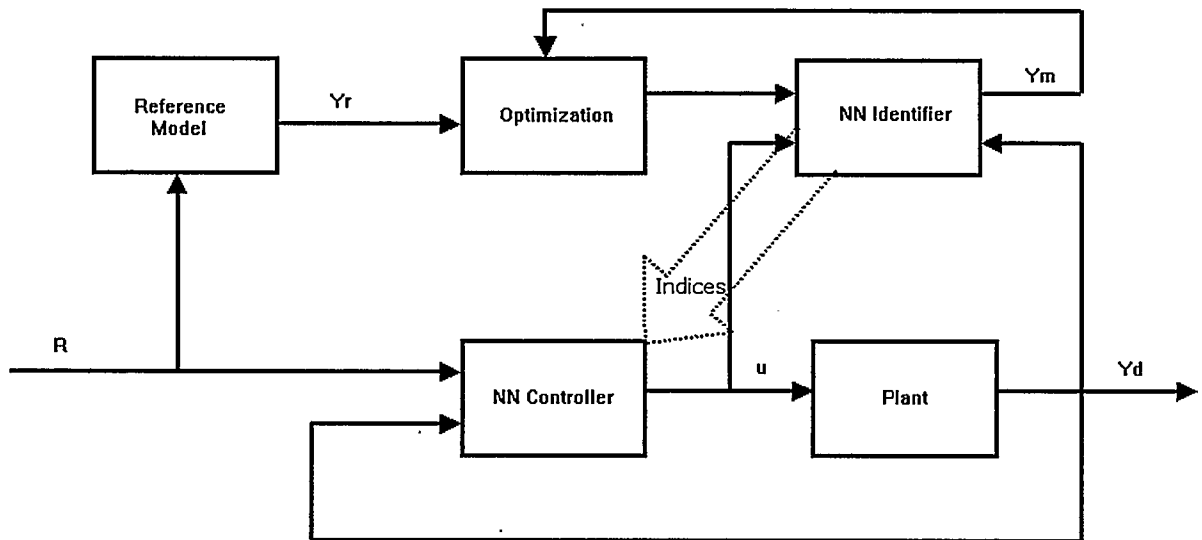


Figure 3.3 Model Predictive Control

The control performance function is a quadratic criterion, J , subject to the constraints of the plant.

$$J = \sum_{j=N_1}^{N_2} [y_r(K+j) - y_m(K+j)]^2 + \sum_{j=1}^{N_2} \lambda_j [u(k+j-1) - u(k+j-2)]^2 \quad (3.5)$$

where the constants N_1 and N_2 define the horizons over which the tracking error and control increments are considered. The advantage of the algorithm is that it does not need a training period.

3.3.4 Neural Network Based Indirect Control Design

This indirect control theory [8,19] also needs two networks but without the reference model. The first network functions as a neural identifier, which will track the dynamic activity of the non-linear plant and will be a channel for the back propagation to train the controller network. The second one acts as a neural controller to provide proper control signals to the plant. The controller structure is similar to the model reference controller. The structure of indirect control is shown in Fig. 3.4.

The cost function of the neuro-identifier is Eq (3.6) and the updating function of its weights is Eq (3.7).

$$J(k) = \frac{1}{2} [\hat{y}(k) - y(k)]^2 \quad (3.6)$$

$$W(k+1) = W(k) - \alpha \nabla_w J(k) \quad (3.7)$$

where $W(k)$ is the weight of the identifier at time k , α is the positive learning rate and $\nabla_w J(k)$ is the instantaneous gradient of J . For the neuro-controller, the performance index is Eq (3.8). Its weight-updating algorithm is the same as Eq (3.7).

$$J(k) = \frac{1}{2} [\hat{y}(k) - R]^2 \quad (3.8)$$

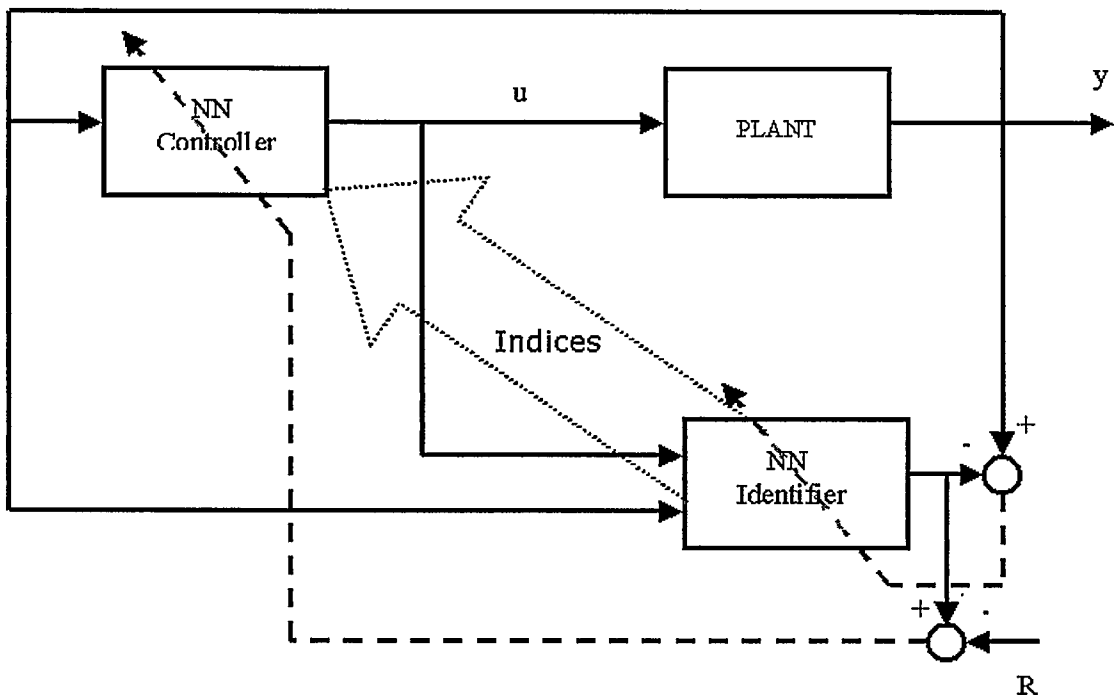


Figure 3.4 Neural Network Indirect Control

3.4 Proposed Multilayer Neural Network Based Direct Control Design

Comparing the control approaches discussed above, all these approaches need two neural networks as the system identifier and the controller. Two networks mean the controller needs more computational resources. In recent years the neural network based

direct control theory has emerged as an effective and efficient control design algorithm that only needs one neural network for both parameter identification and control. Since it only uses one network, the computation burden of the entire controller is greatly reduced.

Therefore, the direct control theory described in [22,26,32] is selected to design the proposed SVC controller. Besides, the projection algorithm is used to improve the network learning speed compared to the above control theories that use the fixed learning rate. The passivity system design guarantees the entire closed loop system stability.

3.4.1 Tracking Problem

A given nonlinear system model described in Eq (3.4) may be changed to a tracking problem. This tracking problem can be described as: for a given desired trajectory in terms of $x_{ndes}(k)$ and its delayed values, a control input $u(k)$ can be found so that the system tracks the desired bounded error in the presence of disturbances while all states and controls remain bounded [22]. The following assumptions are employed to keep the system valid.

- $g_{\min} \leq \|g(x(k))\| \leq g_{\max}$, $g_{\min}, g_{\max} > 0$.
- The desired trajectory and its delayed values are measurable and bounded.

For each desired trajectory $x_{ndes}(k)$ and its delays, the tracking error $e(k)$ is denoted as:

$$e(k) = x_n(k) - x_{ndes}(k) \quad (3.7)$$

and the filtered tracking error $r(k)$ with $n-1$ delays is given as

$$r(k) = e(k) + \lambda_1 e(k-1) + \dots + \lambda_{n-1} e(k-n+1) \quad (3.8)$$

where $e(k-1), \dots, e(k-n+1)$ are delayed values of the error $e(k)$, and $\lambda_{n-1}, \dots, \lambda_1$ are constant matrices selected so as $|z^{n-1} + \lambda_1 z^{n-2} + \dots + \lambda_{n-1}|$ is stable. Using the same way of Eq (3.8), the filtered tracking error at time $k+1$ can be written as:

$$\begin{aligned} r(k+1) &= e(k+1) + \lambda_1 e(k) + \dots + \lambda_{n-1} e(k-n+2) \\ &= x_n(k+1) - x_{ndes}(k+1) + \lambda_1 e(k) + \dots + \lambda_{n-1} e(k-n+2) \end{aligned} \quad (3.9)$$

So far, the entire system control problem is changed to a tracking problem. Recalling the nonlinear system described in Eq (3.4), the tracking problem, Eq (3.9), can be changed to:

$$\begin{aligned} r(k+1) &= f(x(k)) + g(x(k))u(k) + dis(k) \\ &\quad - x_{ndes}(k+1) + \lambda_1 e(k) + \dots + \lambda_{n-1} e(k-n+2) \end{aligned} \quad (3.10)$$

3.4.2 System Dynamics

The above tracking problem, Eq(3.10), can be further modified to the following form, Eq (3.11), by dividing by $g(x(k))$ on the both sides and lumping all the mismatched parts with the system disturbance term, $dis(k)$.

$$\begin{aligned} g^{-1}(x(k))r(k+1) &= g^{-1}(x(k))f(x(k)) - g^{-1}(x(k))x_{ndes}(k+1) + \\ &\quad \lambda_1 e(k) + \dots + \lambda_{n-1} e(k-n+2) + u(k) + dis(k) \end{aligned} \quad (3.11)$$

So the ideal control $u(k)$ for the given tracking system can be derived by cancelling all the terms except the disturbance part on the right hand side of Eq(3.11):

$$u(k) = -g^{-1}(x(k))f(x(k)) + g^{-1}(x(k))x_{ndes}(k+1) + k_v r(k) - \lambda_1 e(k) - \lambda_2 e(k-1) - \dots - \lambda_{n-1} e(k-n+2) \quad (3.12)$$

where k_v is the m by m diagonal gain vector and the term of $k_v r(k)$ is employed to compensate for the system disturbance and make the entire closed loop system stable.

Since $f(x(k))$ and $g(x(k))$ are unknown, a multilayer neural network is introduced to approach the nonlinearly uncertain part in Eq (3.12). The relationship of them can be described as:

$$\hat{W}^T \hat{\Phi}(x(k)) = g^{-1}(x(k))f(x(k)) + \varepsilon(k) \quad (3.13)$$

where $\hat{W}^T \hat{\Phi}(x(k))$ is the actual output of the NN and $\varepsilon(k)$ is the error between the output of the neural network and the actual value of the original system. The actual control $u(k)$ of the closed loop system after employing the neural network can be changed to:

$$u(k) = -\hat{W}^T \hat{\Phi}(x(k)) + g^{-1}(x(k))x_{ndes}(k+1) + k_v r(k) - \lambda_1 e(k) - \lambda_2 e(k-1) - \dots - \lambda_{n-1} e(k-n+2) \quad (3.14)$$

Substituting Eq (3.14) back to the tracking system, Eq (3. 11), the closed-loop tracking error system can be expressed as

$$g^{-1}(x(k))r(k+1) = k_v r(k) + \varepsilon(k) + dis(k) \quad (3.15)$$

The closed-loop tracking error system Eq (3.15) is a state strict passive system if the following condition is satisfied.

$$k_v^T k_v < I / g_{\max}^2 \quad (3.16)$$

where k_v is the m by m diagonal gain vector.

Proof:

The Lyapunov candidate function is chosen as:

$$V = (g^{-1}(x)r(k))^T (g^{-1}(x)r(k)) \quad (3.17)$$

The first difference of the candidate function is

$$\begin{aligned} \Delta V &= r^T(k)k_v^T k_v r(k) + 2r^T(k)k_v(\varepsilon(k) + dis(k)) + (\varepsilon(k) + dis(k))^T(\varepsilon(k) + dis(k)) \\ &\quad - r^T(k)g^{-1T}(x)g^{-1}(x)r(k) \end{aligned} \quad (3.18)$$

$$\begin{aligned} &= -r^T(k)[I/(g^T(x)g(x)) - k_v^T k_v]r(k) + 2r^T(k)k_v(\varepsilon(k) + dis(k)) \\ &\quad + (\varepsilon(k) + dis(k))^T(\varepsilon(k) + dis(k)) \end{aligned} \quad (3.19)$$

The term, $\varepsilon(k) + dis(k)$, is bounded by $\varepsilon_{\max} + dis_{\max}$. Hence, the system is a state strict passive system if the condition in Eq. 3.16 is satisfied.

3.4.3 Selection of the Input for the Proposed NN

The structure of the proposed NN has been selected in Chapter 2. It is a multilayer perceptron structure with one input layer, two hidden layers and one output layer. For the first and the second hidden layers, the hyperbolic tangent function is selected as the basis function. The output layer is a linear layer to adjust the magnitude of the output. The input

of the proposed NN can simply select the same delay order as that used in the control error filter. By using the delays of the system output to reinforce the relationship between the present and the past status, neither $u(k)$ nor its delays are needed by the proposed NN.

After selecting the input of the proposed NN, the structure of the entire closed-loop system with the neural network is shown in Fig 3.5. Note that the desired trajectory is a zero vector for the system oscillation damping. The output 1 of the error delay block added to $e(k)$ equals $r(k)$, the filtered error used to adjust the weights of the NN. Also, multiplying $r(k)$ with the gain k_v and adding at the output 2 of the NN (Eq 3.14) makes the closed system stable. The remaining part of Eq. 3.14, output 2 of the error delay block, is also added at the summing junction as shown in Fig. 3.5.

3.4.4 Weight Update Functions

The NN weight-tuning algorithm used in the proposed controller is developed from the Delta learning rule and the back propagation. The filtered error is back propagated to each layer by updating its weights.

Based on the extension to Lyapunov theory for dynamic systems, theorem 3.3 in [26] is given as: For a given three layer NN, if the desired trajectory $x_{ndes}(k)$, the NN functional reconstruction error $\varepsilon(k)$ and the disturbance $dis(k)$ are bounded, the weight updating function for each layer can be denoted as:

$$\hat{W}_1(k+1) = \hat{W}_1(k) - \alpha_1 \hat{\Phi}_1(k) [\hat{W}_1(k)^T \hat{\Phi}_1(k) + \beta_1 k_v r(k)]^T \quad (3.20)$$

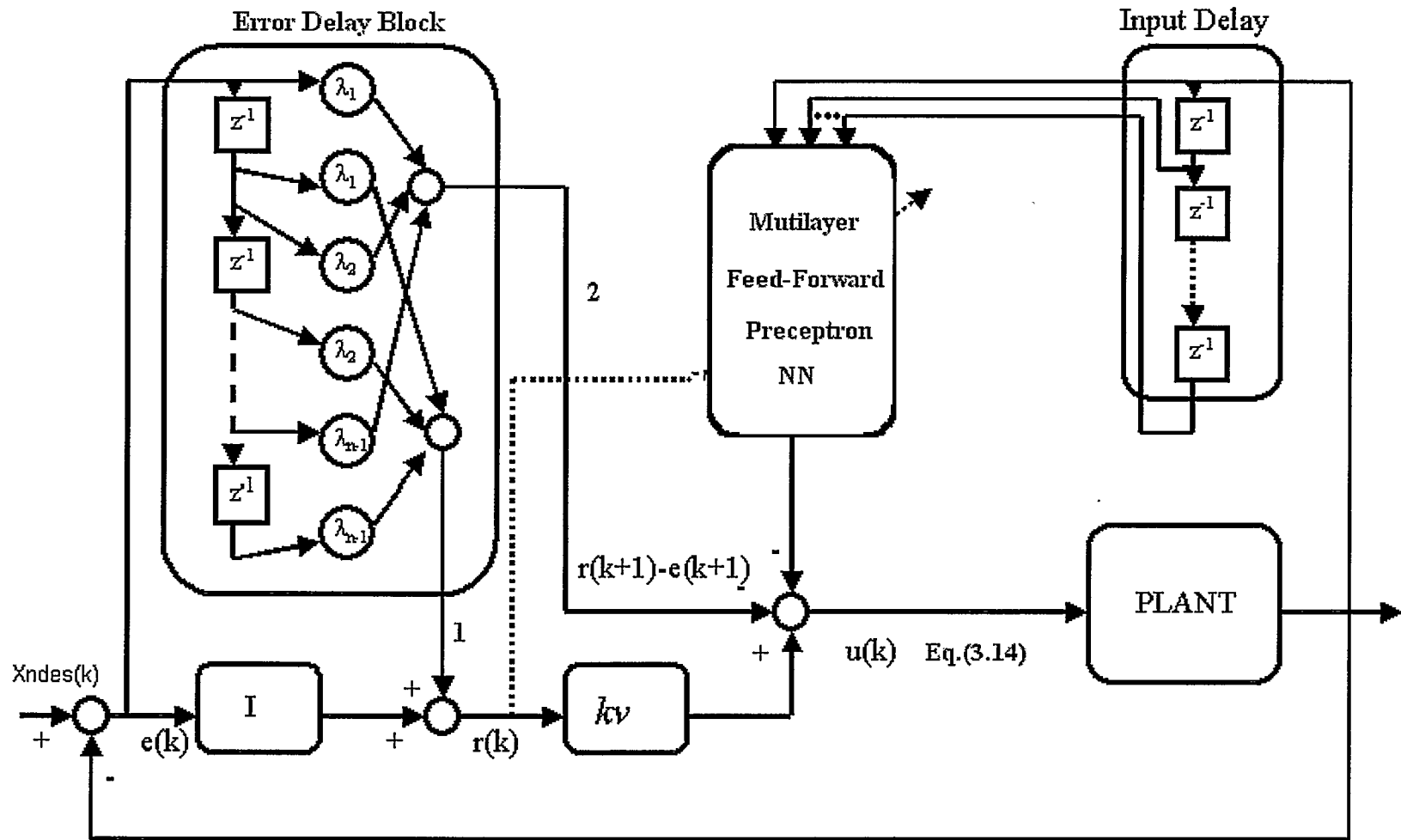


Figure 3.5 Proposed NN Controller

$$\hat{W}_2(k+1) = \hat{W}_2(k) - \alpha_2 \hat{\Phi}_2(k) [\hat{W}_2(k)^T \hat{\Phi}_2(k) + \beta_2 k_v r(k)]^T \quad (3.21)$$

$$\hat{W}_3(k+1) = \hat{W}_3(k) + \alpha_3 \hat{\Phi}_3(k) r(k+1) \quad (3.22)$$

where \hat{W}_1 , \hat{W}_2 and \hat{W}_3 are the weights of the first layer, second layer and the third layer, respectively. $\hat{\Phi}_1$ is the input vector of the network. $\hat{\Phi}_2$ and $\hat{\Phi}_3$ are the vectors of the basis functions of the second and third layer, respectively. α_i , $i=1,2,3$ is the positive constant learning rate for each layer in the algorithm. In addition, $\|\beta_i\| \leq kv_i$, $i=1,2$.

According to [26], the following conditions are needed to make the system converge:

$$\bullet \quad \alpha_i \Phi_{i \max}^2 < 2 \quad \text{for } i=1,2 \quad (3.23)$$

$$\bullet \quad \alpha_3 \Phi_{3 \max}^2 < 1 \quad \text{for layer 3} \quad (3.24)$$

Lemma 3.1 [26]: if $A(k) = I - \alpha \Phi(x(k)) \Phi^T(x(k))$ in the system described in Eq (3.15), where $0 < \alpha < 2$ and $\Phi(x(k))$ is a vector of basis functions, then $\|\Pi_{k_0}^{k_1-1} A(k)\| < 1$ is guaranteed. If there is an $L > 0$ such that $\sum_{k=k_0}^{k_1+L-1} \Phi(x(k))^T \Phi(x(k)) > 0$ for all k , then the system is exponential stable.

From the conclusion of Lemma 3.1 in [26], the algorithm requires a persistent excitation (PE) for the network to keep the system stable. This PE condition sometime is not easy to derive in dynamic systems. Another problem affecting the learning rate of the NN is the fixed learning rate α_i and this problem is the major drawback of the Delta rule.

3.4.5 Projection Algorithm

To make the learning rate α_i variable is the main objective of this section. The projection algorithm introduced in [26] provides a way to improve the learning rate of the whole system. It modifies the fixed learning rate to a variable rate to satisfy the stability conditions listed in Eq (3.23) and Eq (3.24). The variable learning rate is:

$$\alpha_i = \frac{\xi_i}{\varsigma_i + \|\hat{\Phi}_i(k)\|^2} \quad , \quad i=1,2,3 \quad (3.25)$$

where ς_i is a positive small number to reduce the numerical difficulty when the norm of $\hat{\Phi}_i(k)$ is close to zero and ξ_i is the new adaptation gain of each layer. It is easy to prove that this modification can satisfy the stability conditions required in Eq (3.23) through Eq (3.24) if the following conditions are selected.

$$\bullet \quad 0 < \xi_i < 2 \quad i=1,2 \quad (3.26)$$

$$\bullet \quad 0 < \xi_i < 1 \quad i=3 \quad (3.27)$$

3.4.6 Modification of the Weight Tuning Functions

A modification of the weight-updating algorithm described in section 3.4.4 is introduced in this section. The following two tuning algorithms overcome the need for persistent excitation in the case of a multilayer NN. This theorem also relies on the extension of the Lyapunov theory for dynamic systems given in [26].

The weight updating equations (3.20)-(3.22) are modified as shown as follows.

$$\begin{aligned}\hat{W}_1(k+1) &= \hat{W}_1(k) - \alpha_1 \hat{\Phi}_1(k) [\hat{W}_1(k)^T \hat{\Phi}_1(k) + B_1 k_v r(k)]^T \\ &\quad - \Gamma \| I - \alpha_1 \hat{\Phi}_1(k) \hat{\Phi}_1^T(k) \| \hat{W}_1(k)\end{aligned}\quad (3.28)$$

$$\begin{aligned}\hat{W}_2(k+1) &= \hat{W}_2(k) - \alpha_2 \hat{\Phi}_2(k) [\hat{W}_2(k)^T \hat{\Phi}_2(k) + B_2 k_v r(k)]^T \\ &\quad - \Gamma \| I - \alpha_2 \hat{\Phi}_2(k) \hat{\Phi}_2^T(k) \| \hat{W}_2(k)\end{aligned}\quad (3.29)$$

$$\begin{aligned}\hat{W}_3(k+1) &= \hat{W}_3(k) + \alpha_3 \hat{\Phi}_3(k) r(k+1) \\ &\quad - \Gamma \| I - \alpha_3 \hat{\Phi}_3(k) \hat{\Phi}_3^T(k) \| \hat{W}_3(k)\end{aligned}\quad (3.30)$$

where Γ is a positive design parameter with the value less than one. The last term of equations (3.28)-(3.30) is designed to relax the dependence on the PE condition required by the pure Delta rule [26].

Corresponding to stability conditions described in Eqs. (3.23)-(3.24), the filtered tracking error $r(k)$ and the NN weights of all the layers in the modified updating algorithm are globally stable if the following conditions are satisfied.

$$\bullet \quad \alpha_i \Phi_{i_{\max}}^2 < 2 \quad \text{for } i=1,2 \quad (3.31)$$

$$\bullet \quad \alpha_3 \Phi_{3_{\max}}^2 < 1 \quad \text{for layer 3} \quad (3.32)$$

$$\bullet \quad 0 < \Gamma < 1 \quad (3.33)$$

$$\bullet \quad K v_{\max} < \frac{1/g_{\max}}{\sqrt{\theta}} \quad (3.34)$$

where

$$\theta = \beta_3 + \sum_{i=1}^2 \beta_i k v_i^2 \quad (3.35)$$

with

$$\beta_i = \alpha_i \Phi_{i \max}^2 + \frac{[(1 - \alpha_i \Phi_{i \max}^2) - \Gamma \|I - \alpha_i \hat{\Phi}_i(k) \hat{\Phi}_i^T(k)\|]^2}{2 - \alpha_i \Phi_{i \max}^2} \quad \text{for } i=1,2 \quad (3.36)$$

$$\beta_3 = 1 + \alpha_3 g_{\max}^2 \Phi_{3 \max}^2 + g_{\max}^2 \frac{[\alpha_3 \Phi_{3 \max}^2 + \Gamma \|I - \alpha_3 \hat{\Phi}_3(k) \hat{\Phi}_3^T(k)\|]^2}{1 - \alpha_3 \Phi_{3 \max}^2} \quad \text{for } i=3 \quad (3.37)$$

The effect of the adaptation of the learning rates on the weights estimation error and the tracking error can be observed through Lyapunov stability analysis. Larger values of learning rates in the first and second layers force smaller weight estimation errors whereas the tracking error is unaffected. On the other hand, a larger learning rate in the output layer can force smaller tracking error and weight estimation errors [26].

3.4.7 Proof of Stability

Based on [26], the Lyapunov stability theorem can be used to prove that the entire closed-loop system is uniformly ultimately Bounded (UUB). The Lyapunov function candidate of the closed-loop system can be defined as:

$$\begin{aligned} V = & (g^{-1}(x)r(k))^T (g^{-1}(x)r(k)) + \frac{1}{\alpha_1} \text{tr}(\tilde{W}_1^T(k)\tilde{W}_1(k)) \\ & + \frac{1}{\alpha_2} \text{tr}(\tilde{W}_2^T(k)\tilde{W}_2(k)) + \frac{1}{\alpha_3} \text{tr}(\tilde{W}_3^T(k)\tilde{W}_3(k)) \end{aligned} \quad (3.38)$$

The Lyapunov function candidate V , Eq. (3.38), is positive definite. The first difference of V is

$$\begin{aligned} \Delta V = & (g^{-1}(x)r(k+1))^T (g^{-1}(x)r(k+1)) - r^T(k)g^{-1T}(x)g^{-1}(x)r(k) \\ & + \frac{1}{\alpha_1} \text{tr}(\tilde{W}_1^T(k+1)\tilde{W}_1(k+1) - \tilde{W}_1^T(k)\tilde{W}_1(k)) \end{aligned}$$

$$\begin{aligned}
& + \frac{1}{\alpha_2} \text{tr}(\tilde{W}_2^T(k+1)\tilde{W}_2(k+1) - \tilde{W}_2^T(k)\tilde{W}_2(k)) \\
& + \frac{1}{\alpha_3} \text{tr}(\tilde{W}_3^T(k+1)\tilde{W}_3(k+1) - \tilde{W}_3^T(k)\tilde{W}_3(k))
\end{aligned} \tag{3.39}$$

For the desired weights W_1 , W_2 and W_3 , the revised dynamics relative to weight estimation errors, $\tilde{W}_i(k) = W_i - \hat{W}_i(k)$ $i=1,2,3$, in the hidden layers and output layer are given by

$$\begin{aligned}
\tilde{W}_1(k+1) = & [I - \alpha_1 \hat{\Phi}_1(k) \hat{\Phi}_1^T(k)] \tilde{W}_1(k) + \alpha_1 \hat{\Phi}_1(k) [W_1^T(k) \hat{\Phi}_1(k) + B_1 k_v r(k)]^T \\
& - \Gamma \| I - \alpha_1 \hat{\Phi}_1(k) \hat{\Phi}_1^T(k) \| \hat{W}_1(k)
\end{aligned} \tag{3.40}$$

$$\begin{aligned}
\tilde{W}_2(k+1) = & [I - \alpha_2 \hat{\Phi}_2(k) \hat{\Phi}_2^T(k)] \tilde{W}_2(k) + \alpha_2 \hat{\Phi}_2(k) [W_2^T(k) \hat{\Phi}_2(k) + B_2 k_v r(k)]^T \\
& - \Gamma \| I - \alpha_2 \hat{\Phi}_2(k) \hat{\Phi}_2^T(k) \| \hat{W}_2(k)
\end{aligned} \tag{3.41}$$

$$\begin{aligned}
\tilde{W}_3(k+1) = & [I - \alpha_3 \hat{\Phi}_3(k) \hat{\Phi}_3^T(k)] \tilde{W}_3(k) - \alpha_3 \hat{\Phi}_3(k) [g(x) [k_v r(k) + \varepsilon(k) + \text{dis}(k)] - \tilde{W}_3^T(k) \hat{\Phi}_3(k)]^T \\
& - \Gamma \| I - \alpha_3 \hat{\Phi}_3(k) \hat{\Phi}_3^T(k) \| \hat{W}_3(k)
\end{aligned} \tag{3.42}$$

where $\hat{\Phi}_i$ and \hat{W}_i are the actual values of Φ_i and W_i , respectively. Substituting Eqs.(3.40) through (3.42) back to Eq. (3.39), the first difference of the Lyapunov candidate function V is changed to

$$\begin{aligned}
\Delta V = & -r(k)^T (I / (g^T(x)g(x)) - k_v^T \theta_1 k_v) r(k) + 2r^T(k) k_v \gamma_1 + \rho_1 \\
& - \sum_{i=1}^2 \{ [2 - \alpha_i \hat{\Phi}_i^T(k) \hat{\Phi}_i(k)] [\tilde{W}_i^T(k) \hat{\Phi}_i(k) \\
& - \frac{[(1 - \alpha_i \hat{\Phi}_i^T(k) \hat{\Phi}_i(k)) - \Gamma \| I - \alpha_i \hat{\Phi}_i(k) \hat{\Phi}_i^T(k) \|]}{2 - \alpha_i \hat{\Phi}_i^T(k) \hat{\Phi}_i(k)} (W_i^T(k) \hat{\Phi}_i(k) + B_i k_v r(k))]^T
\end{aligned}$$

$$\begin{aligned}
& \times [\tilde{W}_i^T(k) \hat{\Phi}_i(k) - \frac{[(1 - \alpha_i \hat{\Phi}_i^T(k) \hat{\Phi}_i(k)) - \Gamma \|I - \alpha_i \hat{\Phi}_i(k) \hat{\Phi}_i^T(k)\|]}{2 - \alpha_i \hat{\Phi}_i^T(k) \hat{\Phi}_i(k)} \\
& \times (W_i^T(k) \hat{\Phi}_i(k) + B_i k_v r(k))] \} \\
& - [1 - \alpha_3 \hat{\Phi}_3^T(k) \hat{\Phi}_3(k)] \times [\tilde{W}_3^T(k) \hat{\Phi}_3(k) \\
& \frac{[\alpha_3 \hat{\Phi}_3^T(k) \hat{\Phi}_3(k) + \Gamma \|I - \alpha_3 \hat{\Phi}_3(k) \hat{\Phi}_3^T(k)\|][g(x)(k, r(k) + \varepsilon(k) + dis(k))]}{1 - \alpha_3 \hat{\Phi}_3^T(k) \hat{\Phi}_3(k)}]_T \\
& \times [\tilde{W}_3^T(k) \hat{\Phi}_3(k) \\
& \frac{[\alpha_3 \hat{\Phi}_3^T(k) \hat{\Phi}_3(k) + \Gamma \|I - \alpha_3 \hat{\Phi}_3(k) \hat{\Phi}_3^T(k)\|][g(x)(k, r(k) + \varepsilon(k) + dis(k))]}{1 - \alpha_3 \hat{\Phi}_3^T(k) \hat{\Phi}_3(k)}] \\
& + \sum_{i=1}^3 \left\{ \frac{1}{\alpha_i} \|I - \alpha_i \hat{\Phi}_i(k) \hat{\Phi}_i^T(k)\|^2 \times tr(\Gamma^2 \hat{W}_i^T(k) \hat{W}_i(k)) \right. \\
& \left. + \frac{2}{\alpha_i} \|I - \alpha_i \hat{\Phi}_i(k) \hat{\Phi}_i^T(k)\| tr[\Gamma \hat{W}_i^T(k) (I - \alpha_i \hat{\Phi}_i(k) \hat{\Phi}_i^T(k))^T \tilde{W}_i(k)] \right\} \quad (3.43)
\end{aligned}$$

where

$$\begin{aligned}
\theta_1 = & I + g^T(x)g(x) \left\{ \alpha_3 \hat{\Phi}_3^T(k) \hat{\Phi}_3(k) + \frac{[\alpha_3 \hat{\Phi}_3^T(k) \hat{\Phi}_3(k) + \Gamma \|I - \alpha_3 \hat{\Phi}_3(k) \hat{\Phi}_3^T(k)\|]^2}{1 - \alpha_3 \hat{\Phi}_3^T(k) \hat{\Phi}_3(k)} \right\} \\
& + I \sum_{i=1}^2 \left\{ \alpha_i \hat{\Phi}_i^T(k) \hat{\Phi}_i(k) + \frac{[(1 - \alpha_i \hat{\Phi}_i^T(k) \hat{\Phi}_i(k)) - \Gamma \|I - \alpha_i \hat{\Phi}_i(k) \hat{\Phi}_i^T(k)\|]^2}{2 - \alpha_i \hat{\Phi}_i^T(k) \hat{\Phi}_i(k)} \right\} \quad (3.44)
\end{aligned}$$

$$\begin{aligned}
\gamma_1 = & (\varepsilon(k) + dis(k)) + [\alpha_3 \hat{\Phi}_3^T(k) \hat{\Phi}_3(k) + \frac{\alpha_3 \hat{\Phi}_3^T(k) \hat{\Phi}_3(k) + \Gamma \|I - \alpha_3 \hat{\Phi}_3(k) \hat{\Phi}_3^T(k)\|}{1 - \alpha_3 \hat{\Phi}_3^T(k) \hat{\Phi}_3(k)}] \\
& \times g(x)(\varepsilon(k) + dis(k)) + \Gamma \|I - \alpha_3 \hat{\Phi}_3(k) \hat{\Phi}_3^T(k)\| \hat{W}_3^T(k) \hat{\Phi}_3(k) \\
& + \sum_{i=1}^2 \{B_i + \Gamma \|I - \alpha_i \hat{\Phi}_i(k) \hat{\Phi}_i^T(k)\| \hat{W}_i^T(k) \hat{\Phi}_i(k)\} k_w \quad (3.45)
\end{aligned}$$

$$\begin{aligned}
\rho_1 = & (\varepsilon(k) + dis(k))^T (\varepsilon(k) + dis(k)) + [\alpha_3 \hat{\Phi}_3^T(k) \hat{\Phi}_3(k) + \frac{1}{1 - \alpha_3 \hat{\Phi}_3^T(k) \hat{\Phi}_3(k)} (\alpha_3 \hat{\Phi}_3^T(k) \hat{\Phi}_3(k) \\
& + \Gamma \| I - \alpha_3 \hat{\Phi}_3(k) \hat{\Phi}_3^T(k) \|)] \times [g(x)(\varepsilon(k) + dis(k))]^T [g(x)(\varepsilon(k) + dis(k))] \\
& + 2\Gamma \| I - \alpha_3 \hat{\Phi}_3(k) \hat{\Phi}_3^T(k) \| (\mathcal{W}_3^T(k) \tilde{\Phi}_3(k))^T g(x)(\varepsilon(k) + dis(k)) \\
& + \sum_{i=1}^2 \{B_i + \Gamma \| I - \alpha_i \hat{\Phi}_i(k) \hat{\Phi}_i^T(k) \| \hat{\Phi}_i^T(k) \hat{W}_i(k) \hat{W}_i^T(k) \hat{\Phi}_i(k)\} \tag{3.46}
\end{aligned}$$

Using the inequality principles, ΔV , Eq. (3.43) can be further changed to

$$\begin{aligned}
\Delta V \leq & -(I/g_{\max}^2 - \theta k_{v\max}^2) \|r(k)\|^2 + 2k_{v\max} \gamma \|r(k)\| + \rho \\
& - \sum_{i=1}^2 \{ [2 - \alpha_i \hat{\Phi}_i^T(k) \hat{\Phi}_i(k)] \| \tilde{W}_i^T(k) \hat{\Phi}_i(k) \\
& - \frac{[(1 - \alpha_i \hat{\Phi}_i^T(k) \hat{\Phi}_i(k)) - \Gamma \| I - \alpha_i \hat{\Phi}_i(k) \hat{\Phi}_i^T(k) \|]}{2 - \alpha_i \hat{\Phi}_i^T(k) \hat{\Phi}_i(k)} (\mathcal{W}_i^T(k) \hat{\Phi}_i(k) + B_i k_v r(k)) \|^2 \} \\
& - [1 - \alpha_3 \hat{\Phi}_3^T(k) \hat{\Phi}_3(k)] \times \| \tilde{W}_3^T(k) \hat{\Phi}_3(k) \\
& - \frac{[\alpha_3 \hat{\Phi}_3^T(k) \hat{\Phi}_3(k) + \Gamma \| I - \alpha_3 \hat{\Phi}_3(k) \hat{\Phi}_3^T(k) \|] [g(x)(k_v r(k) + \varepsilon(k) + dis(k))]}{1 - \alpha_3 \hat{\Phi}_3^T(k) \hat{\Phi}_3(k)} \|^2 \\
& + \sum_{i=1}^3 \left\{ \frac{1}{\alpha_i} \| I - \alpha_i \hat{\Phi}_i(k) \hat{\Phi}_i^T(k) \|^2 \times tr(\Gamma^2 \hat{W}_i^T(k) \hat{W}_i(k) + 2\Gamma \hat{W}_i^T(k) \tilde{W}_i(k)) \right\} \tag{3.47}
\end{aligned}$$

where

$$\begin{aligned}
\theta = & 1 + \alpha_3 g_{\max}^2 \Phi_{3\max}^2 + g_{\max}^2 \frac{[\alpha_3 \Phi_{3\max}^2 + \Gamma \| I - \alpha_3 \hat{\Phi}_3(k) \hat{\Phi}_3^T(k) \|^2]}{1 - \alpha_3 \Phi_{3\max}^2} \\
& + \sum_{i=1}^2 \left\{ \alpha_i \Phi_{i\max}^2 + \frac{[(1 - \alpha_i \Phi_{i\max}^2) - \Gamma \| I - \alpha_i \hat{\Phi}_i(k) \hat{\Phi}_i^T(k) \|^2]}{2 - \alpha_i \Phi_{i\max}^2} \right\} \tag{3.48}
\end{aligned}$$

$$\begin{aligned}
\gamma = & \left[1 + \alpha_3 \mathcal{G}_{\max} \hat{\Phi}_{3\max}^2 + \frac{\mathcal{G}_{\max} (\alpha_3 \Phi_{3\max}^2 + \Gamma \| I - \alpha_3 \hat{\Phi}_3(k) \hat{\Phi}_3^T(k) \|)}{1 - \alpha_3 \Phi_{3\max}^2} \right] (\varepsilon_{\max} + dis_{\max}) \\
& + \Gamma \| I - \alpha_3 \hat{\Phi}_3(k) \hat{\Phi}_3^T(k) \| W_{3\max} \Phi_{3\max} \\
& + \sum_{i=1}^2 \{ B_i + \Gamma \| I - \alpha_i \hat{\Phi}_i(k) \hat{\Phi}_i^T(k) \| W_{i\max} \Phi_{i\max} \} k_{vi}
\end{aligned} \tag{3.49}$$

$$\begin{aligned}
\rho = & \left[1 + \alpha_3 \mathcal{G}_{\max}^2 \hat{\Phi}_{3\max}^2 + \frac{\mathcal{G}_{\max}^2}{1 - \alpha_3 \hat{\Phi}_{3\max}^2} (\alpha_3 \hat{\Phi}_{3\max}^2 + \Gamma \| I - \alpha_3 \hat{\Phi}_3(k) \hat{\Phi}_3^T(k) \|) \right] \\
& \times (\varepsilon_{\max} + dis_{\max})^2 + 2\Gamma \| I - \alpha_3 \hat{\Phi}_3(k) \hat{\Phi}_3^T(k) \| W_{3\max} \tilde{\Phi}_{3\max} \mathcal{G}_{\max} (\varepsilon_{\max} + dis_{\max}) \\
& + \sum_{i=1}^2 \{ B_i + \Gamma \| I - \alpha_i \hat{\Phi}_i(k) \hat{\Phi}_i^T(k) \| \Phi_{i\max}^2 W_{i\max}^2 \}
\end{aligned} \tag{3.50}$$

The maximum value [26] of the last term of Eq.(3.47) is:

$$C = \frac{A_{\max}}{A_{\min}} \frac{1}{2 - \Gamma} [(1 - \Gamma)^2 A_{\max} + \Gamma^2 (2 - \Gamma) A_{\min}] W_{\max}^2 \tag{3.51}$$

where A_{\max} and A_{\min} are the maximum and minimum singular values of the diagonal matrix given by Eq. (3.52).

$$\left[\begin{array}{ccc}
\frac{1}{\alpha_1} \| I - \alpha_1 \hat{\Phi}_1(k) \hat{\Phi}_1^T(k) \|^2 & 0 & 0 \\
0 & \frac{1}{\alpha_2} \| I - \alpha_2 \hat{\Phi}_2(k) \hat{\Phi}_2^T(k) \|^2 & 0 \\
0 & 0 & \frac{1}{\alpha_3} \| I - \alpha_3 \hat{\Phi}_3(k) \hat{\Phi}_3^T(k) \|^2
\end{array} \right] \tag{3.52}$$

W_{\max} is the maximum value of the norm of W , where $W = [\|W_1\| \ \|W_2\| \ \|W_3\|]^T$.

W_i $i=1,2,3$ is the desired weight of the layer i and $\|W_i\| \leq W_{i\max}$. The requirements of Eq (3.31) and Eq (3.32), which can be satisfied by using the projection algorithm introduced

in section 3.4.5, can make the fourth and fifth terms of Eq (3.47) to be negative. The summation of the remaining terms of ΔV , Eq. (3.47), is negative with the upper bound on the tracking error given by

$$\|r(k)\| > \frac{1}{(1/g_{\max}^2 - \theta k_{v\max}^2)} [\gamma k_{v\max} + \sqrt{\gamma^2 k_{v\max}^2 + (\rho + C)(1/g_{\max}^2 - \theta k_{v\max}^2)}] \quad (3.53)$$

Hence, the entire close loop system is UUB.

3.5 Summary

In this chapter, plant models and several neural networks based control architectures are discussed. From the comparisons of these control theories, the NN based direct control with guaranteed performance algorithm is selected as the proposed control theory. The algorithm only needs one neural network to perform both the system identification and control functions. Hence, it can reduce the computation complexity and save the system resources.

The modified Delta learning rule and projection algorithm are used in the derivation of the proposed algorithm to improve the learning rate of the network and relax the dependence for the PE, which is needed by most algorithms. Therefore, all the system weights can be simply initialized as zeros that can avoid the system oscillations during the initial iterations of learning. This characteristic improves the system overall reliability in practical applications. Furthermore, the mathematical proof by using Lyapunov stability theory is provided in the discussion and the result can keep the numerical stability of the entire closed loop system.

CHAPTER 4

SIMULATION STUDIES OF NN SVC CONTROLLER IN A SINGLE MACHINE INFINITE BUS SYSTEM

4.1 Introduction

Considerable efforts have been devoted to using SVCs to damp system oscillations [10,12,13,15,18,45,46,47]. These references have demonstrated that a SVC PSS can provide a positive damping function for generator oscillations similar to that of a generator PSS.

In this chapter, the multilayer neural network based direct control theory is used to develop the proposed NN SVC controller (NNPSS) and tests with the proposed NNPSS in a single machine infinite bus system are described.

The traditional PSS control theory is also used to design a conventional SVC PSS (SCPSS) to control the output of the SVC. Comparison of the damping effectiveness between an SCPSS and the proposed NNPSS is done for different operating conditions.

4.2 Modeling of the Single Machine Infinite Bus System with an SVC at the Middle Bus

A schematic representation of the single machine infinite bus power system model with an SVC at the middle bus is shown in Fig. 4.1, where the SVC is composed of a

cascade multi-level inverter and an energy storage device. In practice, DC capacitors are usually used for the energy storage.

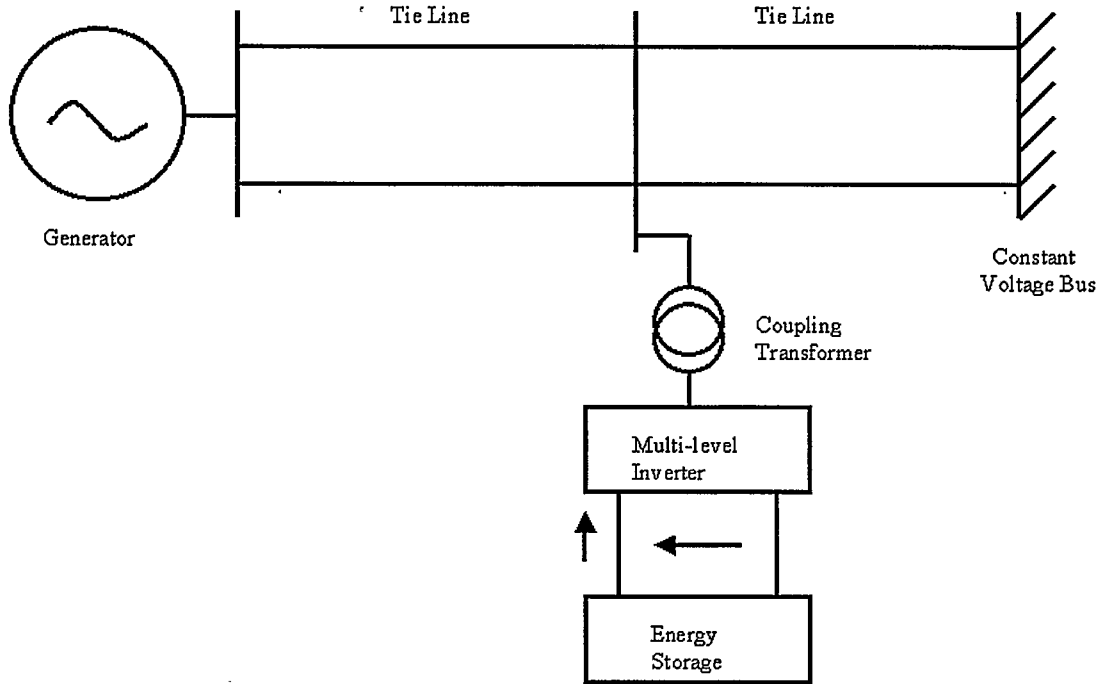


Figure 4.1 Single Machine Infinite Bus System with an SVC

This model is developed from the models described in [4,7,8,12,13,15]. The middle bus has two tie lines connected to the generator bus and the infinite bus, respectively. This configuration is easy to implement short circuit fault tests when a fault occurs on a transmission line. Concerning the generating unit, the Park's seventh order model [7,8] of a synchronous machine is used to represent its dynamics. The generator also has a standard IEEE ST1A AVR (GAVR) [8] to control the generator terminal voltage.

The output of the supplementary controller [15,18] can be added to the system either after the voltage control loop or at the input junction of the voltage control loop to

damp system oscillations. In practice, most PSS designs [15] select the second alternative, as the system voltage performance is better. The proposed SVC controller shown in Fig 4.2 is also designed to add the damping signal at the input junction of the voltage controller. Its structure includes two parts. One part is an AVR used to adjust the output of the SVC [15] to control the voltage at the middle bus. K_a and T_a are the gain and the time constant of the SVC AVR (SAVR). V_{AMAX} and V_{AMIN} are the upper and lower limits of the SAVR output, V_{ref} is the reference voltage of the middle bus and its actual voltage is measured as V_m .

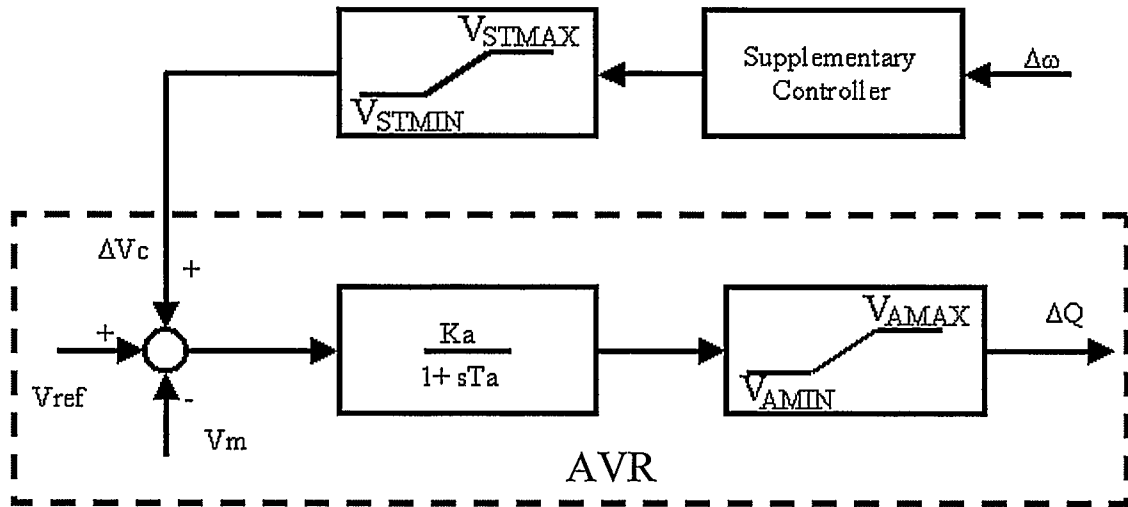


Figure 4.2 SVC Controller Configuration

The supplementary controller is a PSS used to generate the damping signals. V_{STMAX} and V_{STMIN} are the upper and lower hard limits of the output of the supplementary controller. In order to keep the system voltage variation at an acceptable level, in simulations the two limits are selected as ± 0.1 . After applying the limits, the controlled bus voltage is limited within 10% around normal operating voltage. The entire mathematical

model and the parameters are given in Appendix. In order to illustrate the damping performance of the proposed NNPSS, during simulating one system has a conventional PSS and another system has the proposed NNPSS.

In most of the published control designs of PSS, input signals of the supplementary controllers are usually selected as deviations of the angular speed of the generator or a combination of deviations of the angular speed and other signal (signals) that have already been introduced in Chapter 1. In the proposed NNPSS, the deviation of the angular speed of the generator is chosen as the input signal. In order to get the signal locally, the deviation of the frequency may be measured instead, because there is only a second order difference between the two.

4.3 Conventional SVC Supplementary Controller

The conventional SVC supplementary controller (SCPSS) [12] is a phase lead/lag type with the same control structure as that of the generator conventional PSS (GPSS) [5]. The transfer function $G_{PSS}(s)$ of the conventional controller is shown in Eq (4.1).

$$G_{PSS}(s) = K_{PSS} \frac{T_W s}{1 + sT_W} \cdot \frac{(1 + sT_2)(1 + sT_4)}{(1 + sT_1)(1 + sT_3)} \quad (4.1)$$

In simulations, the SCPSS is designed for the operating condition of 0.7 p.u. and p.f =0.85 lag. A small system disturbance, 0.1 p.u step increase in mechanical torque, is applied to the generator. Parameters of the SCPSS are tuned to make the middle bus voltage variation in phase with the deviation of the generator speed [13] and to provide the best damping performance for this condition. These parameters are kept fixed for all simulation studies.

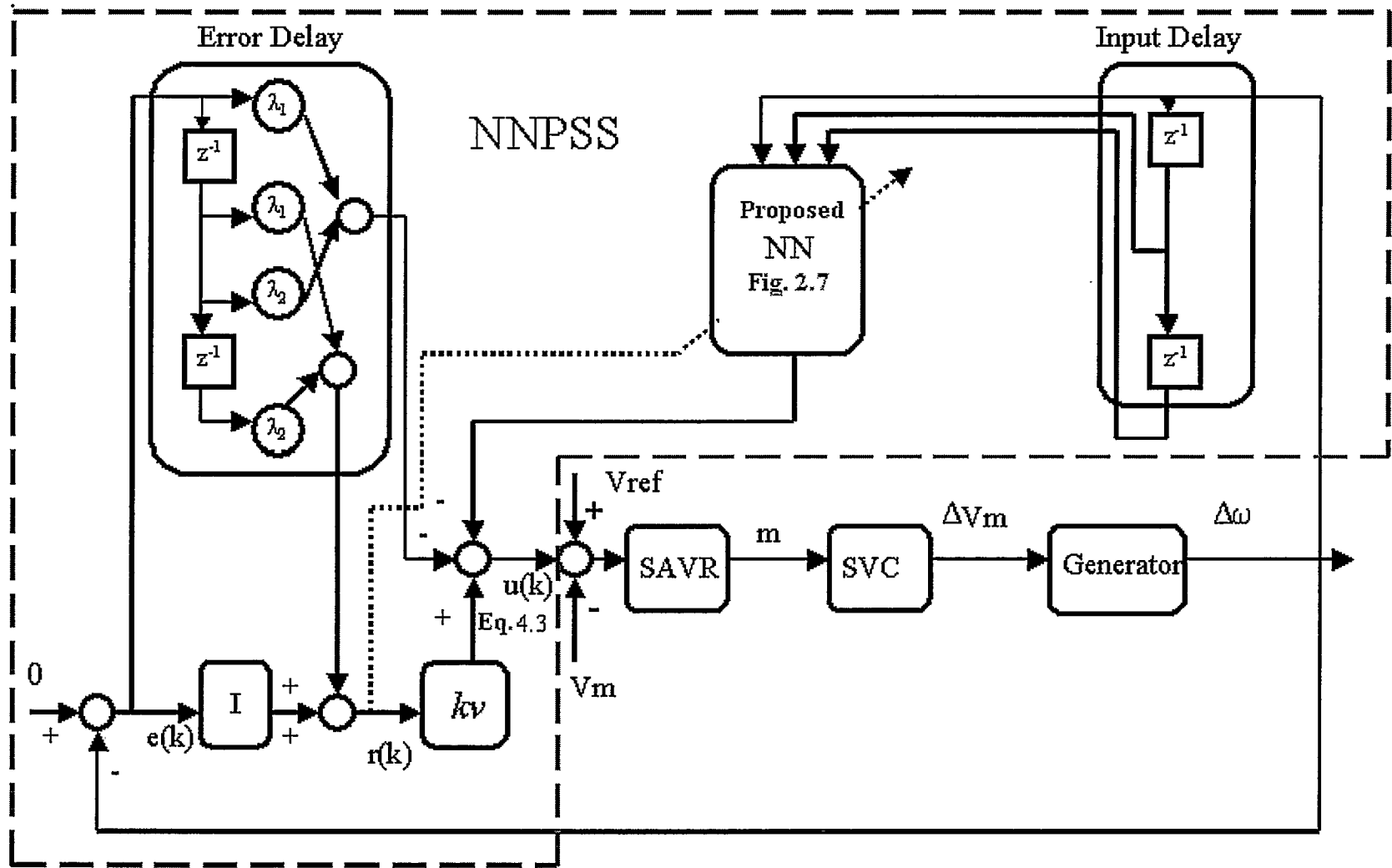


Figure 4.3 Closed Loop System with the Proposed SVC NNPSS

4.4 Design of the Proposed SVC NNPSS

The structure of the entire closed loop system with the proposed SVC NNPSS is shown in Fig. 4.3. The NNPSS consists of a multilayer neural network with the hyperbolic tangent function as the activation function and a filtered error direct control introduced in Chapter 3.

The error filter order of the controller is selected as a third order filter and the desired trajectory is an all zero vector, so the input error of the controller can be expressed as:

$$e(k) = \Delta\omega(k) - 0 \quad (4.2)$$

where $\Delta\omega(k)$ is the generator speed deviation estimated at instant k . The control output $u(k)$ can be calculated according to Eq (4.3)

$$u(k) = -W^T \Phi(\Delta\omega) + k_v r(k) - \lambda_1 e(k) - \lambda_2 e(k-1) \quad (4.3)$$

where $W^T \Phi(\Delta\omega)$ is the output of the proposed neural network. The update functions of the weights of each layer use Eq (3.28) through Eq (3.30) derived in Chapter 3. The sampling frequency is chosen as 40 Hz (The sampling interval equals to 25 ms).

4.5 Control Simulation Studies

A number of simulation studies have been conducted at different system operating conditions to evaluate the system performance of the proposed controller. For comparison, studies have also been conducted with a SCPSS designed by using the conventional methods.

4.5.1 Network Training

The proposed NN is first trained in off-line. In the training period, the initial weights are selected as small random numbers between $[-0.1, +0.1]$ and the controller is applied on the system. The training of the proposed controller can be conducted by applying one or a series of system disturbances on the system until the controller provides the desired damping effect in the simulation studies.

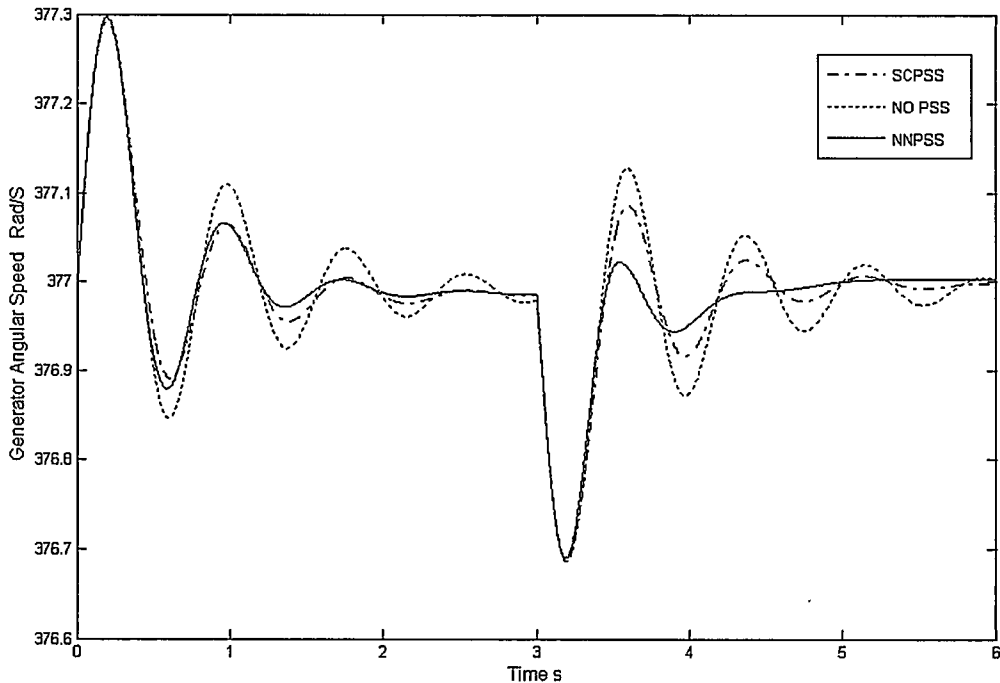


Figure 4.4 Training of the Network. Initial Condition $P=0.7$ p.u., p.f. = 0.85 lag

The training of the controller in this dissertation is conducted by applying a 0.05 p.u step increase in the mechanical torque of the generator at the operating condition of $P= 0.7$ p.u., and a power factor of 0.85 lag. The input torque is returned to the initial value at 3 s. From Fig 4.4, it can be seen that at the second disturbance, the system can provide good damping. The final weights are chosen as the initial weights for the following simulations.

4.5.2 Normal operating Condition

The normal operating condition of the single machine power system is set at $P= 0.7$ p.u. and the power factor equals to 0.85 lag. In the simulation, a 0.2 pu step increase in the mechanical torque of the generator is applied at 0.1 s. A comparison of the angular speed of the system with the proposed SVC controller (NNPSS), with the conventional SVC PSS controller (SCPSS) and without control (NO PSS) is shown in Fig. 4.5. The voltage variation at the middle bus, the output of the SVC PSS controllers and the outputs of SAVRs are shown in Figs. 4.6, 4.7 and 4.8, respectively.

It is easy to see from Fig 4.5 that the proposed SVC controller can effectively damp the system oscillations. In the first peak, there is no difference between the SCPSS and the NNPSS, but from the second peak, the NNPSS can damp the system oscillation much faster than the SCPSS. In Fig 4.6, the voltage of the system without PSS is almost a constant. In contrast, the voltage of the system with the NNPSS has the larger variation especially in the first half cycle and the voltage has already hit the upper boundary. The voltage variation can cause an electrical power variation on the generator and further provides a damping torque on the generator rotor. It can be seen that the NNPSS causes a larger voltage variance at the middle bus compared to the SCPSS.

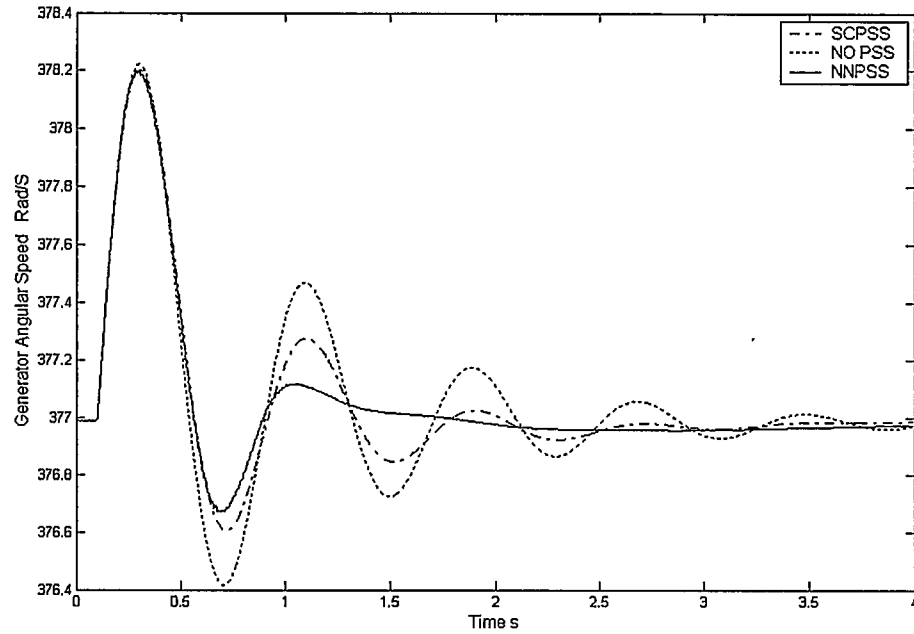


Figure 4.5 Generator Angular Speed in Response to a 0.2 p.u. Step Increase in Torque. Initial Condition $P=0.7$ p.u., p.f. = 0.85 lag

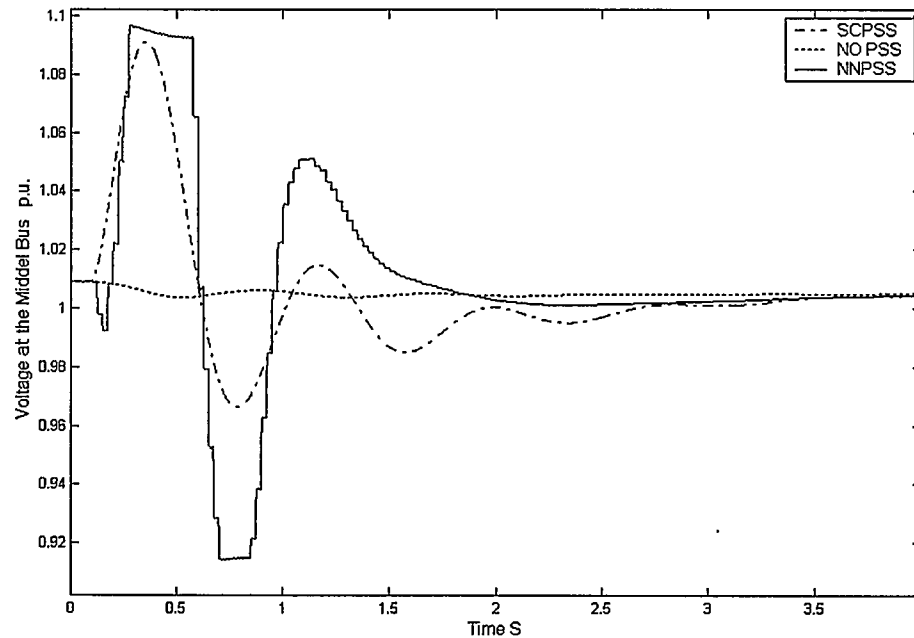


Figure 4.6 Voltage at the Middle Bus in Response to a 0.2p.u. Step Increase in Torque. Initial Condition $P=0.7$ p.u., p.f. = 0.85 lag

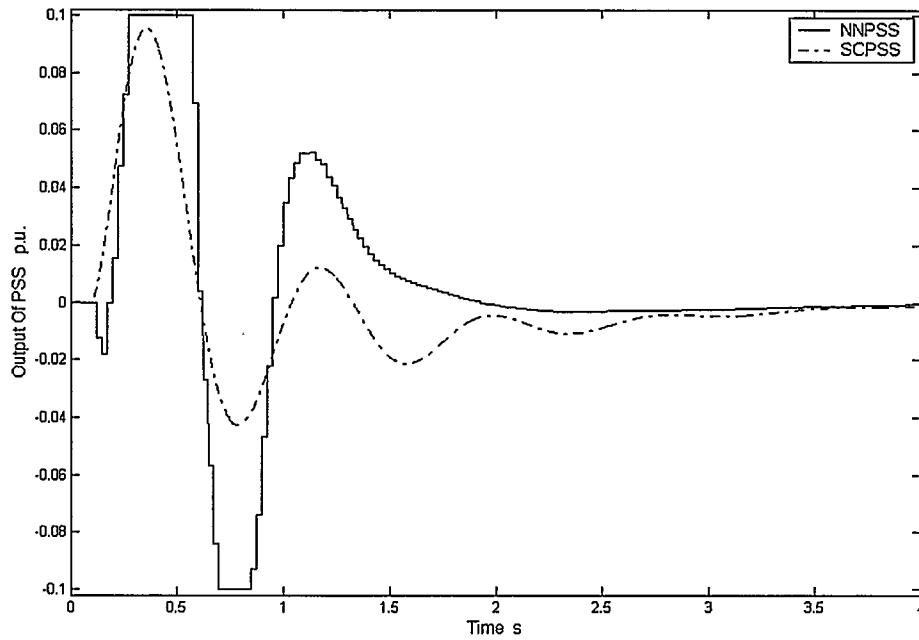


Figure 4.7 Output of PSS in Response to a 0.2 p.u. Step Increase in Torque. Initial Condition $P=0.7$ p.u., p.f. = 0.85 lag

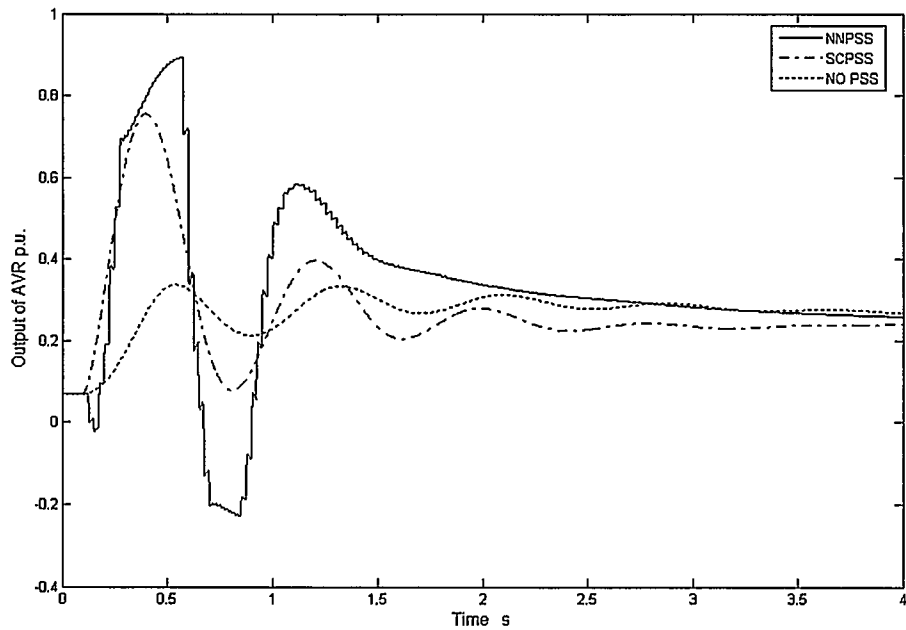


Figure 4.8 Output of SAVR in Response to a 0.2p.u. Step Increase in Torque. Initial Condition $P=0.7$ p.u., p.f. = 0.85 lag

The output of the PSS in Fig. 4.7 and the output of the AVR in Fig. 4.8 show the difference of the response between the SCPSS and the NNPSS. It is obvious that the NNPSS has better response than the CPSS when the SVC capacity is sufficient.

4.5.3 Leading Power Factor Condition

This test is conducted at the condition of $P=0.7$ p.u. and $p.f. = 0.9$ lead. The disturbance is applied at 0.1 s with a 0.2 p.u. step increase in the mechanical torque. The speed deviation of the generator and voltage variation at the middle bus are shown in Figs. 4.9 and 4.10, respectively.

The results show that the NNPSS has a better performance in the oscillation damping than the SCPSS.

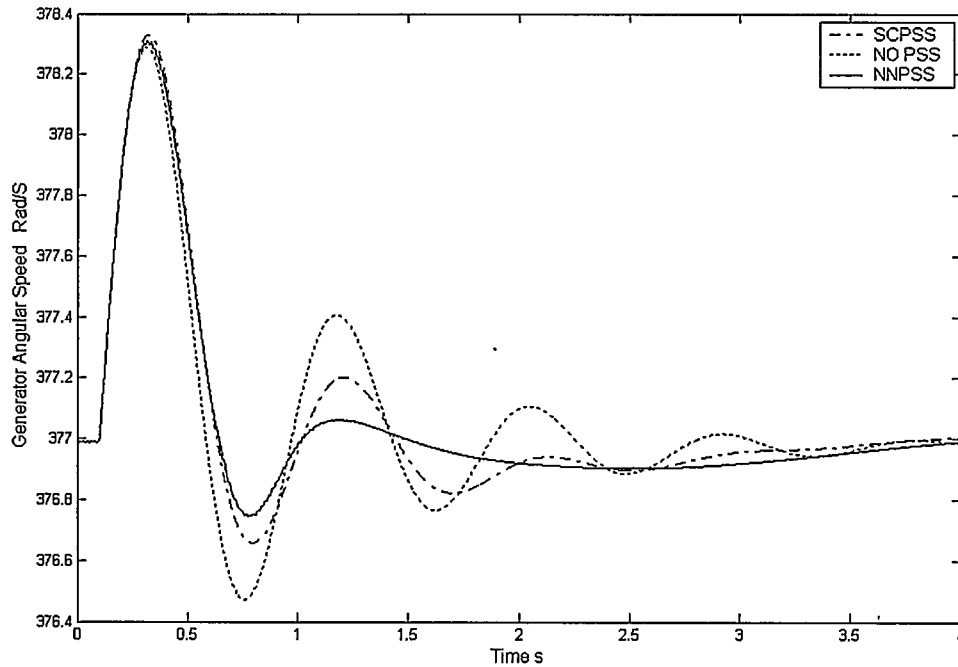


Figure 4.9 Generator Angular Speed in Response to a 0.2p.u. Step Increase in Torque. Initial Condition $P=0.7$ p.u., $p.f. = 0.9$ lead

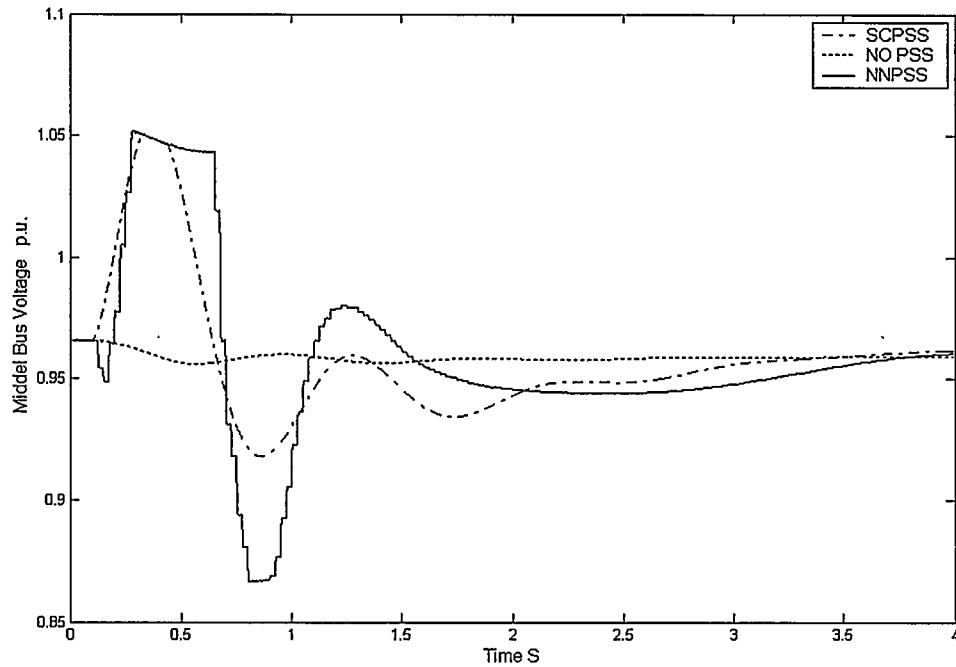


Figure 4.10 Voltage at the Middle Bus in Response to a 0.2p.u. Step Increase in Torque. Initial Condition $P=0.7$ p.u., p.f. = 0.9 lead

4.5.4 Light Load Test

In this section, the generator operating condition is changed to $P = 0.2$ p.u. and p.f. = 0.85 lag, and a 0.2 pu step increase of the input mechanical torque is applied at 0.1 s. The response of the system is shown in Fig. 4.11 and 4.12.

It is seen that at this operating condition both the NNPSS and the SCPSS have better performance at the first peak than in the normal condition. After the first peak, the NNPSS can take full advantage of the SVC capacity to damp the system oscillations. Therefore, the NNPSS has better damping performance than the SCPSS.

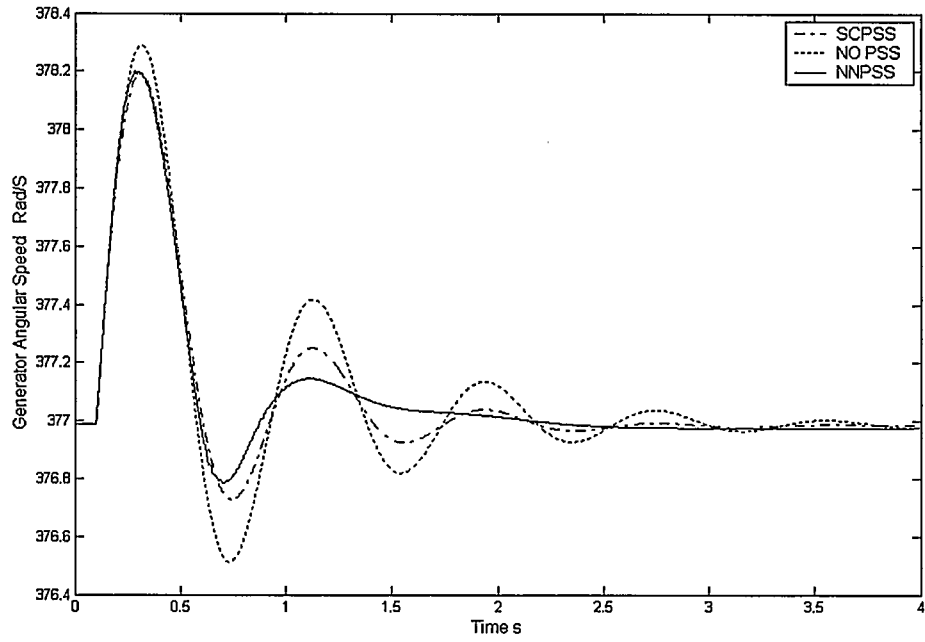


Figure 4.11 Generator Angular Speed in Response to a 0.1 p.u. Step Increase in Torque. Initial Condition P=0.2 p.f.=0.85 lag

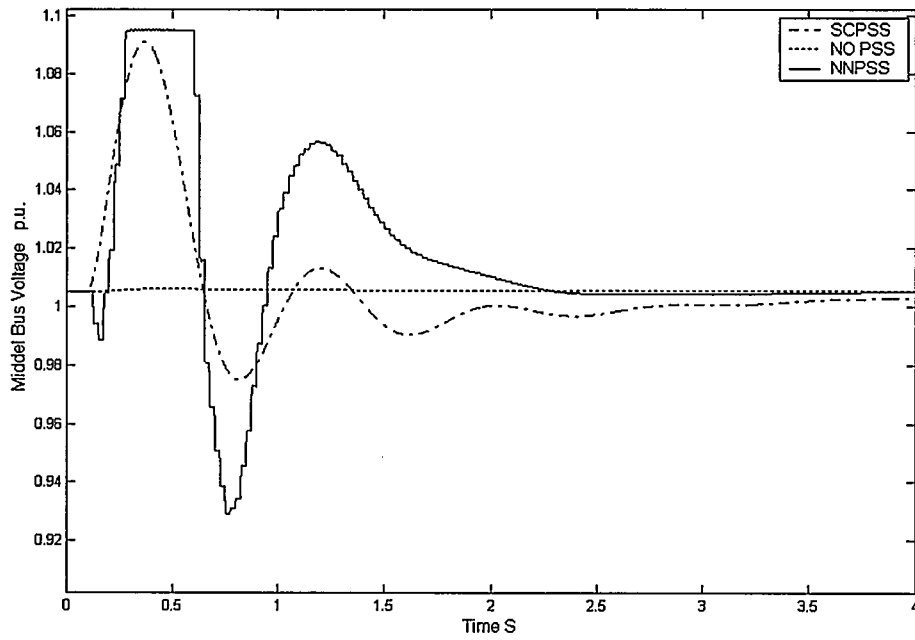


Figure 4.12 Voltage at the Middle Bus in Response to a 0.2p.u. Step Increase in Torque. Initial Condition P=0.2p.u., p.f. = 0.85 lag

4.5.5 Voltage Reference Change of the Generator Bus

The voltage reference of the generator bus has a 0.03 p.u. step increase with the initial condition of $P = 0.7$ p.u. and p.f. = 0.85 lag. Figs 4.13 through 4.14 show the generator speed variation and the voltage response at the middle bus.

The variation of the generator angular speed shows that both the SCPSS and the NNPSS can improve the system stability and there is no obvious difference between these two types of PSSs. The improvement of damping function of the NNPSS in this case is not as obvious as that in a major disturbance. Considering the system oscillation in this case is very small, only 0.1 rad/s, the improvement is not important in the operating condition.

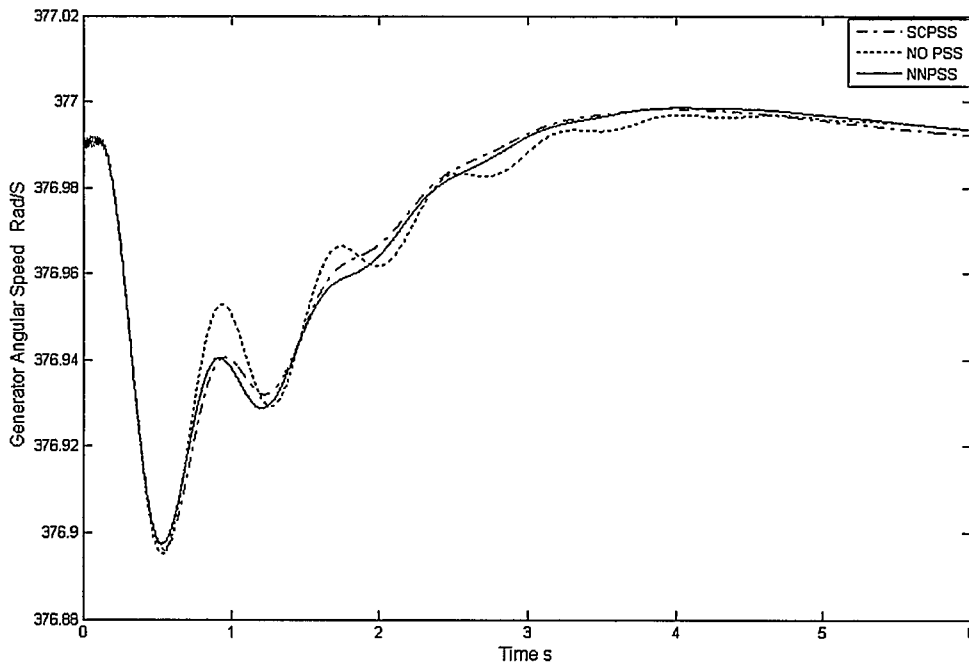


Figure 4.13 Generator Angular Speed in Response to a 0.03 p.u. Step Increase in the Voltage Reference of the Generator Bus. Initial Condition $P=0.7$ p.u., p.f. = 0.85 lag

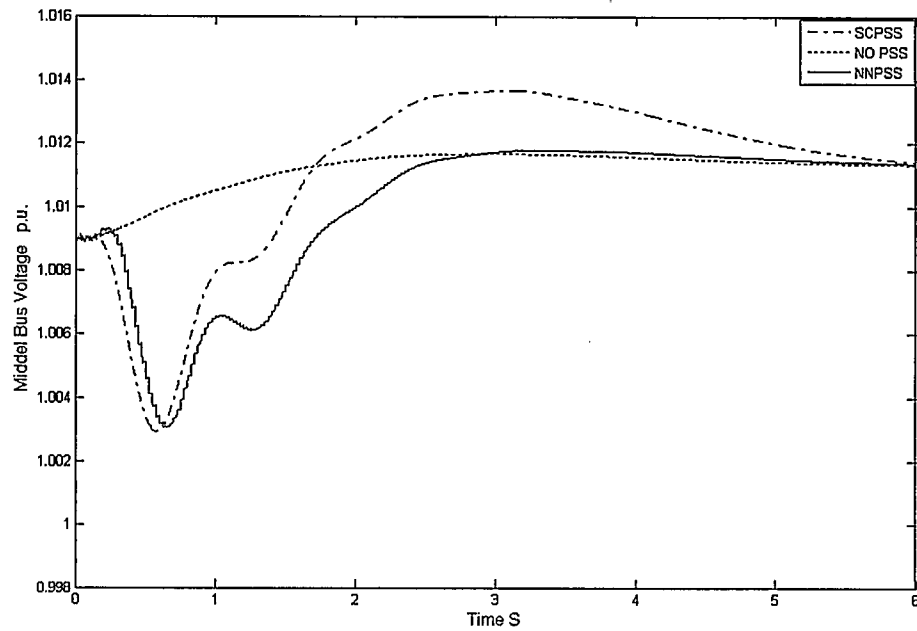


Figure 4.14 Voltage at the Middle Bus in Response to a 0.03 p.u. Step Increase in the Voltage Reference of the Generator Bus. Initial Condition $P=0.7$ p.u., p.f. = 0.85 lag

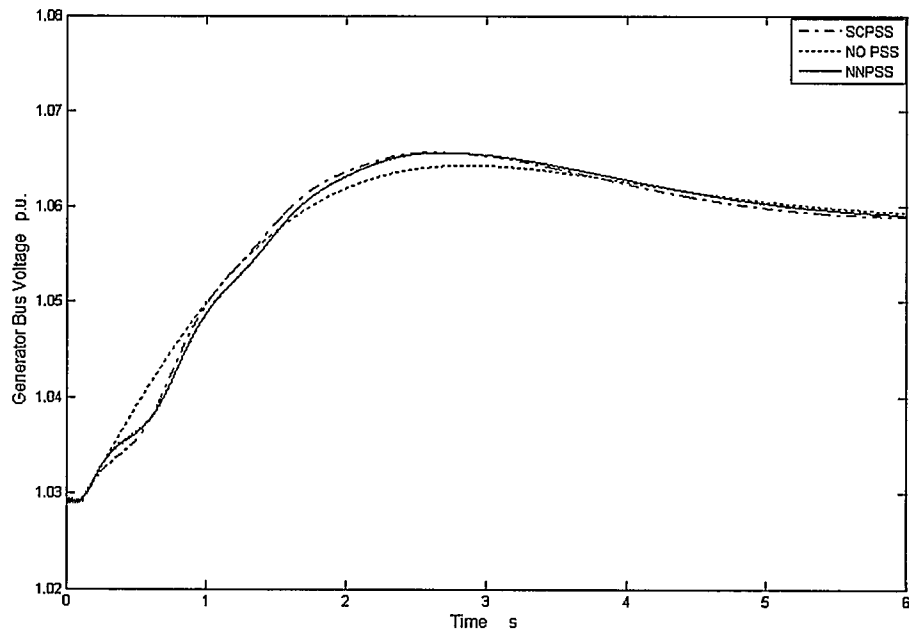


Figure 4.15 Generator Bus Voltage in Response to a 0.03 p.u. Step Increase in The Voltage Reference of The Generator Bus. Initial Condition $P=0.7$ p.u., p.f. = 0.85 lag

However, from the point of view of voltage, the NNPSS can make the middle bus voltage calm down much faster than the SCPSS and does not have any adverse impact on the damping function. Therefore, the NNPSS is better than the SCPSS.

4.5.6 Voltage Reference Change of the Middle Bus

The behaviour of the NNPSS and the SCPSS is shown in Figs. 4.16 through 4.18 when the voltage reference of the middle bus has a 0.04 p.u. step increase in the condition of $P = 0.7$ p.u. and $p.f. = 0.85$ lag.

The result on the generator speed variation shows that there is no obvious difference between the NNPSS and the SCPSS. Just like the last test, the system oscillation caused by

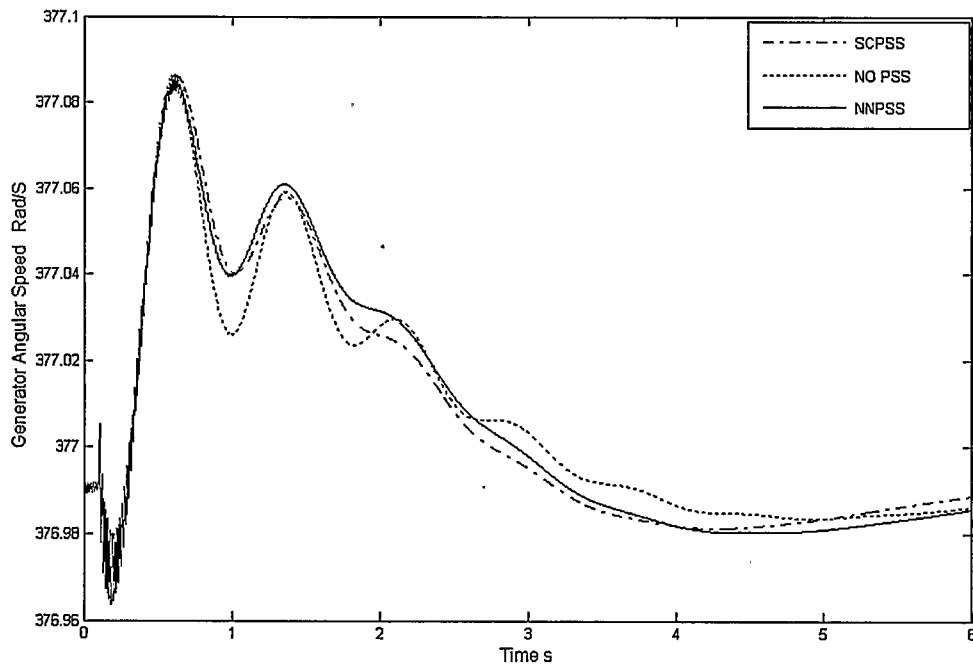


Figure 4.16 Generator Angular Speed in Response to a 0.04 p.u. Step Increase in the Voltage Reference of the Middle Bus. Initial Condition $P=0.7$ p.u., $p.f.=0.85$ lag

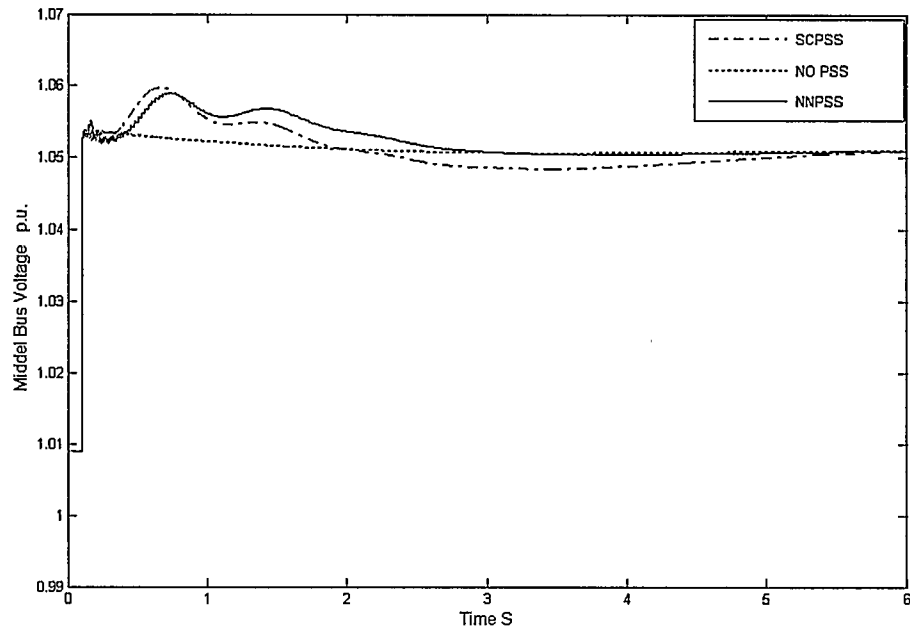


Figure 4.17 Voltage at the Middle Bus in Response to a 0.04 p.u. Step Increase in the Voltage Reference of the Middle Bus. Initial Condition $P=0.7$ p.u., p.f. = 0.85 lag

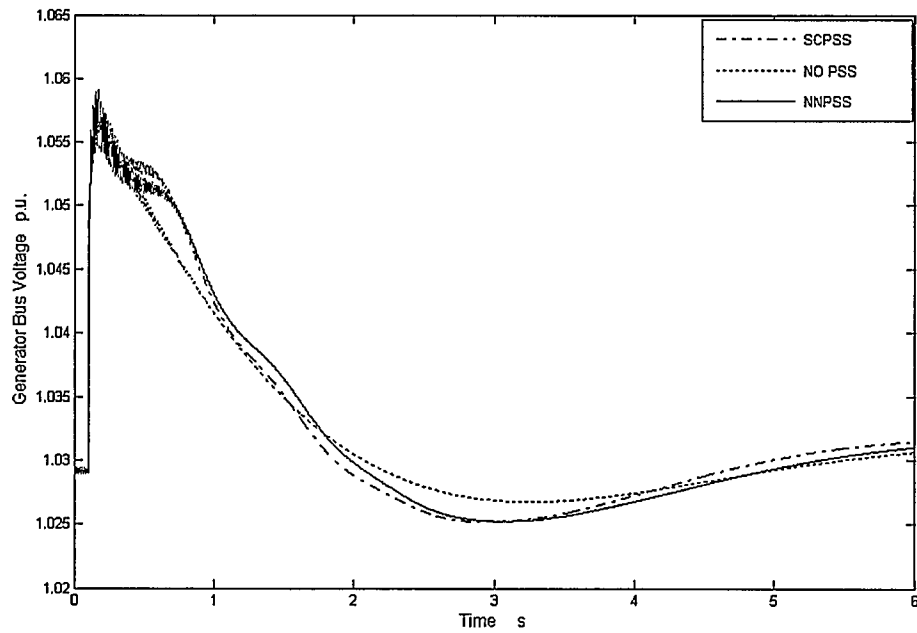


Figure 4.18 Generator Bus Voltage in Response to a 0.04 p.u. Step Increase in the Voltage Reference of the Middle Bus. Initial Condition $P=0.7$ p.u., p.f.=0.85 lag

voltage reference change is very small because two AVRs in the system also improve the system stability.

As different AVR models are selected for the generator and the SVC, the voltage curve, which is different from that in the last test, is a step change rather than a gradually converged curve. In the GAVR, there is a feedback from the output of the GAVR back to the input. This characteristic can make the system voltage change more smoothly. The SAVR does not have the feedback, so its output changes very sharp. The result of the damping function is the same as in the last test. The NNPSS is better than the SCPSS only because the voltage response of the NNPSS converges faster.

4.5.7 Different Sampling Intervals

In this test, three different sampling intervals, 20ms, 25ms and 30ms, have been used to compare the system response to the same system disturbance. The system operating condition is set as $P=0.7$ p.u. and $p.f.=0.85$ lag. In the simulation, a 0.2 pu step increase in the mechanical torque of the generator is applied at 0.1 s and the results are shown in Figs. 4.19 and 4.20.

The results show that all three sampling frequencies can provide effective damping and no obvious difference on the effectiveness of damping exists among them. All three settings can provide satisfactory result.

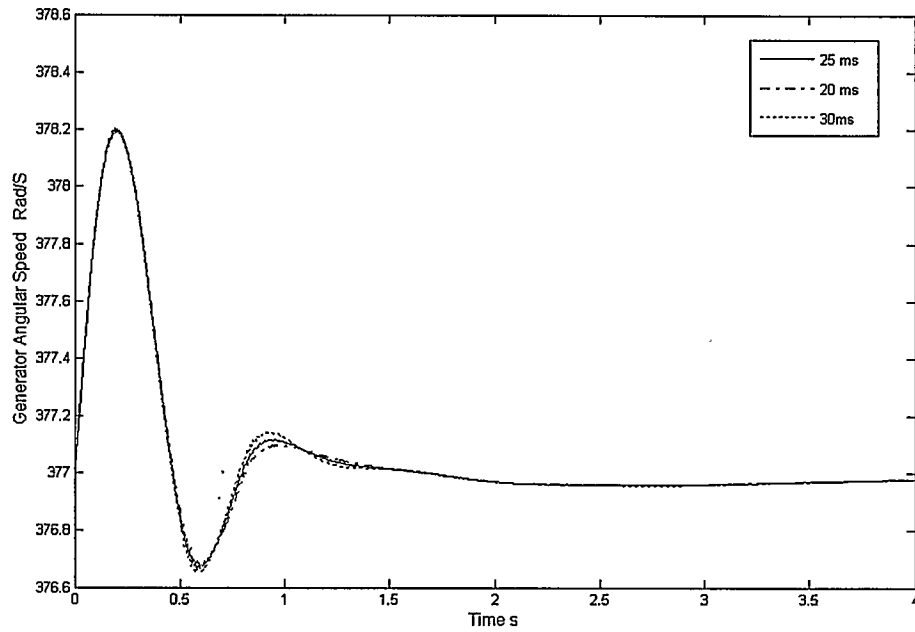


Figure 4.19 Generator Angular Speed in Response to a 0.2 p.u. Torque Increase at Different Sampling Intervals. Initial Condition $P=0.7$ p.u., p.f. = 0.85 lag

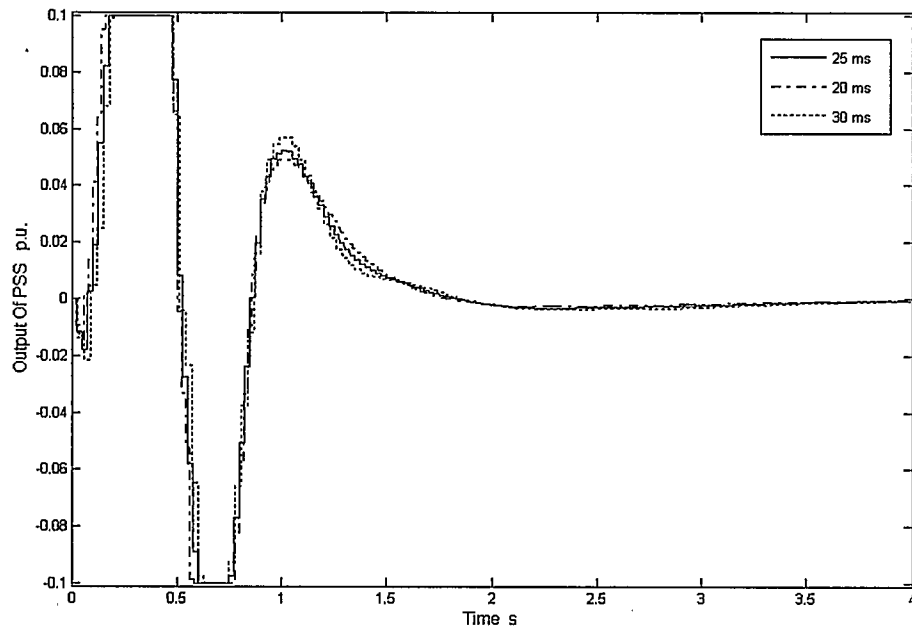


Figure 4.20 Output of PSS in Response to a 0.2 p.u. Torque Increase at Different Sampling Intervals. Initial Condition $P=0.7$ p.u., p.f. = 0.85 lag

4.5.8 Three Phase Short Circuit Test

Short circuit faults are the most common major disturbances in the power system operation. Among the different types of short circuits, three-phase short circuit fault usually is the most severe one. Therefore, three-phase short circuit fault is chosen to do this test. The fault is applied on one transmission line very close to the generator bus and the three-phase short circuit fault lasts for 0.1s. Figs. 4.21 and 4.22 show the performance of the system. Output of the PSS and SAVR is shown in figs. 4.23 and 4.24, respectively.

Starting from the second peak shown in Fig 4.21, both the NNPSS and the SCPSS provide the effective damping of the system. As long as the output of the PSS does not hit the limits, which is obvious in Fig. 4.24, the NNPSS is more effective for damping than SCPSS.

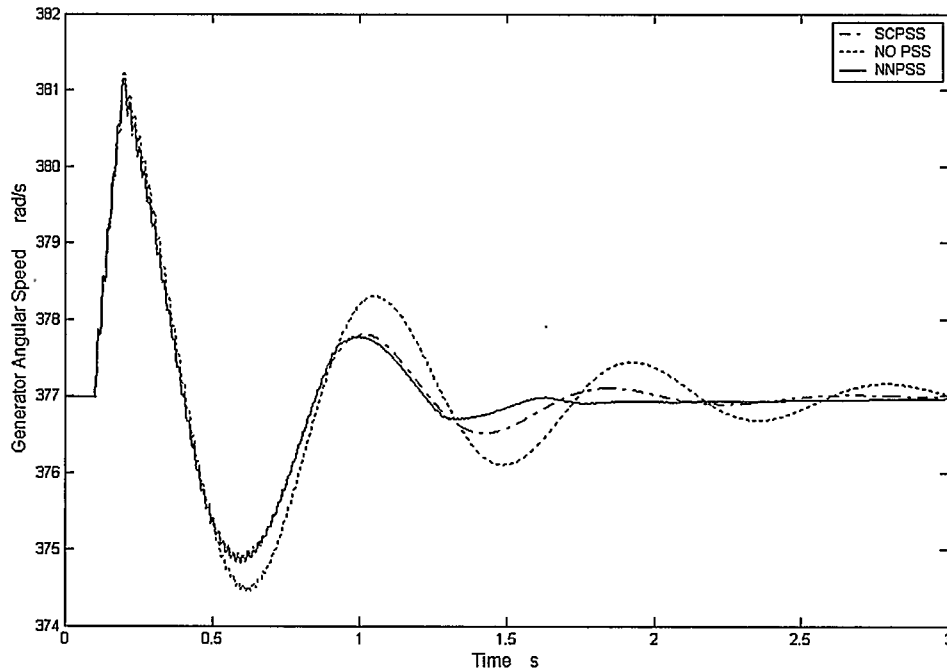


Figure 4.21 Generator Angular Speed in Response to a Three Phase Short Circuit at a Tie Line Close To The Generator Bus. Initial Condition $P=0.7$ p.u., p.f. = 0.85 lag

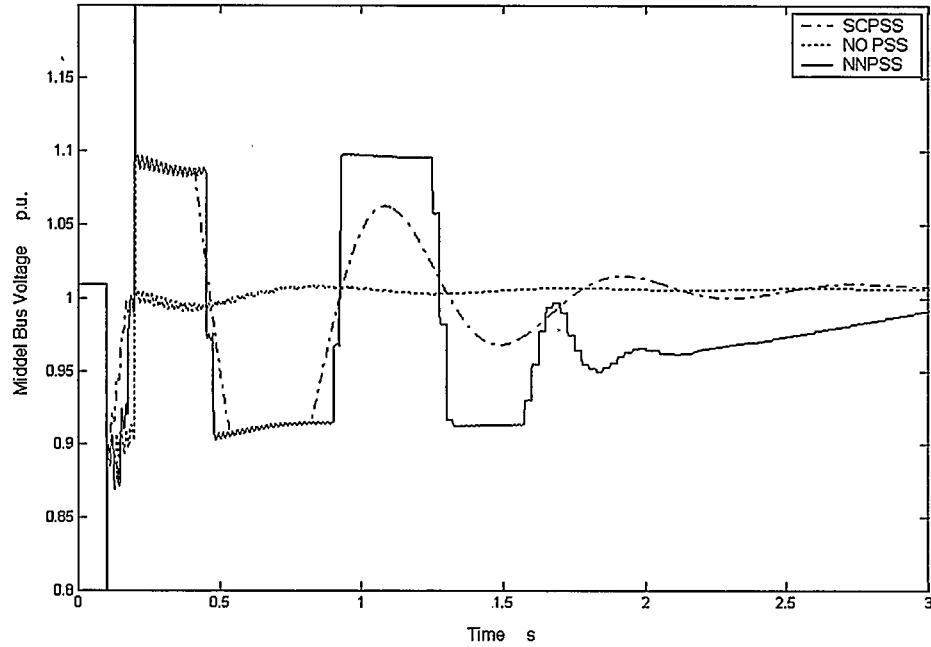


Figure 4.22 Voltage at the Middle Bus in Response to a Three Phase Short Circuit at a Tie Line Close to the Generator Bus . Initial Condition $P=0.7\text{p.u.}$, $\text{p.f.} = 0.85$ lag

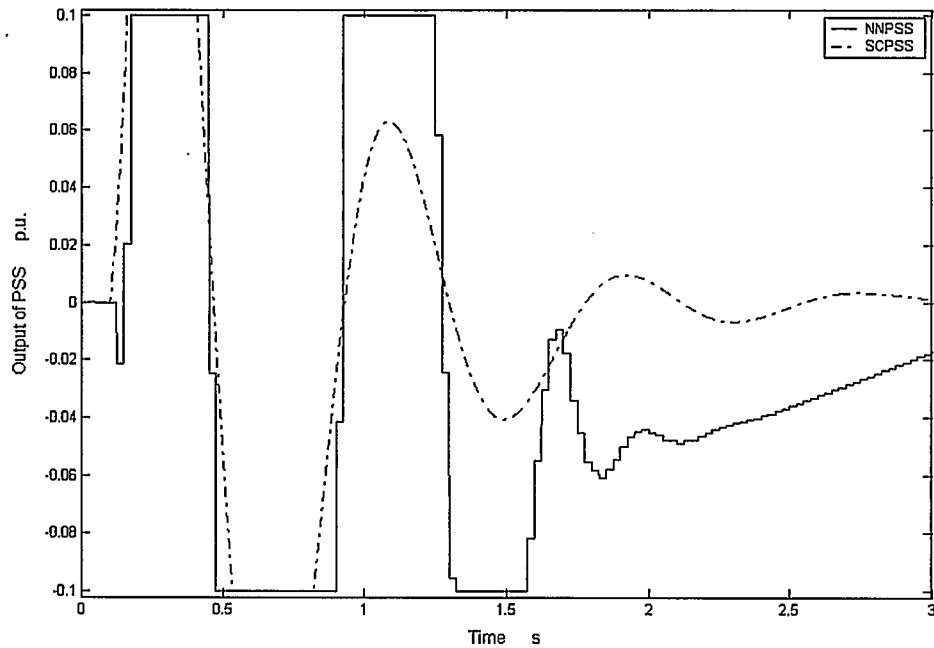


Figure 4.23 Output Of PSS in Response to a Three Phase Short Circuit at a Tie Line Close to the Generator Bus. Initial Condition $P=0.7\text{p.u.}$, $\text{p.f.} = 0.85$ lag

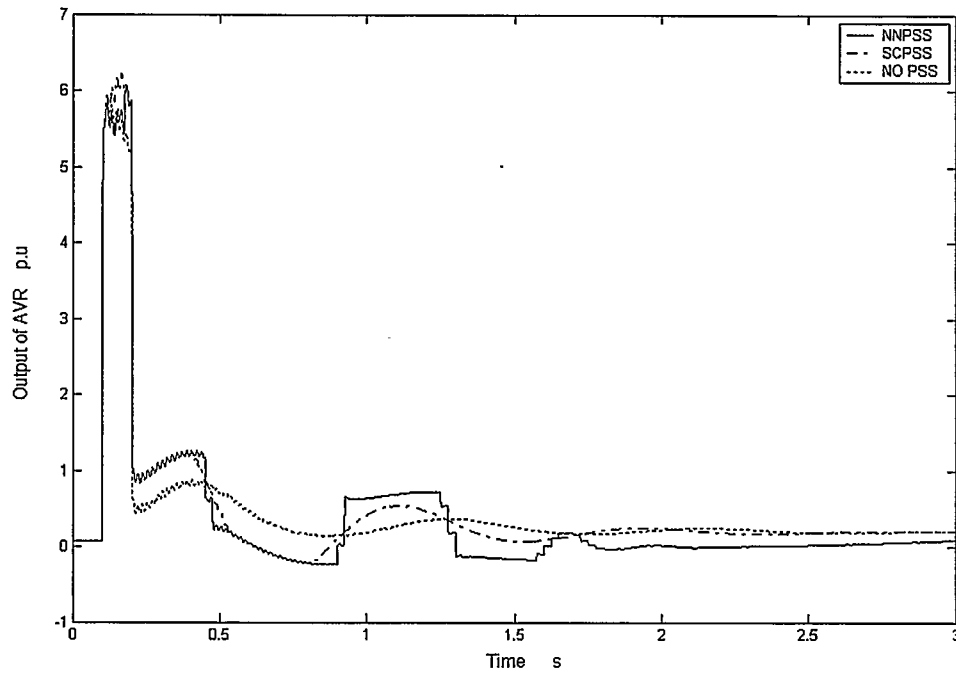


Figure 4.24 Output Of SAVR in Response to a Three Phase Short Circuit at a Tie Line Close to the Generator Bus. Initial Condition $P=0.7\text{p.u.}$, $\text{p.f.} = 0.85$ lag

The middle bus voltage dip during the fault shown in Fig. 4.22 is greatly reduced by the strong output of the SVC AVR shown in Fig. 4.24. Neither the CPSS nor the NNPSS has any adverse impact on the function of the SAVR.

- **Three phase short circuit fault with successful reclosure**

A three-phase short circuit fault occurs at 0.1 s, is cleared at 0.2 s by disconnecting the tie line and the line is reclosed successfully at 5 s. The result in Fig 4.25 shows that the transient performance of the NNPSS is more stable and better than that of the SCPSS.

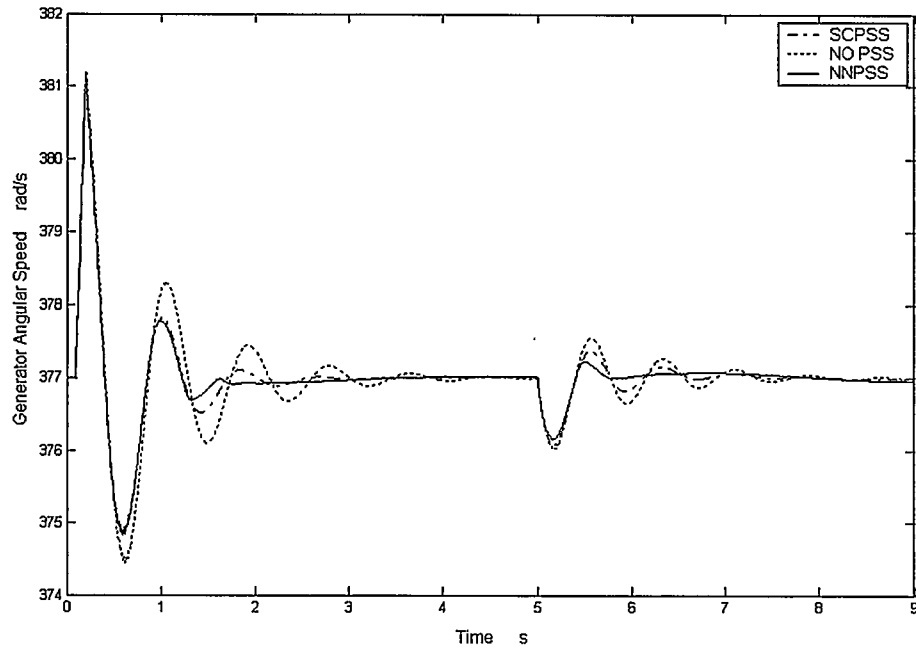


Figure 4.25 Generator Angular Speed in Response to a Three Phase Short Circuit with Successful Reclosure at a Tie Line Close to the Generator Bus. Initial Condition $P=0.7$ p.u., p.f. = 0.85 lag

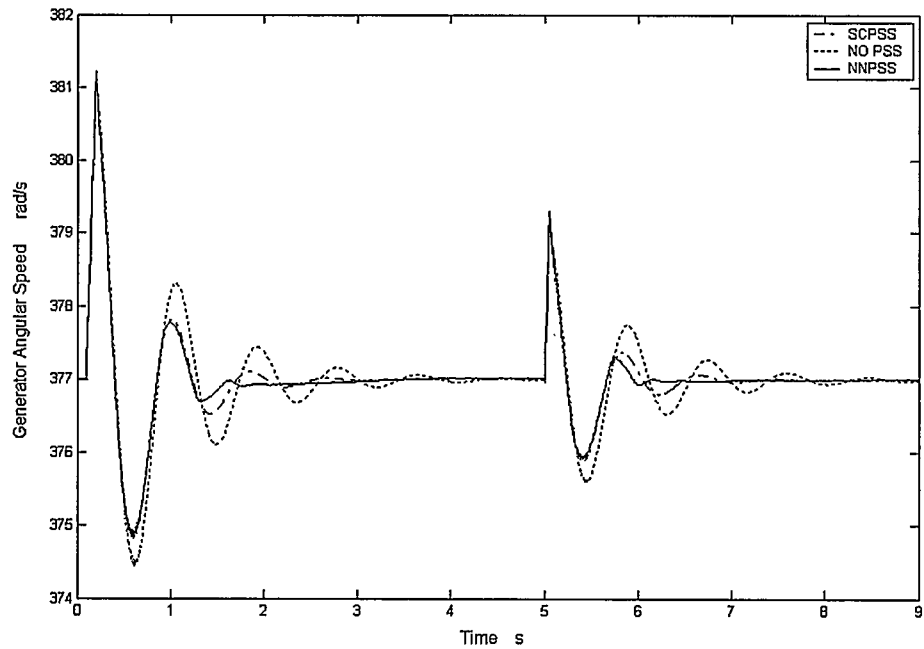


Figure 4.26 Generator Angular Speed in Response to a Three Phase Short Circuit with Unsuccessful Reclosure at a Tie Line Close to the Generator Bus. Initial Condition

4.5.9 Comparisons of the Damping Effectiveness between Generator PSS and the Proposed SVC Controller

A comparison of the system responses to a 0.2 pu increase in torque with different PSS configurations is shown in Fig 4.27 with the system operating at $P=0.7$ pu , 0.85 p.f. lag. It can be seen from the results that the GPSS is general provides more effective damping than the SCPSS as the GPSS can directly control the generator exciter. The damping function of the NNPSS in the first and second peaks is not as effective as the GPSS, but after that, the NNPSS is more effective. From the point view of the overall effectiveness, the NNPSS is the best among the three.

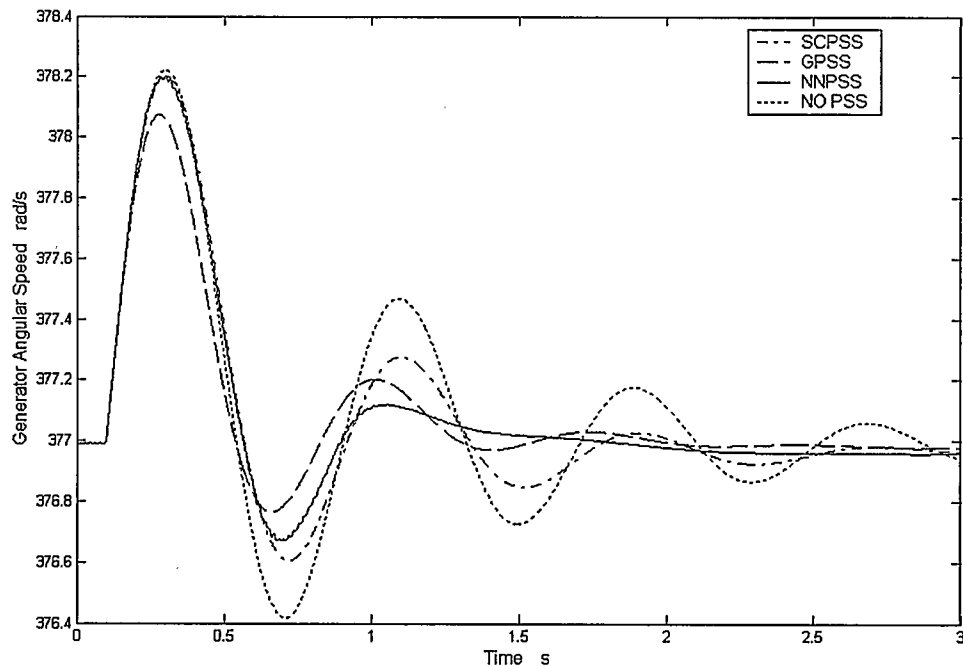


Figure 4.27 Different PSS Configurations in Response to a 0.2 p.u. Increase in Torque.

Initial Condition $P=0.7$ p.u., p.f. = 0.85 lag

4.5.10 Test of the Coordination with the Generator CPSS

In the practical system, SVCs usually are installed separately to improve the system voltage stability. It means that the SVC controller may work together with a generator PSS (GPSS). A test was performed to compare the performance of three PSS combinations, the system with only an NNPSS, the system with an SCPSS and a GPSS, and the system with a GPSS and an NNPSS, during a major disturbance of three-phase short circuit very close to the generator bus. The system performance is shown in Fig. 4.28. In order to make the comparison clearer, Fig 4.28 with the vertical scale enlarged is shown in Fig 4.29.

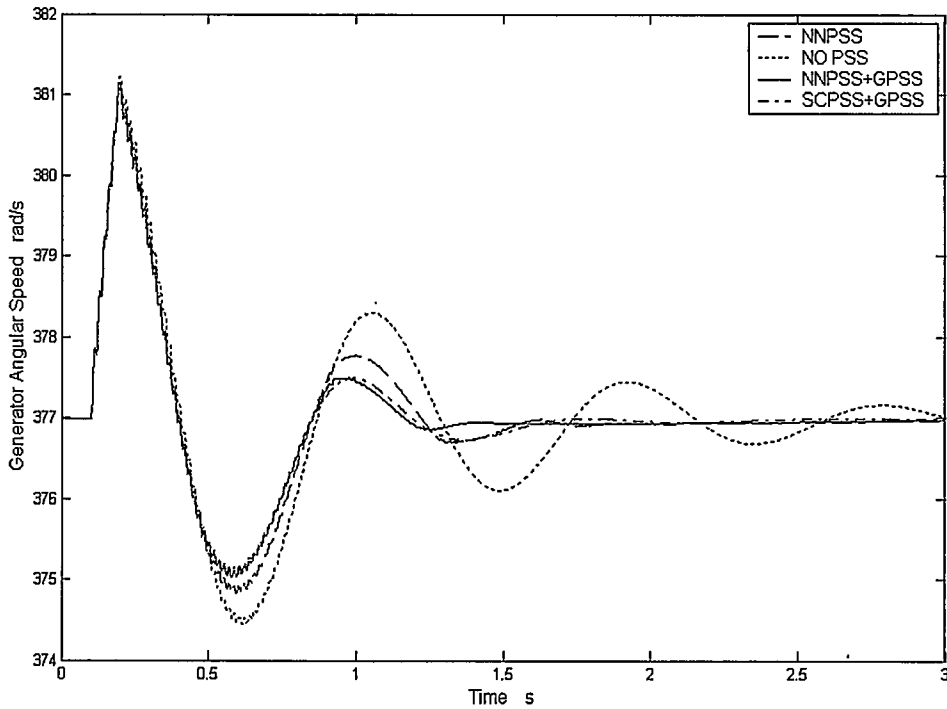


Figure 4.28 Different PSS Combinations in Response to a 3 Phase Short Circuit Lasting for 0.1s. Initial Condition $P=0.7$ p.u., p.f. = 0.85 lag

It can be seen from Fig 4.28 that SVC PSS can coordinate with the GPSS to damp the system oscillation faster and without any adverse impact. A combination of a GPSS and an SVC PSS is more effective than the system having only one of them. The combination of a GPSS with an NNPSS can stabilize the system faster than the combination of an SCPSS with a GPSS. The results in Fig. 4.29 show that the NNPSS can coordinate with a GPSS and the combination has the best performance among the three different configurations.

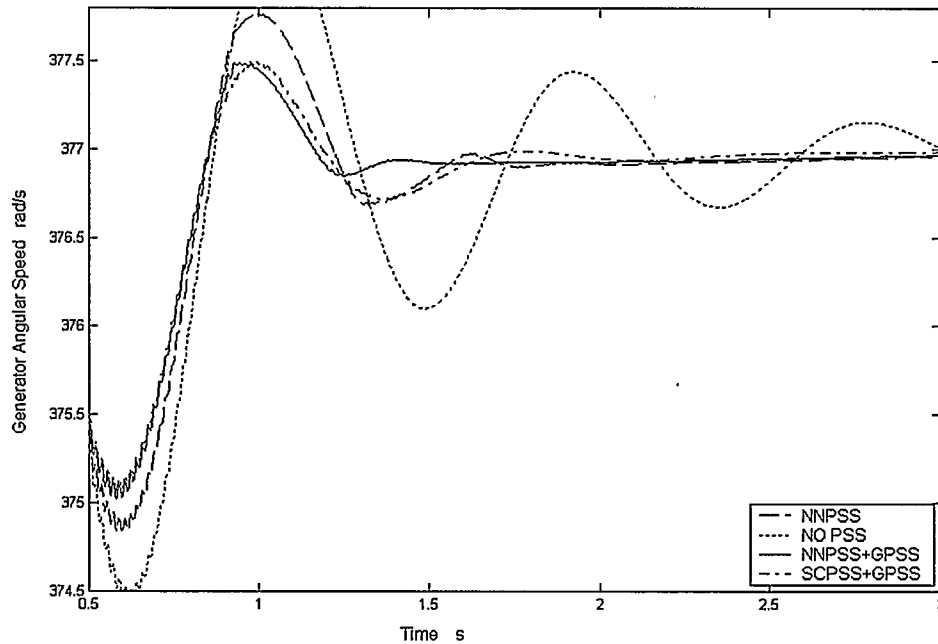


Figure 4.29 Enlarged Fig. 4.27. Initial Condition $P=0.7$ p.u., $p.f. = 0.85$ lag

4.5.11 Test of the Stability Margin

In the simulation, the inputs of the mechanical torque applied on the systems with different PSS configurations are continuously increased at a rate of 0.001 p.u. per second

and the initial condition is $P=1.22$ p.u and $p.f = 0.9$ lag. From the results shown in Fig. 4.30, stability margin of the system with the NNPSS is greater than with the CPSS.

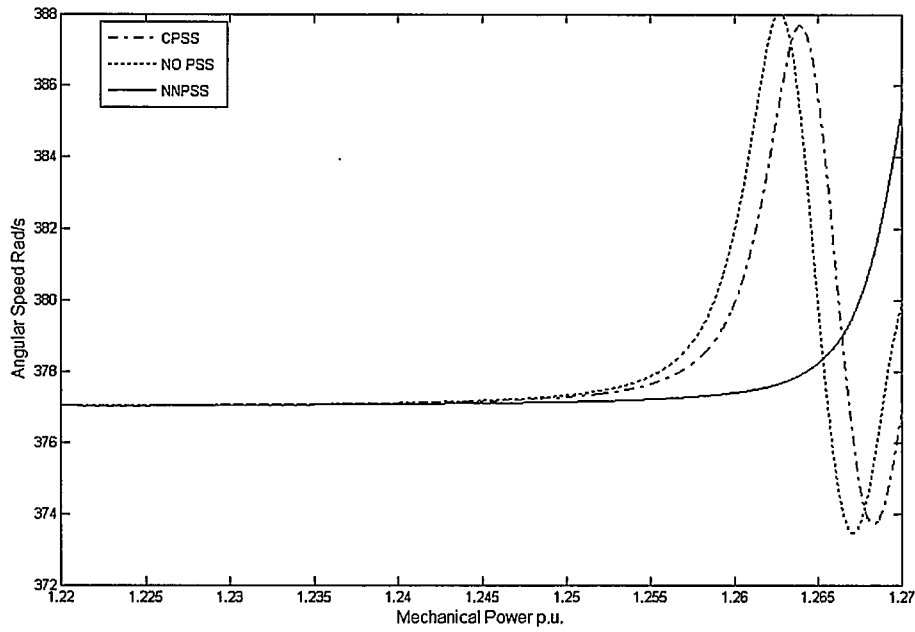


Figure 4.30 Generator Speed in Response to a Continuous Mechanical Torque Increase at the Rate of 0.001 p.u per Second. Initial Condition $P=1.22$ p.u., $p.f. = 0.90$ lag

4.6 Summary

Performance of the proposed neural network based SVC controller has been tested in a single machine infinite bus power system with an SVC at the middle bus. Results of the simulation studies given in this chapter show that the proposed SVC controller has the following advantages:

- The proposed NNPSS is not designed for any fixed operating condition. The NNPSS can operate at a wide range of operating conditions with a stable and

reliable performance. It can be seen from the results that the proposed NN controller can provide better performance than the traditional linearized control design method.

- The design of the proposed controller and simulation studies are based on the seventh order generator model, which can closely simulate the complexity and the nonlinearity of the real power system.
- The proposed NN controller only uses one neural network for both the system parameter identification and control, so the computational complexity is reduced compared to other neural network control design methods.
- The proposed controller can coordinate with another PSS on the generator in the system and work together to make the system oscillation damping more efficient.

In summary, the proposed controller achieves the design objective and has better performance than the conventional controller.

CHAPTER 5

CONCLUSIONS AND FUTURE STUDIES

After many years of development to enhance power system stability, many kinds of power system stabilizers have been developed and applied in practical systems. The application of generator PSSs greatly improved power system stability. The fast development of Flexible AC Transmission System (FACTS) in recent years has provided the potential that these static components can be also used for the system oscillation damping. SVCs are widely used in power systems as dynamic reactive power compensation devices controlled dynamically by adjusting the firing angle of power electronic elements to adjust their output.

The most widely used type of SVCs is the so-called multi-level cascading converter comprised of several levels of converters and storage devices. It can supply reactive power to the system or absorb reactive power from the system through SVC controllers. An SVC controller usually includes an automatic voltage regulator (AVR) and a supplementary controller, power system stabilizer (PSS). AVR is in charge of the voltage regulation to keep the system voltage in a certain level to support the power transmission and PSS is used to damp system oscillations if the system meets any disturbance.

Conventional PSSs (CPSS) use the linearized system model to design the controller, so it usually has better performance for a certain system operating condition. As power systems are highly nonlinear and uncertain, CPSS cannot provide a stable performance for

various operating conditions. In order to solve this problem, advanced control design algorithms such as adaptive control and intelligent control are being investigated.

In this dissertation, a neural network based SVC controller is developed on the base of direct control theory. Conclusions of the research and future studies are summarized below.

5.1 Conclusions

The purpose of the dissertation is to develop a design technique for the neural network based SVC controller with guaranteed performance. The mathematical analysis and simulation studies show that the controller can greatly improve the system stability during internal or external disturbances.

- The proposed controller is based on a multilayer neural network, which has one input layer, two hidden layers and one output layer. There are ten neurons in each hidden layer and one neuron in the output layer. The neurons in the hidden layers use the hyperbolic tangent function as the activation function. The output layer is a linear layer to adjust the magnitude of the output. Simulation studies show that the network can closely approach the nonlinear system and can coordinate with the filtered direct control to damp power system oscillations.
- The discrete time filtered direct control algorithm is used to design the proposed controller that has only one neural network to do both the system identification and control. The weights of the network are dynamically updated according to the filtered error of the entire closed-loop system. The projection algorithm and

the modified Delta rule are used to update the weights of the neural network. By using the Lyapunov stability theory, the stability of the entire control algorithm is verified.

- The input signals of the supplementary controller and the network are selected as the deviation of the generator angular speed and its two delays. The filter order of the controller is three. The simulation results show that the selected filter order is sufficient for the system control to correct the error of the entire close loop system.
- The proposed neural network based PSS (NNPSS) has been tested in a single machine infinite bus system. In the system, a seventh order generator model was used to test the effectiveness of the controller and an SVC was set at the middle bus of the system. The simulation studies were conducted at different operating conditions from light load to heavy load, lagging power factor to leading power factor. The simulation results show that the neural network based SVC controller has a very good performance at the different operating conditions. The controller can improve the stability of the power system and has achieved the expected damping objective.
- Comparison studies between an SVC CPSS and the proposed SVC NNPSS have been conducted in different operating conditions. The results show that the NNPSS gives better performance in various operating and fault conditions than the CPSS. The damping effectiveness of the Generator CPSS, the SVC CPSS and the proposed SVC NNPSS was also compared through simulation studies.

The SVC NNPSS has better performance than the Generator CPSS in the test system whereas the Generator CPSS is better than the SVC CPSS.

- The coordination of an SVC controller and a generator CPSS has been investigated. The simulation studies show that they can cooperate with each other very well without any adverse damping function and the coordination can further improve the system stability

5.2 Future Studies

In order to get the maximum benefits of the proposed neural network based SVC controller in the practical system, further studies may be carried out. Based on this dissertation, the following topics are recommended for future research.

- The performance of the proposed control algorithm in a multi-machine system should be conducted in the future to verify the coordination between the controller and the generators.
- The proposed controller should be physically realized in a laboratory environment to verify the effectiveness of the control theory in a physical system.
- In the dissertation, the proposed controller uses the multilayer perceptron neural network as the objective network. In the recent years, more neural network structures have been developed. These new network structures should be compared to find if any new network structure could have a faster learning rate and better performance to further reduce the computational complexity.

REFERENCE

- [1]. “NERC Planning Standards”, *North American Electrical System Reliability Council*, September, 1997
- [2]. C.K. Lee, S.K. Leung “ Circuit-Level Comparison of STATCOM Technologies”, *IEEE Transaction on Power Electronics*, Vol. 18, No. 4, July 2003, pp 1084 – 1092
- [3]. Z. Zhang, N.R. Fahmi, “Modelling and Analysis of a Cascade 11-level Inverters-Based SVG with Control Strategies for Electric Furnace Application”, *IEE Proceedings, Gener. Transm. Distrib.* , Vol. 150, No.2, March 2003, pp 217 – 223
- [4]. Yiqiang Chen, Boon-Teck Ooi, “ STATCOM Based on Multi-modules of Multilevel Converters Under Multiple Regulation Feedback Control”, *IEEE Transaction on Power Electronics*, Vol. 14, No. 5, September 1999, pp 959 –965
- [5]. Clark Hochgraf, Robert H. Lasseter, “A Transformer-less Static Synchronous Compensator Employing a Multi-level Inverter ” , *IEEE Transaction on Power Delivery*, Vol. 12 , Issue: 2 , April 1997, pp 881 – 887
- [6]. William D. Stevenson, “Elements of Power System Analysis”, McGraw-Hill, 1989
- [7]. P. Kundur, “ Power System Stability and Control”, McGraw-Hill, 1994.
- [8]. Jian He, “Adaptive Power System Stabilizer Based on Recurrent Neural Network ”, *PhD Thesis*, University of Calgary, 1998
- [9]. Antal Soos, “An Optimal Adaptive Power System Stabilizer ”, *M.sc Thesis*, University of Calgary, 1997
- [10]. E. Lerch, “Advanced SVC Control for Damping Power System Oscillations”, *IEEE Transactions On Power Systems*, Vol. 6, May 1991, No.2, pp 524 – 535

- [11]. Mehrdad Ghandhari, "Application of Control Lyapunov Functions to Static Var Compensator", *IEEE Proceedings of the 2002 International Conference on Control Applications*, Vol. 1, Sept. 2002, pp 18-20
- [12]. H.F Wang, "A Unified Model for the Analysis of FACTS Devices in Damping Power System Oscillations. I. Single-machine infinite-bus power systems", *IEEE Transaction on Power Delivery*, Vol. 12, Issue: 2, April 1997, pp 941 - 946
- [13]. H.F Wang, "Applications of Damping Torque Analysis to STATCOM Control", *Electrical Power & Energy Systems*, Vol. 22, 2000, pp 197-204
- [14]. C.A Canizares, Z.T. Faur, "Analysis of SVC and TCSC Controllers In Voltage Collapse", *IEEE Transactions on Power Systems* Vol. 14, February 1999, No.1 pp 158 – 165
- [15]. Ferdi Armansyah, Naoto Yorino, "Robust Synchronous Voltage Sources Designed Controller for Power System Oscillation Damping", *Electrical Power & Energy Systems*, Vol. 24, 2002, pp 41-49
- [16]. N. Hosseinzadeh A. Kalam, "A Direct Adaptive Fuzzy System Stabilizer", 4th *International Conference on Advances in Power System Control*, 1997 HONG KONG. pp 377-382
- [17]. Jang-Hyun Park, "Robustly Stable Fuzzy Controller for Uncertain Nonlinear System with Unknown Input Gain Sign", 2002. *Proceedings of the 2002 IEEE International Conference on Fuzzy Systems*, Vol. 1 , May 12-17, 2002, pp 639-643
- [18]. A.H.M.A Rahim, " Power System Damping Control Through Fuzzy Static Var Compensator Design Including Crisp Optimum Theory", *Intelligent Fuzzy Systems*, IOS Press, Vol. 11, 2001, pp 185-194

- [19]. Wenxin Liu, "Adaptive Neural Network Based Power System Stabilizer Design", *IEEE Proceedings of the International Joint Conference on Neural Networks*, Vol. 4, July 20 - 24, 2003, pp 2970 - 2975
- [20]. Takashi Hiyama, "Fuzzy Logic Control Scheme With Variable Gain for Static Var Compensator to Enhance Power System Stability", *IEEE Transactions On Power Systems*, Vol 14, Feb 1999, pp 186 – 191
- [21]. Martin T. Hagan, "Neural Networks for Control", *Literature*, School of Electrical & Computer Engineering, Oklahoma State University
- [22]. S. Jagannathan, "Discrete-Time CMAC NN Control of Feedback Linearizable Nonlinear Systems Under a Persistence of Excitation", *IEEE Transaction on Neural Networks*, Vol. 10, No. 1, January 1999, pp 128 – 137
- [23]. N. Hosseinzadeh, "A Rule-Based Fuzzy Power System Stabilizer Tuned by a Neural Network", *IEEE Transaction on Energy Conversion*, Vol. 14, No. 3, September 1999, pp 773 –779
- [24]. Shing-Chia Chen, Wen-Liang Chen, "Controller Design Using Walsh-Basis Function Neural Networks", *Proceedings of American Control Conference*, Vol. 5, June 25-27, 2001, pp 3551 – 3556
- [25]. Y J Cao, S J Cheng, "Sliding Mode Control of Non-linear Systems Using Neural Network", *International Conference on Control*, Vol. 1, Mar 21-24, 1994, pp 855 – 859
- [26]. Sarangapani Jagannathan, "Multilayer Discrete-time Neural-net Controller with Guaranteed Performance", *IEEE Transaction on Neural Network*, Vol. 7, No. 1, January 1996, pp 107 - 130

- [27]. Andrzej Janczak, "Neural Network Approach for Identification of Hammerstein Systems", *International Journal of Control*, Vol.76. 2003, pp 1749-1766
- [28]. Jean-Michel Renders " Adaptive Neurocontrol of MIMO Systems Based on Stability Theory", *IEEE International Conference on Neural Networks*, Vol. 4, June 27- July 2, 1994, pp 2476 – 2481
- [29]. Young-moon Park, "A Synchronous Generator Stabilizer Design Using Neuro Inverse Controller and Error Reduction Network", *IEEE Transaction on Power Systems*, Vol. 11, No. 4, November 1996, pp 1969 – 1975
- [30]. Ravi Segal, "Radial Basis Function (RBF) Network Adaptive Power System Stabilizer", *IEEE Transaction on Power Systems*, Vol. 15, No. 2, May 2000, pp 722 –727
- [31]. Ivica N. Kostanic, "Radial Basis Function Neural Network For Regulation of Nonlinear System", *IEEE Proceedings of the Southeastcon '96. 'Bringing Together Education, Science and Technology'*, April 11-14, 1996, pp 413 –416
- [32]. S. Commuri, "Discrete-Time CMAC Neural Networks for Control Applications", *Proceedings of the 34th IEEE Conference on Decision and Control*, Vol. 3, Dec. 13-15, 1995, pp 2420 – 2426
- [33]. S. Jagannathan, "Multilayer Neural Network Controller for A Class of Nonlinear Systems", *Proceedings of the 1995 IEEE International Symposium on Intelligent Control*, Aug. 27-29, 1995, pp 427 – 432
- [34]. Glanz, F.H.; Miller, W.T.; Kraft, L.G., "An Overview of the CMAC Neural Network" *IEEE Conference on Neural Networks for Ocean Engineering*, Aug. 15-17, 1991, pp 301 – 308

- [35]. H.K. Lam, "An ART-Based Construction of RBF Networks", *IEEE Transaction on Neural Networks*, Vol. 13, No. 6, November 2002, pp1308–1321
- [36]. Wood, R.J.; Gennert, M.A., "A Neural Network that Uses a Hebbian Back Propagation Hybrid Learning Rule", *International Joint Conference on Neural Networks*, Vol. 3, June 7-11, 1992, pp 863 – 868
- [37]. Alianna, Maren, "Handbook of Neural Computing Applications", *Academic Press, Inc.* ISBN 0-12-546090-6
- [38]. White, Sofge, "Handbook of Intelligent Control", *Van Nostrand Reinhold*. ISBN 0-442-30857-4
- [39]. Fuchuang Chen, "Back-propagation Neural Networks For Nonlinear Self-Tuning Adaptive Control", *IEEE, Control Systems Magazine*, Vol. 10, Issue: 3, April 1990, pp 44 - 48
- [40]. Nader Sadegh, "A Perceptron Network for Functional Identification and Control of Nonlinear Systems", *IEEE Transaction on Neural Networks*, Vol. 4, No. 6, November1993, pp 982-988
- [41]. Lewis, F.L.; Liu, K.; Yesildirek, A. "A Neural Net Robot Controller with Guaranteed Tracking Performance", *IEEE Transaction on Neural Networks*, Vol. 6, Issue: 3, May 1995, pp 703-715
- [42]. B.Widrow and E.Walach, "Adaptive Inverse Control ", *New Jersey: Prentice Hall*, 1996
- [43]. K.S. Narendra, " Identification and Control of Dynamical Systems Using Neural Networks ", *IEEE Transaction on Neural Networks*, Vol. 1, No. 1, March 1990, pp 4 – 27

- [44]. K.J. Hunt, D. Sbarbaro, "Neural Networks for Control System – A Survey ", *Automatica*, Vol. 28, 1992, pp 1083-1112
- [45]. Nadarajah Mithulananthan, "Comparison of PSS, SVC and STATCOM Controllers for Damping Power System Oscillations", *IEEE Transaction on Power Systems*, Vol. 18, No. 2, May 2003, pp 786–792
- [46]. E.Z. Zhou, "Application of Static Compensators to Increase Power System Damping", *IEEE Transaction on Power Systems*, Vol. 8, No. 2, May 1993, pp 655–661
- [47]. Hanxiang Cheng, "Control Analysis and Stability for Static Var Generator" IFAC Symposium on Power Plants and Power System Control, Korea, September 15-18, 2003, pp 527-532

APPENDIX

1. Generator

The generator model is based on the Park's seventh order model [7][8].

$$\dot{\lambda}_d = v_{gd} + r_s i_d + \omega_b (\omega + 1) \lambda_q$$

$$\dot{\lambda}_q = v_{gq} + r_s i_q - \omega_b (\omega + 1) \lambda_d$$

$$\dot{\lambda}_{kd} = -r_{kd} i_{kd}$$

$$\dot{\lambda}_{kq} = -r_{kq} i_{kq}$$

$$\dot{\lambda}_f = E_f - r_f i_f$$

$$\dot{\omega} = \frac{\omega_b}{2H} (T_m + gov + K_d \dot{\delta} - Te)$$

$$\dot{\delta} = \omega \omega_b$$

2. SVC

According to [12,22], the SVC can be modeled as a voltage source behind a step up transformer. The voltage along d and q axis is a function of the magnitude and angle of the DC voltage. The value of m can be controlled to adjust the output of the SVC.

$$e_d = (1 + m)V_{dc} \cos(\Psi)$$

$$e_q = (1 + m)V_{dc} \sin(\Psi)$$

From the SVC voltage resource to the middle bus, the whole SVC unit can be expressed as:

$$v_{md} = e_d + r_T i_{sd} - x_T i_{sq}$$

$$v_{mq} = e_q + r_T i_{sq} + x_T i_{sd}$$

3. Transmission System

From the generator bus to the middle bus, the system can be written as:

$$v_{gd} = v_{md} + r_e i_d - x_e i_q$$

$$v_{gq} = v_{mq} + r_e i_q + x_e i_d$$

From the middle bus to the infinite bus, the system can be written as:

$$v_{md} = v_b \sin \delta + r_e (i_d + i_{sd}) - x_e (i_q + i_{sq})$$

$$v_{mq} = v_b \cos \delta + r_e (i_q + i_{sd}) + x_e (i_d + i_{sq})$$

4. Governor Model

The transfer function of the governor is selected as:

$$gov = \left[a_g + \frac{b_g}{1 + sT_g} \right]$$

5. IEEE Standard ST1A AVR Model

The AVR and the exciter model used in the system is from the IEEE standard P421.5, 1992, Type ST1A as shown in Fig A.1.

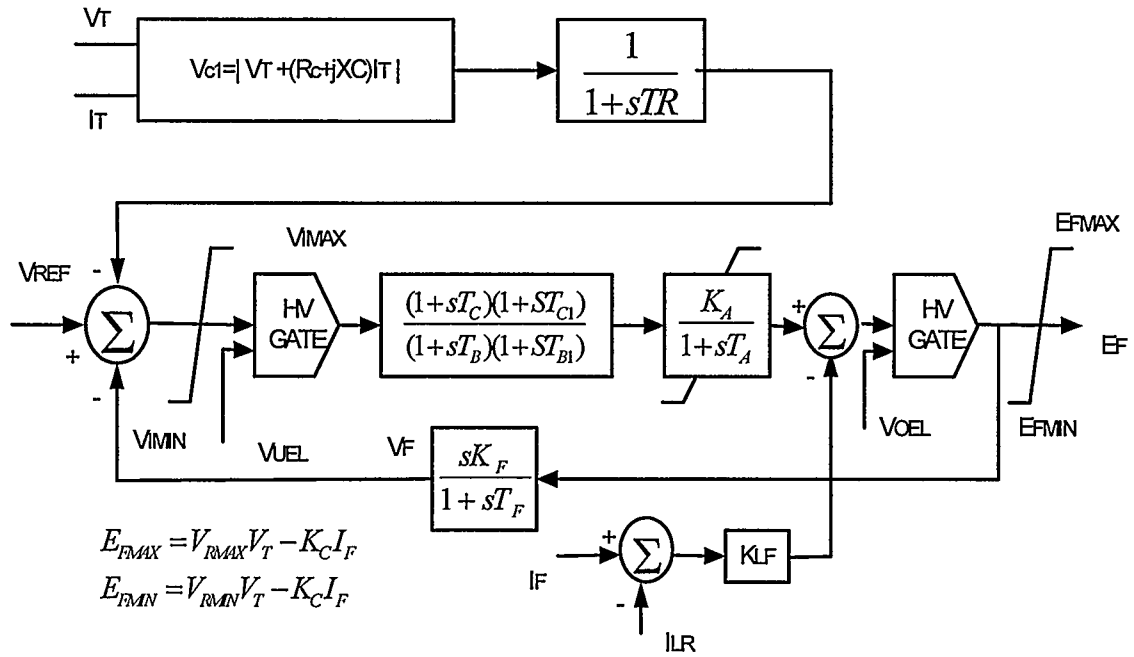


Figure A.1 AVR and Exciter Model

6. Parameters Used In The Simulations

- Generator and Tie Line parameters [8]

$$\begin{array}{lll}
 r_s = 0.007 & r_f = 0.00089 & r_{kq} = 0.023 \\
 r_{kd} = 0.023 & x_q = 0.743 & x_d = 1.24 \\
 x_{md} = 1.126 & x_{mq} = 0.626 & x_f = 1.33 \\
 x_{kd} = 1.1500 & x_{kq} = 0.625 & H = 3.46 \\
 Kd = -0.027 & r_e = 0.0 & x_e = 0.3
 \end{array}$$

- Governor Parameters ,Generator AVR and Generator CPSS

$$\begin{array}{lll}
 a_g = -0.001328 & T_c = 0.05 & T_1 = 0.17 \\
 b_g = -0.17 & T_b = 0.03 & T_2 = 0.01 \\
 T_g = 0.25 & K_F = 0.05 & T_3 = 0.17 \\
 K_A = 200 & T_A = 0.01 & T_4 = 0.01 \\
 T_F = 1.0 & K_{PSS} = 0.05 & T_w = 1.65 \\
 V_{IMIN} = -999 & V_{AMAX} = 999 & V_{UEL} = -999 \\
 V_{IMAX} = 999 & V_{RMIN} = -999 & V_{OEL} = 999 \\
 V_{AMIN} = -999 & V_{RMAX} = 999 & V_{STMIN} = -0.1 \\
 V_{STMAX} = 0.1 & &
 \end{array}$$

- SVC, SVC AVR and SVC CPSS

$$\begin{array}{ll}
 x_T = 1.0 & T_1 = 0.05 \\
 r_T = 0.0 & T_2 = 0.03 \\
 K_a = 50 & T_3 = 0.05 \\
 T_a = 0.01 & T_4 = 0.07 \\
 V_{AMAX} = 999 & T_w = 1.65 \\
 V_{AMIN} = -999 & V_{STMIN} = -0.1 \\
 K_{PSS} = 0.1 & V_{STMAX} = 0.1
 \end{array}$$

All resistances and reactances are in per unit and time constant in seconds.